博士論文

Systematic analysis of brain structure and neural network from a view of neuroblast lineages in *Drosophila melanogaster*

（幹細胞の系譜から見たショウジョウバエの脳構造と神経ネットワークの体系的解析）

Masayoshi Ito

伊藤　正芳

Table of Contents

Summary

Background:

During development neurons are generated by sequential divisions of neural stem cells, or neuroblasts. In the insect brain progeny of certain stem cells form lineage-specific sets of projections that arborize in distinct brain regions, called clonal units. Though this raises the possibility that the entire neural network in the brain might be organized in a clone-dependent fashion, only a small portion of clones has been identified.

Results:

Using *Drosophila melanogaster*, I randomly labeled one of about 100 stem cells at the beginning of the larval stage and analyzed the projection patterns of their progeny in the adult, and identified 96 clonal units in the central part of the fly brain, the cerebrum. Neurons of all the clones arborize in distinct regions of the brain, though many clones feature heterogeneous groups of neurons in terms of their projection patterns and neurotransmitters. Arborizations of clones overlap preferentially to form several groups of closely associated clones. Fascicles and commissures were all made by unique sets of clones. Whereas well-investigated brain regions such as the mushroom body and central complex consist of relatively small numbers of clones and are specifically connected with a limited number of neuropils, seemingly disorganized neuropils surrounding them are composed by a much larger number of clones and have extensive specific connections with many other neuropils.

Conclusions:

My study showed that the insect brain is formed by a composition of cell-lineage dependent modules. Clonal analysis reveals organized architecture even in those neuropils without obvious structural landmarks.

Introduction

Drosophila melanogaster as a useful model for neuroanatomy

Neural computation in the brain is accomplished by its complex neural network. Synergistic performance of a large number of neurons is usually involved even for the organization of simple behaviors from sensory inputs to motor outputs. A broad and detailed knowledge of neural projection patterns is a prerequisite to understand how such networks are organized (Ramon y Cajal, 1909).

The *Drosophila melanogaster* is a useful model for the neuroanatomy in the brain. The size of the brain is small enough (about 500 μm width, 250 μm height and 150 μm thickness) that the whole brain could fall into the range of laser-scam microscopy. The whole *Drosophila* brain consists of about 100,000 neurons, much smaller number of neurons than in the mammal brain.

The *Drosophila* brain can be divide into three parts; the optic lobe, the cerebrum and the subesophageal ganglion (SEG). The optic lobe is the most lateral part of the brain and it composed by visual projection neurons. The optic lobe contains about 30,000 neurons for each side. The SEG is the most ventral part of the brain and it composed by gustatory neurons from labellum, somatic sensory neuron and motor command neuron which connecting thoracic ganglion. The SEG is estimated to have about 5,000 neurons each side of the midline. The cerebrum is a central part of the brain and it contains many kinds of neurons, which are related to other sensory pathways, integration of different sensory inputs, learning and memory, etc. The cerebrum is estimated to have about 15,000 neurons each side of the midline (Shimada, Kato et al., in preparation).

In the *Drosophila* brain, many kinds of neurons have been identified. Lower order sensory neurons of olfactory (Tanaka et al. 2008), visual (Otsuna and Ito. 2006), auditory (Kamikouchi et al. 2004), and gustatory (Miyazaki and Ito. 2010) system were identified by screening of the Gal4 enhancer trap strains. Higher order neurons in the characteristic neuropils such as mushroom body and central complex have been studied using behavioral experiments of olfactory learning in the mushroom body and visual learning in the central complex. However, there is little knowledge about higher order neurons in the non-characteristic neuropils, which are so called diffused neuropils.

Clonal progeny in the mammal and *Drosophila* brain

During development, a neural stem cell divides asymmetrically to give birth to a family of clonally associated neurons (Sawa, 2010, Molyneaux et al., 2007). Growing evidences, both from vertebrate and invertebrate brains, suggest the importance of clonal organization in the network formation and function. In vertebrates, neural stem cells in the ventricular zone produce a wide variety of neurons. Each neural stem cell divides asymmetrically and produces two daughters. One of the daughter cells remains a stem cell while the other becomes a neuronal progenitor. In the mammalian brain, sibling neurons of the same lineage tend to have more synaptic contacts with each other, suggesting closer functional association (Costa, and Hedin-Pereira, 2010). Clonally related neurons can share characteristic functions such as those in the visual cortex that detect similar visual features (Ohtsuki et al., 2012, Li et al. 2012).

Neurons of the insect brain are also formed by the stem cells, called neuroblasts. In *Drosophila melanogaster* as well as in several other insect species, progeny of certain neuroblasts compose specific brain components such as the antennal lobe (AL), the mushroom body (MB), and the central complex (CX) (Ito et al., 1997, Boyan and Williams, 2010, Lai et al., 2008, Ito and Awasaki, 2008) The set of clonally related neurons and their specific arborizations is called a clonal unit (Ito et al., 1997, Ito and Awasaki, 2008), which serves as the building block that constructs the neural network of at least some of the brain's neuropils.

Differentiation of neuroblasts and neurons in the *Drosophila* brain

In the early *Drosophila* embryo there are identical 106 neuroblasts. Each neuroblast has a unique identity, which is determined by the cell body location in the neuroectoderm, and by the combination of genes it expresses (Urbach and Technau, 2003). Specification of individual neuroblast fates depend on the positional information in the neuroectoderm which provided by the early patterning genes; gap genes empty spiracles, hunchback, huckebein, sloppy paired 1 and tailless, tailless; the homeotic gene labial; and many other genes expressed in the early neuroectoderm (Fig. 1A-C)

Several kinds of neurons derived from a single neuroblast are generated by the two factors of producing different cell types; birth order and hemi-lineage. Birth order is the case

that neurons have different projection patterns according to the stages when they are produced from a neuroblast. In the mushroom body, 3 types of neurons; γ, α'/β', α/β neurons are produced according to the birth order (Lee et al, 1998). Reduction of Chinmo expression during development controls the differentiations of them. Hemi-lineage is the case that a pair of neurons which are produced by a single cell division of a neuroblast has deferent projection patterns. On the other hand, the projection targets of olfactory receptor neurons are different between two daughter cells of GMC. Uneven distributions of proteins such as Numb activates Notch signaling pathway only one of them (Endo et al, 2012).

Proliferation of neuroblasts and clone labeling technique

The cerebral neurons are generated by 106 neuroblasts during development (Ito and Hotta, 1992, Urbach and Technau 2003). Most neuroblasts, except for the four MB neuroblasts and one lateral AL neuroblast, have two phases of proliferation during early-mid embryonic and early larval-early pupal stages, producing neurons of the primary and secondary lineages, respectively (Ito and Hotta, 1992, Prokop and Technau, 1991). Neuroblasts are classified as type I and II. Most neuroblasts are type I; their daughter cells called the ganglion mother cells (GMCs) divide once again to give birth to two neurons each. In contrast, eight type II neuroblasts give birth to intermediate neural progeny, which divides several times to generate a larger number and more varieties of neurons (Fig. 1D) (Bello et al., 2008, Bone and Doe, 2008).

The progeny of single neuroblast could be labeled by using the Mosaic Analysis with a Repressible Cell Marker (MARCM) technique (Fig. 1E). The MARCM system features GAL80 which works antagonistically to transcription factor GAL4. GAL80 suppresses expression of the UAS-linked reporter even in the presence of GAL4. Heat shock flippase induce somatic recombination between the FRT sequences and GAL80 gene is removed from one of the daughter cells. The reporter gene will be expressed specifically in one of the daughter cell and its progeny. Inducing heat shock before the neuroblast proliferation, only a few clonal units would be randomly labeled in the adult brain.

Remaining questions about clonal units

In spite of extensive studies performed so far, including the clonal analysis of diverse *fruitless*-expressing neurons (Cachero et al., 2010, Yu et al., 2010), several key questions remain unanswered. Given the number of neuroblasts, as many as 100 clonal units should exist in the adult brain. Do they all feature specific arborizations that contribute to distinct brain components? Is each clone unique? How do neurons of different lineages overlap to form a closely associated functional group, called the clan (Ito and Awasaki, 2008)? Are the neurons of a clone structurally and biochemically uniform, or diverse? To answer these questions, I performed a large-scale analysis for the thorough identification of clonal structures.

In spite of the recent advances in the systematic single neuron labeling and multicolor cell labeling methods such as Brainbow (Chiang et al., 2011, Hampel et al., 2011), complete identification of tens of thousands of neurons is not technically easy. Comprehensive analysis of the much fewer number of clonal units, the combination of which should contain the entire neural projection patterns, provides a systematic overview of brain-wide neural network efficiently. It also gives indispensable insights for understanding how complex brain architecture is developmentally and evolutionarily organized.

Material and Methods

Fly strains and clone labeling

Following genetic cross and heat shock conditions were used to label clones: *elav^{c155}-Gal4 hs-FLP; FRT^{G13} tub-GAL80* crossed with *UAS-DsRed; FRT^{G13}; UAS-n-Syb::GFP* (heat shock at 36°C for 45 min); *elav^{c155}-Gal4 hs-FLP; FRT^{G13} tub-GAL80* crossed with *UAS-Syt::HA; FRT^{G13} UAS-GFP*; *UAS-mCD8::GFP* (36°C for 45 min); *hs-FLP tub-GAL80 FRT^{19A}; actin-Gal4* crossed with *UAS-DsRed FRT^{19A}; +; UAS-n-Syb::GFP* (36°C for 30 min); *hs-FLP tub-GAL80 FRT^{19A}; actin-Gal4* crossed with *FRT^{19A}; UAS-GFP* (37°C for 30 min). In all cases heat shock was applied between 12-36 hours after egg laying. Heat-shock condition was adjusted so that progeny of one or only a few neuroblasts should be labeled in a brain sample. To label dopaminergic cells for registration, *TH-GAL4* strain was crossed with *UAS-mCD8::GFP* strain.

Sample preparation

Flies were raised at 25°C with 12h/12h light/dark cycle, and female flies between 4 and 10 days after eclosion were examined. Brains were dissected in phosphate-buffered saline (PBS), fixed with 4% formaldehyde/PEM (0.1M PIPES, 2mM EGTA, 1mM $MgSO_4$, pH 6.95) for 2 hours at 4°C, and washed with PBS containing 0.5% Triton X-100 (PBT). Brains were blocked with 10% normal goat serum/PBT (blocking solution; BS) for 1hour and incubated in the BS with primary antibodies for overnight at 4°C on a rotary shaker, followed by the rinse with PBT and incubation in the BS with secondary antibodies for overnight at 4°C. After washed with PBS, the brains were incubated in 50% glycerol/PBS for 2 hours and 80% glycerol/H_2O for overnight at 4°C, and mounted in 80% glycerol/H_2O.

Following primary antibodies were used: rabbit anti-DsRed antibody (TAKARA BIO; #632496, 1:1000), rat anti-GFP (nacalai tesque; #GF090R, 1:1000), rabbit anti-GFP (Molecular Probe; #A11122, 1:1000), rat anti-HA (Roche; #11 867 423 001, 1:500), mouse nc82 (gift from E. Buchner and A. Hofbauer, 1:20), rabbit anti-GABA (SIGMA-ALDRICH; A2052, 1:1000), rabbit anti-5HT (Dia-Sorin, Stillwater, MN, 20080, lot 051007, 1:2,000), mouse antiH (ImmunoStar, #907001, 1:500), and rabbit antiDC2 (Abcam, #GR84243-2, 1:1000).

Following secondary antibodies were used: Alexa Fluor 488-conjugated anti-rat IgG (Molecular Probes; #A-11006, 1:250), Alexa Fluor 568-conjugated anti-rabbit IgG (Molecular Probes; #A-11036, 1:250), Alexa Fluor 488-conjugated anti-rabbit IgG (Molecular Probes; #A-11034, 1:250), Alexa Fluor 568-conjugated anti-rat IgG (Molecular Probes; #A-11077, 1:250) and Alexa Fluor 647-conjugated anti-mouse IgG (Molecular Probes; #A-21236, 1:250).

Image processing

Confocal image stacks were acquired by a Zeiss LSM 510 confocal microscope at 1024 ×1024 pixel resolution every 1.28μm (0.32×0.32×1.28 μm) using water-immersion 40× Plan-Apochromat objective (NA=1.2). For the samples with relatively weak labeling, noise was suppressed using 3D deconvolution software cellSens Dimension (Olympus). Image stacks were imported to 3D modeling software Amira 5.2.2 (Mercury Inc.). Signals of cell body clusters, bundles of neural fibers, and arborization areas of a clonal unit were manually selected in each layer. Signals of unselected regions including background noise and signals of other neurons were erased using a macro program of ImageJ (NIH). Cleaned image stacks were registered using brain aligner (Peng et al., 2011) or registration plugin in Fiji (Schindelin et al., 2012) to the standard brain template presented in Cachero et al' (Chachero et al., 2010). 3D reconstruction images were produced with Fluorender (Wan et al., 2009). Cell bodies and neural fibers were presented in magenta (RGB ratio; 255, 0, 255), presynaptic sites in yellow green (128, 255, 0), and neuropil structures in bluish gray (32, 32, 64). To compose stereo images, red channel and green/blue channels of the images reconstructed from slightly different viewing angles were merged with Photoshop (Adobe).

Mapping of clones

Projection patterns of the clonal units were documented using newly developed formulae (see Supplemental Table S3). Cell body numbers of the clones were estimated by averaging the count of cellular objects observed in the enhanced signals of n-Syb::GFP/ Syt::HA and background labeling of nc82 antibody, because cytoplasmic GFP/DsRed signals tend to be saturated. Two individuals counted each sample to avoid biases.

Overlap analysis

Registered image stacks were downsized into $256 \times 256 \times 128$ voxels and converted to binary data. Image data of all clonal units were piled up and color-coded according to the degree of overlap at each voxel. For cluster analysis, distance between a pair of clones was measured by the ratio between the number of voxels occupied by only one of the clones versus the total number of voxels occupied by the two clones (=0 if the two clones match completely, and 1 if there are no shared voxels). Cluster analysis using Ward's method based on these distances was performed with Mathematica 7 (Wolfram).

Construction of projection network

Neuropils arborized by a single projection subgroup of a clone were translated to a combination of neuropil pairs between which connections were observed. For the projection subgroups with symmetric distribution of presynaptic sites, I assigned non-directional connections. For those with asymmetric distribution of presynaptic sites, I assigned directional links from the neuropil lacking presynaptic sites to those with them, and no links between the neuropils lacking presynaptic sites or between the neuropils featuring them. Connection data were visualized with Cytoscape (National Resource for Network Biology) as an assembly of nodes and edges that represent neuropils and clonal projections, respectively.

Detection of network communities

I used Blondel's algorithm adopted for weighted networks (Blondel et al., 2008), because it provides partitioning with larger *Q* values than other algorithms for various types of networks (Blondel et al., 2008, Fortunato, 2010). *Q* value, also called modularity, is calculated by a combination of a given network and the partitioning result (Fortunato, 2010, Newman et al., 2004). *Q* values larger than 0.3 suggest that the given network has community structure (Newman et al., 2004).

Results

Visualization of clonal units in the adult *Drosophila* brain

To visualize clonal units, I labeled the progeny of single neuroblasts using the mosaic analysis with a repressible cell marker (MARCM) technique (Lee and Luo 1999). I used actin-GAL4 or elav-GAL4 to drive expression in all the neurons, and induced flippase mediated chromosomal recombination with mild heat shock in late embryos or early first-instar larvae to label all the neurons of the secondary lineages. To estimate the direction of information in the labeled neurons, I visualized neural fibers and presynaptic sites using combinations of cytoplasmic reporters (DsRed or GFP) and synaptic vesicle-targeted fusion reporters (neuronal synaptobrevin (n-Syb)::GFP or synaptotagmin (Syt)::HA). Considering the potential cell-specific variability in the labeling intensity and flipping frequency, I used various combinations of drivers, reporters and the locations of recombination targets to reveal a wider variety of clones.

I analyzed in total about 5,000 brain samples, and the labeled clones that share locations of cell bodies and characteristic projection patterns were classified (Fig. 2). I sometimes found clone samples that visualize characteristic subsets of arborizations found in other samples. Because this could happen either because flippase-mediated recombination would have occurred later during development, or because of the variety of expression driver activity among cells, I determined these samples as labeling the same clone.

I identified 80 groups of neuroblast clones with a single cluster of cell bodies. In addition, I found 14 groups of cells that feature two or three clusters of cell bodies in different parts of the brain. Because these clusters are co-labeled reproducibly in all the samples examined, including those in the companion study (Yu et al, submitted), it is highly likely that the labeled neurons belong to a single neuroblast clone despite their distant locations. Most of the two-cell clones, labeled by the flippase activity in the GMCs, showed projection patterns that were subsets of the above clones. However, I found two notable exceptions whose arborization patterns do not match with any of the above. Because their lineage identity is not yet resolved, I treated them as visualizing projections of potentially distinct neuroblast clones. Thus, I identified in total 96 clonal units (94 clearly identified and

two potential clones, Supplemental Fig. S1, Table S1).

3D data of the clones acquired from different samples were put into a standard template (Chiang et al., 2011) using linear and nonlinear registration methods (Peng et al., 2011, Schindelin et al., 2012) and overlaid for comparison (Fig. 4A). Arborizations of the clones together covered nearly entire volume of the cerebrum. The opposite hemisphere was also covered extensively, because 51 of the identified clones project also to the contralateral brain. The ventralmost part of the cerebrum was covered less extensively, because the current study excluded the clones of the SEG many of which arborize in this region.

To document the arborization patterns of the identified clones (Supplemental Table S2, 3), I used the systematic nomenclature system of the entire fly brain proposed by the Insect Brain Name Working Group (Ito et al., submitted), which separate the brain into 44 regions (neuropils) per side (Supplemental Table S2A). Arborizations of a distinct part of 36 clones matched well with the proposed neuropil boundaries (Supplemental Fig. S2, Table S2B). Arborizations that cross these boundaries were also observed often but, when arborizations of multiple clones were overlaid, they tend to show correlation with certain boundaries (Fig. 3J-R)

I developed a unified naming scheme of the clonal units in collaboration with the companion study (Yu et al., submitted), so that identical clones should have the same name. Clones are named using three designators: neuropil, cell body location, and number. They were first categorized according to the associated neuropils. Because many clones innervate multiple neuropils, I took the neuropil where the neurites emerging from the cell bodies form the first arborizations, or in which the clone arborizes most prominently. The clones were subsequently categorized according to the location of the cell body clusters (anterior, posterior, lateral, dorsal or ventral, in body axis). For the clones with multiple cell body clusters, two characters were added to indicate their relative locations.

Clones in each subcategory were numbered according either to the simplicity or to fine location of cell body clusters. Number was added even when there is only one clone type in the subcategory, so that other clones that might be identified in the future can easily be distinguished. Six of the clones that derive from the eight PAN (posterior *asense*-negative) cell lineages (Yu et al., submitted) were named DM1-6 to keep

consistency with previous studies (Izergina et al., 2009). Remaining two PAN clones were named DL1 and 2 because of their more lateral locations.

Precise descriptions of identified clonal units

ALad1

ALad1 is an already known clonal unit. Cell bodies lie on superior position to AL, and mean cell number is 63. ALad1 has 2 projection subgroups. ALad1A projects from AL to SEG via vALF. ALad1B projects from AL to CA and LH via mALT. Presynaptic signals are distributed in the entire arborization areas.

ALl1

ALl1 is an already known clonal unit. Cell bodies lie on lateral position to AL, and mean cell number is 196. ALl1 has 8 projection subgroups. ALl1A innervate only AL. ALl1B innervates both sides of AL. ALl1C projects from AL to SEG via vALF. ALl1D projects from AL to CA and LH via mALT. ALl1E projects from AL to PLP via mlALT. ALl1F projects from AL to LH via lALT. ALl1G projects from AL to SLP, SIP and CRE via lALT. ALl1H projects from AMMC and both sides of SAD to both sides of WED and AVLP. Presynaptic signals are distributed in the entire arborization areas.

ALlv1

ALlv1 is an already known clonal unit. Cell bodies lie on inferior lateral position to AL, and mean cell number is 54. ALlv1 has 3 projection subgroups. ALlv1A projects from AL to FLA and SEG via vALF. ALl1B projects from AL to SCL and SLP via mALT. ALl1C projects from AL to SIP and SMP via mALT. Presynaptic distribution is unknown.

ALv1

ALv1 is an already known clonal unit. Cell bodies lie on inferior position to AL, and mean cell number is 61. ALv1 has 3 projection subgroups. ALv1A projects from AL to SEG via vALF. ALv1B projects from AL to LH via mlALT. ALv1C projects from AL to PLP, SIP, SMP and CRE via mlALT. Presynaptic signals are localized in LH, PLP, SLP, SIP and CRE.

AOTUv1

AOTUv1 is a newly identified clonal unit. Cell bodies lie on anterior position to CRE, and mean cell number is 57. AOTUv1 has 2 projection subgroups. AOTUv1A projects from AOTU, SIP and SMP to CRE and LAL. AOTUv1B projects from AOTU, SIP and SMP to contralateral side of CRE and LAL. Presynaptic signals are localized in both sides of CRE and LAL.

AOTUv2

AOTUv2 is a newly identified clonal unit. Cell bodies lie on inferior position to AOTU, and mean cell number is 48. AOTUv2 has 4 projection subgroups. AOTUv2A innervates both sides of AOTU, SIP, SCL, and SMP. AOTUv2B innervates AOTU, SLP and LH. AOTUv2C projects from AOTU to PLP and SPS. AOTUv2D projects from AOTU to LO. Presynaptic signals are localized in SLP, LH and both sides of AOTU, SIP, SCL and SMP.

AOTUv3

AOTUv3 is a newly identified clonal unit. Cell bodies lie on inferior position to AOTU, and mean cell number is 80. AOTUv3 has 3 projection subgroups. AOTUv3A innervates BU, AOTU, SIP, SMP, CRE, LAL, AMMC and SAD. AOTUv3B innervates both sides of AOTU, SIP, SMP, ATL and IB. AOTUv3C innervates both sides of LAL, VES and SPS. Presynaptic signals are localized in BU and contralateral side of LAL, VES and SPS.

AOTUv4

AOTUv4 is a newly identified clonal unit. Cell bodies lie on inferior position to AOTU, and mean cell number is 99. AOTUv4 has 2 projection subgroups. AOTUv4A projects from AOTU, SIP, SMP and SLP to BU. AOTUv4B innervates FB, both sides of LAL, CRE, SIP and SMP. Presynaptic signals are localized in BU and both sides of LAL, CRE, SMP and SIP.

CLp1

CLp1 is a newly identified clonal unit. Cell bodies lie on posterior position to SMP, and mean cell number is 105. CLp1 has 2 projection subgroups. CLp1A innervates SMP, SCL, ICL, SLP and PLP. CLp1B innervates both sides of SCL, SPS, ATL and IB. Presynaptic signals are distributed in the entire arborization areas.

CREa1

CREa1 is a newly identified clonal unit. Cell bodies lie on anterior position to CRE, and mean cell number is 107. CREa1 has 2 projection subgroups. CREa1A projects from both sides of ML to CRE SIP, SMP and SLP. CREa1B projects contralateral side of FLA, SAD and SEG to contralateral side of SLP. Presynaptic signals are localized in both sides of ML and contralateral side of SLP.

CREa2

CREa2 is a newly identified clonal unit. Cell bodies lie on anterior position to CRE, and mean cell number is 118. CREa2 has 4 projection subgroups. CREa2A projects from both sides of ML to FB. CREa2B projects SIP, SMP and SLP to both sides of ML. CREa2C projects from SMP and SLP to SIP, CRE and LAL. CREa2D projects from AOTU, SIP, SMP and ATL to PLP, SPS, LAL and WED. Presynaptic signals are localized in SIP, CRE, LAL, WED, PLP, SPS and both sides of ML.

DM1

DM1 is an already known clonal unit. Cell bodies lie on posterior position to PB, and mean cell number is 237. DM1 has 12 projection subgroups. DM1A projects from PB to FB and EB. DM1B projects from PB to FB and contralateral side of NO. DM1C projects from PB to FB and contralateral side of CRE (RU). DM1D projects from PB to FB and contralateral side of LAL (GA). DM1E projects from LAL, WED to CRE, SMP and SIP. DM1F projects from IB, VES, GOR, CAN to SAD and AMMC. DM1G projects from IB, VES, GOR, CAN to ICL, SCL, SLP and AOTU. DM1H projects from contralateral side of IB, VES, GOR, CAN to contralateral side of SAD and AMMC. DM1I projects from contralateral side of IB, VES, GOR, CAN to contralateral side of ICL, SCL, SLP and AOTU. DM1J projects from both sides of IPS, SEG to ME. DM1K projects from both sides of IPS, SEG to LOP. DM1L projects from both sides of IPS, SEG to contralateral side of ME. Presynaptic signals are localized in PB, FB, EB, LAL, WED and ME, contralateral side of NO, CRE, LAL, LOP and ME, and both sides of SAD, AMMC, SCL, ICL, SLP and AOTU.

DM2

DM2 is an already known clonal unit. Cell bodies lie on posterior position to PB, and mean

cell number is 215. DM2 has 5 projection subgroups. DM2A projects from PB to FB and EB. DM2B projects from PB to FB and contralateral side of NO. DM2C projects from PB to FB and contralateral side of CRE (RU). DM2D projects from PB to FB and contralateral side of LAL (GA). DM2E projects from SLP, SMP to FLA and PRW. Presynaptic signals are localized in PB, FB, EB, SLP, SMP, FLA and PRW, contralateral side of NO, CRE and LAL.

DM3

DM3 is an already known clonal unit. Cell bodies lie on posterior position to PB, and mean cell number is 227. DM3 has 6 projection subgroups. DM3A projects from PB to FB and EB. DM3B projects from PB to FB and contralateral side of NO. DM3C projects from PB to FB and contralateral side of CRE (RU). DM3D projects from PB to FB and contralateral side of LAL (GA). DM3E innervates VL, ML, and PED. DM3F innervates both sides of SMP, SIP, CRE and SLP. Presynaptic signals are localized in PB, FB, EB, VL, ML and PED, contralateral side of NO, CRE and LAL, and both sides of SMP, SIP, CRE and SLP.

DM4

DM4 is an already known clonal unit. Cell bodies lie on posterior position to PB and IPS. Mean cell numbers are 96 and 20. DM4 has 6 projection subgroups. DM4A projects from PB to FB and EB. DM4B projects from PB to FB and contralateral side of NO. DM4C projects from PB to FB and contralateral side of CRE (RU). DM4D projects from PB to FB and contralateral side of LAL (GA). DM4E projects FB to SMP, SIP and AOTU. DM4F projects from WED and PLP to contralateral side of WED. Presynaptic signals are localized in PB, FB, EB, SMP, SIP, AOTU, WED and PLP, contralateral side of NO, CRE and LAL.

DM5

DM5 is an already known clonal unit. Cell bodies lie on posterior position to SPS, and mean cell number is 103. DM5 has 1 projection subgroups. DM5A projects from LAL, WED to contralateral side of LAL and WED. Presynaptic signals are localized in contralateral side of LAL and WED.

DM6

DM6 is an already known clonal unit. Cell bodies lie on posterior position to SPS, and mean

cell number is 251. DM5 has 5 projection subgroups. DM5A innervates FB, EB, both sides of NO, LAL, WED, CRE, SMP and SIP. DM5B projects from SMP, SLP, SIP and CRE to contralateral side of SMP and SLP. DM5C projects from contralateral side of ICL, SCL, SLP, PVLP and AVLP to contralateral side of LO. DM5D innervates both sides of VES, CAN, SAD and FLA. DM5E innervates AMMC and both sides of WED, PLP, SPS and IPS. Presynaptic signals are distributed in FB, EB, NO, LAL, WED, CRE, SMP, SIP, AMMC PLP, SPS and IPS and contralateral side of ICL, SCL, SLP, PVLP, AVLP, WED, PLP, SPS and IPS.

DL1

DL1 is an already known clonal unit. Cell bodies lie on posterior position to LH and PLP. Mean cell numbers are 137 and 48. DL1 has 4 projection subgroups. DL1A projects from SIP, SMP to FB (upper layer). DL1B projects from SIP, SMP to FB (lower layer). DL1C projects from PLP and WED to LO via AOT. DL1D projects from LAL and AVLP to LO via AOT. Presynaptic signals are distributed in SIP, SMP, FB, PLP, WED and LO.

DL2

DL2 is an already known clonal unit. Cell bodies lie on posterior position to LH and PLP. Mean cell numbers are 114 and 18. DL2 has 4 projection subgroups. DL2A projects from LH to SLP, SIP and SMP via PYF. DL2B innervates both sides of SIP, SMP, α lobe of VL, CRE and LAL. DL2C innervates PVLP, AVLP and SLP. DL2D innervates both sides of SCL, SLP, ICL, VES and GOR via GORC. Presynaptic signals are distributed in the entire arborization areas.

EBa1

EBa1 is an already known clonal unit. Cell bodies lie on superior lateral position to AL, and mean cell number is 86. EBa1 has 3 projection subgroups. EBa1A projects from LAL and BU to EB. EBa1B projects from AOTU, LAL, CRE and SIP to contralateral side of AOTU via aSEC. EBa1C projects from FB to contralateral side of CRE, SIP and LAL via aSEC. Presynaptic signals are localized in EB and contralateral side of AOTU, CRE, SIP and LAL.

EBp1

EBp1 is a newly identified clonal unit. Cell bodies lie on posterior position to SPS, and mean cell number is 6. EBp1 has 1 projection subgroups. EBp1A innervates both sides of LAL, BU and EB via MEF. Presynaptic signals are distributed in the entire arborization areas.

FLAa1

FLAa1 is a newly identified clonal unit. Cell bodies lie on inferior medial position to AMMC, and mean cell number is 8. FLAa1 has 1 projection subgroups. FLAa1A projects from FLA, VES and SAD to LAL and CRE. Presynaptic signals are localized in LAL and CRE.

FLAa2

FLAa2 is a newly identified clonal unit. Cell bodies lie on inferior position to AL, and mean cell number is 60. FLAa2 has 3 projection subgroups. FLAa2A projects from both sides of PRW and FLA to SIP and both sides of SMP via MBDL. FLAa2B projects from both sides of PRW and FLA to α lobe of VL via MBDL. FLAa2C projects from PRW, FLA, SAD and SEG to α'lobe of VL via MBDL. Presynaptic signals are localized in SMP, SIP, α lobe of VL, PRW, FLA, SAD, SEG and contralateral side of SMP.

LALv1

LALv1 is a newly identified clonal unit. Cell bodies lie on inferior position to AL, and mean cell number is 105. LALv1 has 1 projection subgroups. LALv1A projects from FB, EB, and both sides of NO to CRE, SMP, SIP and SLP. Presynaptic signals are localized in both sides of FB, EB and NO.

LHa1

LHa1 is a newly identified clonal unit. Cell bodies lie on lateral position to LH, and mean cell number is 58. LHa1 has 1 projection subgroups. LHa1A innervates SLP and LH. Presynaptic signals are distributed in the entire arborization areas.

LHa2

LHa2 is a newly identified clonal unit. Cell bodies lie on lateral position to SLP, and mean cell number is 55. LHa2 has 1 projection subgroups. LHa2A innervates LH and SLP. Presynaptic signals are distributed in the entire arborization areas.

LHa3

LHa3 is a newly identified clonal unit. Cell bodies lie on lateral position to AVLP, and mean cell number is 47. SLPav4 has 1 projection subgroups. SLPav4A innervates LH and SLP. Presynaptic signals are distributed in the entire arborization areas.

LHa4

LHa4 is a newly identified clonal unit. Cell bodies lie on lateral position to AVLP, and mean cell number is 50. LHa4 has 1 projection subgroups. LHa4A innervates LH and SLP. Presynaptic signals are distributed in the entire arborization areas.

LHd1

LHd1 is a newly identified clonal unit. Cell bodies lie on anterior position to SIP, and mean cell number is 55 LHd1 has 3 projection subgroups. LHd1A projects from AOTU to SPS and PLP. LHd1B innervates both sides of AOTU, SIP and SMP via AOTUC. LHd1C projects from AOTU to LH and both sides of SLP via PYF and ADC. Presynaptic signals are localized in LH and both sides of AOTU, SIP, SMP and SLP.

LHl1

LHl1 is a newly identified clonal unit. Cell bodies lie on lateral position to LH, and mean cell number is 49. LHl1 has 3 projection subgroups. LHl1A innervates LH, SLP and AVLP. LHl1B innervates SLP, SIP and LH via PYF. LHl1C innervates SCL, SLP and SIP. Presynaptic signals are distributed in the entire arborization areas.

LHl2

LHl2 is a newly identified clonal unit. Cell bodies lie on lateral position to SLP, and mean cell number is 97. LHl2 has 2 projection subgroups. LHl2A innervates SMP, SLP and LH. LHl2B innervates both sides of AVLP, PVLP, SLP, SCL, ICL and GOR via SAC. Presynaptic signals are localized in SMP, SLP and LH.

LHl3

LHl3 is a newly identified clonal unit. Cell bodies lie on lateral position to SLP, and mean cell number is 46. LHl3 has 2 projection subgroups. LHl3A projects LH and SLP to AVLP.

LHl3B projects from PLP to LO. Presynaptic signals are localized in AVLP and PLP.

LHl4

LHl4 is a newly identified clonal unit. Cell bodies lie on lateral position to LH, and mean cell number is 107. LHl4 has 2 projection subgroups. LHl4A innervates LH and SLP. LHl4B projects from PLP, SPS, SCL, ICL and SLP to LO. Presynaptic signals are localized in LH, SLP, PLP, SPS, SCL, ICL and SLP

LHp1

LHp1 is a newly identified clonal unit. Cell bodies lie on posterior position to LH, and mean cell number is 30. LHp1 has 1 projection subgroups. LHp1A innervates LH and SLP. Presynaptic distribution is unknown.

LHp2

LHp2 is a newly identified clonal unit. Cell bodies lie on posterior position to SLP, and mean cell number is 100. LHp2 has 2 projection subgroups. LHp1A innervates LH, SLP and SMP. LHp1A innervates both sides of PLP, WED, AVLP, SAD, LAL and ATL via PLF and sPLPC. Presynaptic signals are distributed in the entire arborization areas.

MBp1

MBp1 is an already known clonal unit. Cell bodies lie on posterior position to CA, and mean cell number is 475. MBp1 has 3 projection subgroups. MBp1A innervates CA, PED, SPU and γ lobe of ML. MBp1B innervates CA, PED, α' lobe of VL and β' lobe of ML. MBp1C innervates CA, PED, α lobe of VL and β lobe of ML. Presynaptic signals are distributed in the entire arborization areas.

MBp2

MBp2 is an already known clonal unit. Cell bodies lie on posterior position to CA, and mean cell number is 482. MBp2 has 3 projection subgroups. MBp2A innervates CA, PED, SPU and γ lobe of ML. MBp2B innervates CA, PED, α' lobe of VL and β' lobe of ML. MBp2C innervates CA, PED, α lobe of VL and β lobe of ML. Presynaptic signals are distributed in the entire arborization areas.

MBp3

MBp3 is an already known clonal unit. Cell bodies lie on posterior position to CA, and mean cell number is 512. MBp3 has 3 projection subgroups. MBp3A innervates CA, PED, SPU and γ lobe of ML. MBp3B innervates CA, PED, α' lobe of VL and β' lobe of ML. MBp3C innervates CA, PED, α lobe of VL and β lobe of ML. Presynaptic signals are distributed in the entire arborization areas.

MBp4

MBp4 is an already known clonal unit. Cell bodies lie on posterior position to CA, and mean cell number is 506. MBp4 has 3 projection subgroups. MBp4A innervates CA, PED, SPU and γ lobe of ML. MBp4B innervates CA, PED, α' lobe of VL and β' lobe of ML. MBp4C innervates CA, PED, α lobe of VL and β lobe of ML. Presynaptic signals are distributed in the entire arborization areas.

PSa1

PSa1 is a newly identified clonal unit. Cell bodies lie on inferior position to AL, and mean cell number is 64. PSa1 has 2 projection subgroups. PSa1A projects from SPS, VES, FLA, SAD and SEG to both sides of ICL, SCL, GOR, PVLP and AVLP. PSa1B projects from ICL, SCL, GOR, PVLP and AVLP to ME and LOP. Presynaptic signals are localized in ICL, SCL, GOR, PVLP, AVLP, ME, LOP and contralateral side of ICL, SCL, GOR, PVLP and AVLP.

PSp1

PSp1 is a newly identified clonal unit. Cell bodies lie on posterior position to SPS, and mean cell number is 28. PSp1 has 1 projection subgroups. PSp1A innervates SPS, ICL, SCL, GOR, SLP, IPS, PLP, IB, ATL, LAL CRE and contralateral side of SPS. Presynaptic signals are distributed in the entire arborization areas.

PSp2

PSp2 is a newly identified clonal unit. Cell bodies lie on posterior position to SPS, and mean cell number is 33. PSp2 has 1 projection subgroups. PSp2A projects from SPS and IPS to thoracic ganglion via cervical connective. Presynaptic distribution is unknown.

PSp3

PSp3 is a newly identified clonal unit. Cell bodies lie on posterior position to ICL, and mean cell number is 45. PSp3 has 3 projection subgroups. PSp3A projects from PLP, ICL and SCL to LO. PSp3B projects PLP, both sides of SPS, ATL and IB to LO. PSp3C projects from VES, FLA, LAL, AVLP, PVLP and AMMC to thoracic ganglion via cervical connective. Presynaptic signals are localized in PLP, ICL, SCL, VES, FLA and LAL and both sides of SPS, ATL and IB.

SIPa1

SIPa1 is a newly identified clonal unit. Cell bodies lie on lateral position to SLP, and mean cell number is 70. SIPa1 has 2 projection subgroups. SIPa1A innervates SLP, PLP, SCL and ATL. SIPa1B innervates SLP, SIP and SMP. Presynaptic signals are distributed in the entire arborization areas.

SLPa&l1

SLPa&l1 is a newly identified clonal unit. Cell bodies lie on inferior position to AOTU and lateral position to SLP. Mean cell numbers are 86 and 70. SLPav1 has 2 projection subgroups. SLPa&l1A innervates SLP, PLP, SCL and ICL. SLPa&l1B projects from PLP, IPS and LO to LAL and VES via AOT. Presynaptic signals are localized in SLP, PLP, SCL, ICL, LAL and VES.

SLPad1

SLPad1 is a newly identified clonal unit. Cell bodies lie on posterior position to SLP, and mean cell number is 147. SLPad1 has 4 projection subgroups. SLPad1A projects from LH to SLP, SIP and SMP via PYF. SLPad1B innervates SLP, SCL, ICL and PVLP. SLPad1C projects from PLP and SPS to SLP, PVLP and AVLP. SLPad1D projects from PLP to both sides of ATL. Presynaptic signals are localized in SLP, SIP, SMP, SCL, ICL, PVLP and AVLP.

SLPal1

SLPal1 is a newly identified clonal unit. Cell bodies lie on lateral position to SLP, and mean cell number is 64. SLPal1 has 1 projection subgroups. SLPal1A innervates SLP, LH and SIP. Presynaptic signals are distributed in the entire arborization areas.

SLPal2

SLPal2 is a newly identified clonal unit. Cell bodies lie on lateral position to SLP, and mean cell number is 61. SLPal2 has 1 projection subgroups. SLPal2A innervates SLP, SCL and LH. Presynaptic signals are distributed in the entire arborization areas.

SLPal3

SLPal3 is a newly identified clonal unit. Cell bodies lie on lateral position to AOTU, and mean cell number is 61. SLPal3 has 3 projection subgroups. SLPal3A innervates AOTU, SIP, SMP and ATL. SLPal3B innervates SLP and SCL via PYF. SLPal3C projects from SLP, PLP and SIP to contralateral side of SIP, SMP CRE and LAL. Presynaptic signals are localized in SLP and SCL, contralateral side of SIP, SMP, CRE and LAL.

SLPav1

SLPav1 is a newly identified clonal unit. Cell bodies lie on lateral position to SLP, and mean cell number is 60. SLPav1 has 4 projection subgroups. SLPav1A innervates SLP and both sides of SMP. SLPav1B projects from PLP, SPS, ICL, SCL and SLP to LO. SLPav1C projects from PLP and SLP to AME. SLPav1D projects from PLP and SLP to ICL and SPS via AOT. Presynaptic signals are localized in SLP, SMP, PLP, SPS, ICL, SCL and contralateral side of SMP.

SLPav2

SLPav2 is a newly identified clonal unit. Cell bodies lie on lateral position to SLP, and mean cell number is 37. SLPav2 has 1 projection subgroups. SLPav2A innervates AOTU, both sides of SMP, SLP, SCL, CRE, LAL and ATL, and contralateral side of PLP via aSEC. Presynaptic signals are distributed in the entire arborization areas. SLPav2 includes dorsal giant inter (DGI) neuron.

SLPav4

SLPav4 is a newly identified clonal unit. Cell bodies lie on lateral position to SLP, and mean cell number is 29. SLPav5 has 1 projection subgroups. SLPav4A innervates SLP, SMP, SCL and ICL. Presynaptic signals are distributed in the entire arborization areas.

SLPp&v1

SLPp&v1 is a newly identified clonal unit. Cell bodies lie on lateral position to LH and posterior position to PLP. Mean cell numbers are 56 and 5. SLPp&v1 has 3 projection subgroups. SLPp&v1A innervates SLP, LH, PLP, SCL and ICL. SLPp&v1B innervates both sides of IPS, SPS, IB and ATL via PLF and sPLPC. SLPp&v1C innervates EPA, PVLP, ICL, AVLP, SIP, AOTU, SAD and SEG. Presynaptic signals are localized in SLP, LH, PLP, SCL, ICL, EPA, PVLP, SAD, SEG and contralateral side of IPS, SPS, IB and ATL.

SLPpl1

SLPpl1 is a newly identified clonal unit. Cell bodies lie on posterior position to LH, and mean cell number is 62. SLPpl1 has 2 projection subgroups. SLPpl1A projects PLP, SLP and SMP to AME and ME via PLF. SLPpl1B projects SLP, SCL, ICL and SMP to LO via PLF. Presynaptic signals are localized in SLP, SCL, ICL, SMP, AME and ME.

SLPpl4

SLPpl4 is a newly identified clonal unit. Cell bodies lie on superior position to LH, and mean cell number is 45. SLPpl4 has 1 projection subgroups. SLPpl4A innervates SLP and SMP. Presynaptic signals are distributed in the entire arborization areas.

SLPpm1

SLPpm1 is a newly identified clonal unit. Cell bodies lie on posterior position to SLP and mean cell number is 72. SLPpm1 has 1 projection subgroups. SLPpm1A innervates SLP, SCL, ICL and PLP. Presynaptic signals are distributed in the entire arborization areas.

SLPpm4*

SLPpm4 is a newly identified clonal unit. Cell bodies lie on posterior medial position to SMP, and mean cell number is 2. SLPpm4 is a potentially GMC clone. SLPpm4 has 1 projection subgroups. SLPpm4A innervates SLP, SCL and PLP. Presynaptic signals are distributed in the entire arborization areas.

SMPad1

SMPad1 is a newly identified clonal unit. Cell bodies lie on anterior medial position to SMP, and mean cell number is 28. SMPad1 has 2 projection subgroups. SMPad1A innervates SIP and both sides of SMP. SMPad1B projects from both sides of SMP to both sides of

FLA via MBDL. Presynaptic signals are distributed in the entire arborization areas.

SMPad2

SMPad2 is a newly identified clonal unit. Cell bodies lie on anterior position to SMP, and mean cell number is 50. SMPad2 has 3 projection subgroups. SMPad2A innervates SMP, SIP and AOTU. SMPad2B projects from SMP and CRE to both sides of VES via MBDL. SMPad2C innervates SMP, SLP, SCL, ICL, PLP and both sides of IB and SPS. Presynaptic distribution is unknown.

SMPad4*

SMPad4 is a newly identified clonal unit. Cell bodies lie on anterior position to SMP, and mean cell number is 2. SMPad4 is a potentially GMC clone. SMPad4 has 1 projection subgroups. SMPad4A projects from CRE, SMP, SIP and SLP to both sides FB and NO. Presynaptic signals are distributed in the entire arborization areas.

SMPp&v1

SMPp&v1 is a newly identified clonal unit. Cell bodies lie on posterior position to SMP and SPS. Mean cell numbers are 63 and 34. SMPp&v1 has 5 projection subgroups. SMPp&v1A innervates SMP, SCL, ICL, SIP and CRE. SMPp&v1B projects from both sides of SMP and ATL to contralateral side of SMP, SCL, ICL, SIP and CRE. SMPp&v1C innervates both sides of SMP, SIP and AOTU via AOTUC. SMPp&v1D innervates both sides of IB, SPS, ATL, SMP, SIP and AOTU. SMPp&v1E projects from both sides of ICL, SCL, SLP and PLP to contralateral side of LOP and ME via POC. Presynaptic signals are distributed in the entire arborization areas except a part of ICL, SCL, SLP and PLP.

SMPp&v2

SMPp&v2 is a newly identified clonal unit. Cell bodies lie on posterior position to SMP and PB. Mean cell numbers are 55 and 12. SMPp&v2 has 5 projection subgroups. SMPp&v2A projects from SMP, SCL and ICL to SPS and IB. SMPp&v2B projects from SMP, SCL and ICL to contralateral side of FLA and VES. SMPp&v1C innervates both sides of SMP, SIP and AOTU via ADC. SMPp&v2D innervates both sides of IB, ATL and SMP. SMPp&v2E projects from SCL, ICL, SLP, PLP, PVLP, and AVLP to contralateral side of PLP, SCL, ICL,

SLP and ME. Presynaptic signals are distributed in the entire arborization areas except a part of SPS, IB, SCL, ICL, SLP, PLP, PVLP and AVLP.

SMPpd1

SMPpd1 is a newly identified clonal unit. Cell bodies lie on posterior position to SMP, and mean cell number is 59. SMPpd1 has 2 projection subgroups. SMPpd1A innervates SLP, SCL, PLP, SMP, SIP and contralateral side of SMP. SMPpd1B innervates SMP, SIP AOTU, PVLP and AVLP. Presynaptic signals are localized in SLP, SCL, PLP, SMP, SIP and contralateral side of SMP.

SMPpd2

SMPpd2 is a newly identified clonal unit. Cell bodies lie on posterior position to SMP, and mean cell number is 17. SMPpd2 has 1 projection subgroups. SMPpd2A innervates SLP, SCL, SMP and contralateral side of SMP. Presynaptic signals are distributed in the entire arborization areas.

VESa1

VESa1 is a newly identified clonal unit. Cell bodies lie on inferior position to AL, and mean cell number is 29. VESa1 has 3 projection subgroups. VESa1A innervates FLA, VES, GOR, ICL and SPS. VESa1B projects from SAD and CAN to AVLP, WED and EPA. VESa1C projects from FLA, VES, GOR and ICL to contralateral side of VES, GOR and ICL. Presynaptic signals are distributed in the entire arborization areas.

VLPa1

VLPa1 is a newly identified clonal unit. Cell bodies lie on anterior position to AVLP, and mean cell number is 94. VLPa1 has 1 projection subgroups. VLPa1A innervates AVLP and PVLP. Presynaptic signals are distributed in the entire arborization areas.

VLPa2

VLPa2 is a newly identified clonal unit. Cell bodies lie on lateral position to AL, and mean cell number is 77. VLPa2 has 2 projection subgroups. VLPa2A projects from IPS and SEG to both sides of PVLP, AVLP and ME via GC. VLPa2B projects from WED, SAD and AMMC to both sides of PVLP and AVLP. Presynaptic signals are localized in both sides of PVLP,

AVLP and ME.

VLPd&p1

VLPd&p1 is a newly identified clonal unit. Cell bodies lie on anterior and posterior position to SLP. Mean cell numbers are 51 and 50. VLPd&p1 has 3 projection subgroups. VLPd&p1A projects from PVLP and AVLP to contralateral side of PVLP via LVF. VLPd&p1B innervates LH, SLP, SCL, SMP, SIP and AOTU. VLPd&p1C projects from PLP to LO. Presynaptic signals are distributed in the entire arborization areas except PLP and LO.

VLPd1

VLPd1 is a newly identified clonal unit. Cell bodies lie on anterior position to SLP, and mean cell number is 57. VLPd1 has 3 projection subgroups. VLPd1A projects from PVLP, SCL, ICL and SLP to FLA, SAD and SEG via mlALT. VLPd1B projects from PVLP, AVLP and SLP to FLA, SAD and SEG. VLPd1C projects from PVLP, SCL, ICL and SLP to LO. Presynaptic signals are localized in PVLP, SCL, ICL, SLP, FLA, SAD and SEG.

VLPd2

VLPd2 is a newly identified clonal unit. Cell bodies lie on anterior position to AOTU, and mean cell number is 50. VLPd2 has 1 projection subgroups. VLPd2A projects from PVLP, AVLP and SLP to ICL, SCL and GOR. Presynaptic signals are localized in ICL, SCL and GOR.

VLPl&d1

VLPl&d1 is a newly identified clonal unit. Cell bodies lie on anterior and lateral position to AVLP. Mean cell numbers are 63 and 66. VLPl&d1 has 4 projection subgroups. VLPl&d1A projects from AVLP, PVLP, WED and AMMC to contralateral side of AVLP and PVLP. VLPl&d1B projects AVLP and PVLP to SCL, ICL and SLP. VLPl&d1C projects from AVLP and PVLP to contralateral side of SCL, ICL and SLP via pSEC. VLPd1D projects from AVLP and PVLP to contralateral side of AVLP via pSEC. Presynaptic signals are distributed in the entire arborization areas.

VLPl&p1

VLPl&p1 is a newly identified clonal unit. Cell bodies lie on lateral position to AVLP and posterior position to PLP. Mean cell numbers are 78 and 43. VLPl&p1 has 5 projection subgroups. VLPl&p1A projects AVLP and PVLP to SCL, ICL and SLP. VLPl&p1B projects from AVLP and PVLP to contralateral side of SCL, ICL and SLP via pSEC. VLPl&p1C projects from AVLP and PVLP to contralateral side of AVLP via pSEC. VLPl&p1D projects from PVLP, SCL, ICL and GOR to SIP, SMP, CRE and LAL via PLF. VLPl&p1E projects from LAL, CRE, SMP and SIP to contralateral side of SMP, SIP and CRE. Presynaptic signals are distributed in the entire arborization areas.

VLPl&p2

VLPl&p2 is a newly identified clonal unit. Cell bodies lie on lateral position to AVLP and posterior position to PLP. Mean cell numbers are 92 and 40. VLPl&p2 has 6 projection subgroups. VLPl&p2A projects from AVLP to LH via lALT. VLPl&p2B projects AVLP and PVLP to SCL, ICL and SLP. VLPl&p2C projects from AVLP and PVLP to contralateral side of SCL, ICL and SLP via pSEC. VLPl&p2D projects from AVLP and PVLP to contralateral side of AVLP via pSEC. VLPl&p1E projects from AMMC to PVLP, AVLP, contralateral side of EPA, PVLP and AVLP via GC. VLPl&p1F projects from WED, AMMC and SAD to PVLP, AVLP, contralateral side of EPA, PVLP and AVLP via GC. Presynaptic signals are distributed in the entire arborization areas except AMMC, WED and SAD.

VLPl1

VLPl1 is a newly identified clonal unit. Cell bodies lie on lateral position to WED, and mean cell number is 100. VLPl1 has 2 projection subgroups. VLPl1A innervates AVLP, PVLP and WED. VLPl1B innervates WED, SAD and AMMC. Presynaptic signals are distributed in the entire arborization areas.

VLPl2

VLPl2 is a newly identified clonal unit. Cell bodies lie on anterior position to AVLP, and mean cell number is 194. VLPl2 has 5 projection subgroups. VLPl2A projects from AVLP to LH via lALT. VLPl2B innervates AVLP, SLP, PVLP and EPA. VLPl2C projects from AVLP and PVLP to LO. VLPl2D projects from AVLP, SLP, PVLP and EPA to contralateral side of AVLP and PVLP via GC. VLPl2E projects from ICL, GOR, SCL and SLP to contralateral

side of ICL, GOR, SCL and SLP via SAC. Presynaptic signals are distributed in the entire arborization areas except LO.

VLPl3

VLPl3 is a newly identified clonal unit. Cell bodies lie on anterior position to AVLP, and mean cell number is 125. VLPl3 has 2 projection subgroups. VLPl3A innervates AVLP, PVLP, ICL and SCL. VLPl3B innervates AVLP, SLP, SCL and ICL Presynaptic signals are distributed in the entire arborization areas.

VLPp&l1

VLPp&l1 is a newly identified clonal unit. Cell bodies lie on posterior position to PLP and LOP. Mean cell numbers are 53, 27 and 18. VLPp&l1 has 3 projection subgroups. VLPp&l1A innervates PVLP AVLP and SLP. VLPp&l1B projects from LO to PLP, SCL, ICL and SLP. VLPp&l1C projects from LOP to IPS. Presynaptic signals are distributed in the entire arborization areas except LO and LOP.

VLPp1

VLPpT1 is a newly identified clonal unit. Cell bodies lie on lateral position to PLP, and mean cell number is 34. VLPp1 has 1 projection subgroups. VLPp1A innervates AVLP and PVLP. Presynaptic signals are distributed in the entire arborization areas.

VLPp2

VLPp2 is a newly identified clonal unit. Cell bodies lie on posterior position to SPS, and mean cell number is 47. VLPp2 has 2 projection subgroups. VLPp –T2A projects from VES, PVLP and ICL to VES, CAN, SPS and IPS. VLPp2B projects from VES, PVLP and ICL to contralateral side of VES, CAN, SPS and IPS. Presynaptic signals are localized in contralateral side of VES, CAN, SPS and IPS.

VPNd1

VPNd1 is a newly identified clonal unit. Cell bodies lie on lateral position to PLP, and mean cell number is 123. VPNd1 has 2 projection subgroups. VPNd1A projects from LO and LOP to PLP (PGe and PGg) and PVLP (VGi). VPNd1B projects from PLP, SPS, ICL, SCL and SLP to contralateral side of ICL, SCL, SPS, PLP and LO. Presynaptic signals are

distributed in the entire arborization areas.

VPNd2

VPNd2 is a newly identified clonal unit. Cell bodies lie on lateral position to LH, and mean cell number is 44. VPNd2 has 1 projection subgroups. VPNd2A projects from LO to AOTU. Presynaptic signals are localized in AOTU.

VPNd3

VPNd3 is a newly identified clonal unit. Cell bodies lie on lateral position to LH, and mean cell number is 42. VPNd3 has 2 projection subgroups. VPNd3A projects from LO to PVLP (VGb). VPNd3B projects from LO to PVLP (VGk). Presynaptic signals are distributed in the entire arborization areas.

VPNd4

VPNd4 is a newly identified clonal unit. Cell bodies lie on lateral position to PLP, and mean cell number is 93. VPNd4 has 1 projection subgroups. VPNd4A projects from LO to SLP, contralateral side of SLP, PVLP and AVLP. Presynaptic signals are localized in SLP and contralateral side of SLP, PVLP and AVLP.

VPNl&d1

VPNl&d1 is a newly identified clonal unit. Cell bodies lie on lateral position to AVLP and SLP. Mean cell numbers are 106 and 18. VPNa1 has 2 projection subgroups. VPNa1A innervates both sides of ME, IPS and SPS via POC. VPNa1B innervates LH and SLP. Presynaptic signals are localized in LH, SLP and both side of ME.

VPNp&v1

VPNp&v1 is a newly identified clonal unit. Cell bodies lie on lateral and posterior position to PLP. Mean cell number is 87 and 44. VPNp1 has 7 projection subgroups. VPNp&v1A innervates PLP, PVLP and AVLP. VPNp&v1B innervates PLP, WED and AVLP. VPNp&v1C projects from PLP, SCL, ICL and SLP to LO. VPNp&v1D innervates both sides of PLP, SCL, ICL and SLP via sPLPC. VPNp&v1E projects from PLP and SLP to CA. VPNp&v1F innervates both sides of SPS and IB. VPNp&v1G innervates both sides of PLP, PVLP, ATL and IB via sPLPC. Presynaptic signals are distributed in the entire arborization

areas except LO and both sides of SPS, IB and ATL.

VPNp1

VPNp1 is a newly identified clonal unit. Cell bodies lie on lateral position to PLP, and mean cell number is 145. VPNp1 has 5 projection subgroups. VPNp1A projects from LO to PVLP and AVLP. VPNp1B projects from LO to VES, LAL and CRE via GC. VPNp1C projects from LO to contralateral side of VES, LAL and CRE via GC. VPNp1D projects from LO to contralateral side of PVLP and PLP via GC. VPNp1E projects from LO to contralateral side of LO and ME via GC. Presynaptic signals are distributed in the entire arborization areas except LO.

VPNp2

VPNp2 is a newly identified clonal unit. Cell bodies lie on lateral position to PLP, and mean cell number is 34. VPNp2 has 1 projection subgroups. VPNp2A projects from LO to PVLP (VGf). Presynaptic distribution is unknown.

VPNp3

VPNp3 is a newly identified clonal unit. Cell bodies lie on lateral position to PLP, and mean cell number is 40. VPNp4 has 2 projection subgroups. VPNp3A projects from LO to PVLP (VGd). VPNp3B projects from LO to PVLP (VGe). Presynaptic signals are localized in PVLP.

VPNp4

VPNp4 is a newly identified clonal unit. Cell bodies lie on lateral position to PLP, and mean cell number is 45. VPNp4 has 1 projection subgroups. VPNp4A projects from LO to PLP, ICL, SCL and SLP. Presynaptic signals are localized in PLP, ICL, SCL and SLP.

VPNv1

VPNv1 is a newly identified clonal unit. Cell bodies lie on lateral position to WED, and mean cell number is 51. VPNv1 has 1 projection subgroups. VPNv1A projects from LO to PVLP (VGf). Presynaptic distribution is unknown.

VPNv2

VPNv2 is a newly identified clonal unit. Cell bodies lie on lateral position to WED, and mean cell number is 59. VPNv2 has 1 projection subgroups. VPNv2A projects from LO to PVLP (VGa). Presynaptic signals are localized in PVLP.

VPNv3

VPNv3 is a newly identified clonal unit. Cell bodies lie on lateral position to WED, and mean cell number is 42. VPNv3 has 1 projection subgroups. VPNv3A projects from LO to PVLP (VGj), EPA and AVLP. Presynaptic signals are distributed in the entire arborization areas.

WEDa1

WEDa1 is a newly identified clonal unit. Cell bodies lie on lateral position to AMMC, and mean cell number is 67. WEDa1 has 1 projection subgroups. WEDa1A innervates AMMC, SAD, WED, SEG and IPS. Presynaptic signals are distributed in the entire arborization areas.

WEDa2

WEDa2 is a newly identified clonal unit. Cell bodies lie on lateral position to AMMC, and mean cell number is 75. WEDa2 has 2 projection subgroups. WEDa2A innervates WED, PLP, SLP, SIP and SMP. WEDa2B innervates LAL, CRE, SIP and SMP. Presynaptic signals are distributed in the entire arborization areas.

WEDd1

WEDd1 is a newly identified clonal unit. Cell bodies lie on anterior position to AOTU, and mean cell number is 62. WEDd1 has 1 projection subgroups. WEDd1A projects from VES and WED to thoracic ganglion via cervical connective. Presynaptic distribution is unknown.

WEDd2

WEDd2 is a newly identified clonal unit. Cell bodies lie on superior position to AL, and mean cell number is 24. WEDd2 has 1 projection subgroups. WEDd2A projects from WED and PLP to contralateral side of WED, PLP, VES, CAN and SAD. Presynaptic signals are distributed in the entire arborization areas.

Clonally composed architecture in the brain

Identified clones showed strong correlation with the functional architecture of the brain (Fig. 2). I first found clear association between clonal units and sensory pathways. As reported previously (Ito et al., 1997, Lai et al., 2008), the clones associated with the AL and MB – the primary and major secondary olfactory centers – are formed by specific clones (Fig. 2A, B). Higher olfactory pathways are also formed by distinct clones. The associative lobe regions of the MB are innervated by specific clones that contain MB-extrinsic neurons (Tanaka et al., 2008) (Fig. 2C, D), and the other major secondary olfactory center – the lateral horn (LH) – is contributed by clones that either arborize locally (Fig. 2E) or send projections to other neuropils (Fig. 2F).

The visual pathways are also formed by distinct clonal units. Each pathway of the visual projection neurons (VPNs) (Otsuna and Ito, 2006), from the primary visual center in the optic lobe to the secondary visual centers in the cerebrum, is formed by distinct clones (Fig. 2G, H). One of the secondary visual centers, the PVLP (see Supplemental Table S2A for abbreviations of neuropils), is also contributed by distinct clones that either arborize locally (Fig. 2I) or project to other neuropils (Fig. 2J). Another secondary visual center, the AOTU, is contributed by specific VPN clones (Fig. 2H) and clones that project to distinct neuropils in the cerebrum (Fig. 2K), forming a clonally organized visual pathway from the optic lobe via the AOTU to higher visual centers. I also found several clones that arborize in the auditory (Fig. 2L) and gustatory (Fig. 2M) primary centers (Kamikouchi et al., 2006, Miyazaki and Ito, 2010). The motor pathway is also associated with clones; the descending neurons I identified derive from three distinct clones (Fig. 2N).

In addition to these clones, I found 38 clones that arborize preferentially in other neuropils than the known sensory or motor centers. For example, the SLP and SMP are contributed by clones that arborize locally (Fig. 2O, Q) or in multiple neuropils connected via projections (Fig. 2P, R). Such clones are also observed in the more ventral parts of the cerebrum (Fig. 2S, T). The eight PAN clones also belong to this category (Fig. 2U-X), sending projections to many brain regions including the CX.

The CX is composed by three major types of clones. Four clones in the posterior brain provide so-called small-field neurons (Hanesch et al., 1989) (Fig. 3A), whereas six

clones in the anterior and posterior brain give rise to large-field neurons of the fan-shaped body (FB, Fig. 3B). In addition, large-field neurons of the ellipsoid body (EB) are formed by two clones in the anterior and posterior brain (Fig. 3C).

Fine structures of the CX are also organized clonally. The small-field neurons of the four clones arborize in largely segregated areas of the FB but converge to form overlapping output sites in the anterior brain called rubus and gall (Ito et al., submitted) (Fig. 3D). Tangential arborizations of large-field neurons are known to have layered organization, each of which may have different functions (Liu et al., 2006). I found that these layers are clonally organized, with each clone contributing to specific layers (Fig. 3E). The ring structure of the EB also has anterior and posterior segregation formed preferentially by the anterior and posterior clones, respectively (Fig. 3F).

Because of the relatively homogeneous appearance when visualized with classic labeling methods, brain regions other than the AL, MB, and CX are often collectively referred to as “diffuse neuropils”, whose structure and functions have hardly been investigated so far. The identified clonal units feature clearly organized projections also in these neuropils.

The clonal VPNs arising from the optic lobe form bulbous masses of terminals called the optic glomeruli (Otsuna and Ito, 2006, Mu et al., 2012) Optic glomeruli are therefore clonally constructed structures (Fig. 3G). The VLP (combination of AVLP and PVLP) and PLP, which houses these optic glomeruli, appear similar when examined with conventional silver stain or synaptic labeling with nc82 antibodies. However, they are very different when I compare the architecture of the cerebral clones other than the VPN-clones in these regions. These clones tend to have broad and overlapping projections in the VLP (Fig. 3H), but arborize in small discrete domains in the PLP (Fig. 3I). In addition, the VLP has many clones that arborize locally in the neuropil, whereas the PLP is devoid of such local clones (Fig. 4I).

Clonal units tend to form broad and overlapping arborizations in the dorsal brain region around the MB and CX, such as the SLP, SMP, SCL and ICL. Clone-dependent organization also exists in these neuropils. In the SLP, when arborizations of the clonal units that also innervate the neighboring VLP, LH, and SMP are overlaid separately, they have preferential arborizations in its anterior, middle, and posterior subregions, respectively

(Fig. 3J-L). Likewise, clones associated with the AOTU and CRE arborize in the anterior SMP, whereas those associated with the SCL and ICL arborize in its posterior part (Fig. 3M-O). In the SCL and ICL, clones associated with the VLP, SLP, and PLP arborize in their anterior, middle, and posterior volumes, respectively (Fig. 3P-R). Thus, subregions of these diffuse neuropils have preferential connections with specific other neuropils.

Structural feature of the clonal units

From these data I was able to deduce several common characteristics of the clonal units. First, cell bodies of all the clones form one or a few tightly packed clusters in the cell body rind (also called the cortex). The number of cells per clone is rather varied (Fig. 4C), suggesting dynamic regulation of mitosis and apoptosis during development.

Second, all the neural fibers arising from a cell body cluster form one or a few tight bundles (Fig. 4D). Different bundles tend to project differently, and neurons projecting via the same initial bundle may further segregate to innervate different neuropils. Considering these, at least 60% of clones contain heterogeneous population of neurons in terms of their arborization patterns.

Thirdly, a clonal unit arborizes within distinct parts of the brain (Fig. 4E). The complexity of innervation pattern varies considerably. About 40% of the clones arborize in up to five neuropils, whereas about 10% arborize in more than 15, some in as many as 36 neuropils. Not only clones deriving from type-II neuroblasts (e.g., Fig. 2U, X) but also several clones made by type-I neuroblasts form complex projections (e.g., Fig. 2J, R, T). I found no clear correlation between the complexity of arborizations and the number of cells in the clone. Left/right asymmetry was not observed at the current resolution of clonal comparison.

Lastly, about 80% of clones (Fig. 4F) feature multiple arborization sites that are connected with the axons of projection neurons (e.g. Fig. 2A, C, F, J, P, R, T). Other clones form single arborizations of local neurons that are either limited within a single neuropil or extend across a few neighboring neuropils (e.g. Fig. 2E, I, O). Interestingly, these locally-arborizing clones were found preferentially in the anterior ventrolateral and posterior dorsal parts of the cerebrum (Fig. 4I).

Number of clones contributing to distinct neuropils

Because of the spatial overlap between clones, each neuropil is contributed to by multiple clonal units. Whereas some neuropils receive contributions from less than 10 clones, a few neuropils are contributed by abundant clones, some as many as 61 (Fig. 4G, Supplemental Table S2B). The number of clones contributing to a particular neuropil may not directly indicate actual overlap, however, because some clones may arborize in its non-overlapping subregions. For a more precise analysis, I divided the brain into small cuboids (voxels) and calculated the number of clones that arborize within each (Fig. 4R-V; size of the voxel= 1.2 × 1.2 × 1.5 μm). Neuropils of the AL, MB and CX appear dark in the color-coded section images, showing that voxels in these regions are contributed by significantly fewer clones – utmost 8 clones per voxel – than those in the surrounding diffuse neuropils like the SLP, SMP, PVLP and SCL.

Correlation between clonal units and neural fiber bundles

Different parts of the brain are connected by many fiber bundles. I therefore analyzed how they are correlated with clonal composition. I identified in total 150 fiber bundles (Fig. 4B, Supplemental Table S2A, C), among which 128 connect ipsilateral parts of the brain (called fascicles, Fig. 4J, K) and 22 connect bilateral neuropils (called commissures, Fig. 4L, M). All the bundles are formed either by single or unique sets of a few clones (Fig. 4N, O), indicating that the composition of fiber bundles is tightly associated with clonal units. Commissures tend to consist of more clones than fascicles: 38% of fascicles and 77% of commissures are contributed by multiple clones of the same side and, because I found no apparent left-right asymmetry concerning clonal structures, each commissure is likely to be contributed by the same number of clones of both sides.

During development, clonally related neurons send fiber bundles into neuropils. For the bundles contributed by multiple clones, fibers arising from different clones may converge right after they emerge out of the cell body clusters (Fig. 4J, L), or they may run a certain distance through the neuropils before they merge (Fig. 4K, M). Both cases occur at about the same rate for the 49 fascicles with multiple clones, (Fig. 4P). For the 17 multi-clone commissures, on the contrary, bundles of 76% of clones converge only when they have extended deep in the neuropil.

Neural fibers have a structural polarity from the cell body to the distal ends of neurites. When fibers from different clones converge during development, they may project either in the same (Fig. 4J, L) or in opposite directions (Fig. 4K, M). 84% of fascicles and 88% of commissures within the hemisphere contain parallel fibers running in the same direction (Fig. 4Q). Thus, developmentally it is much more common that fibers deriving from different clones form parallel rather than opposite-running bundles.

Neural fibers also have functional polarity in terms of the direction of signal propagation. I found 46 clones in which at least some of their projections show clear asymmetric distribution of presynaptic sites (Supplemental Fig. S3A-C). It is often believed that the arborizations proximal to the cell bodies are dendritic. However, 23 out of the 46 clones contain projections with presynaptic sites only in their proximal arborizations (Fig. 4H), indicating clear directional flow from further ends of these neurites.

Spatial overlap between clonal units and segmental origin of the brain

In order to communicate with neurons of other clones, arborizations of different clones must overlap (Ito and Awasaki, 2008). Although spatial overlap does not directly indicate the presence of synaptic connections, clones whose arborizations overlap extensively should have a tighter functional relationship than those that hardly do. Cluster analysis based on the "distance" between all the combinations of clones by calculating the degree of overlap between them revealed that the clones could be classified into four groups (Fig. 5A). Three clone groups arborize primarily in the dorsal-lateral, dorsal-medial, and ventral regions of the cerebrum, respectively, and the fourth group consists of the visual projection neurons that share large arborizations in the optic lobe (Fig. 5B-E).

Developmentally and evolutionarily, the insect cerebrum consists of three neuromeres: the proto-, deuto- and tritocerebra (Strausfeld, 2012). During neurogenesis neural fibers deriving from each neuromere merge extensively making, in the adult, the identification of neuromere boundary extremely difficult. I expected that the boundaries might be resolved by analyzing the spatial overlap of clones that belong to each neuromere. Contrary to my expectation, putative deuto- and tritocerebral clones, whose cell bodies lie at the level ventral (developmentally more posterior) to the AL, did not form distinct overlap cluster but were split into three above-mentioned major clusters together

with protocerebral clones (Fig. 5B-D). Cluster analysis specifically of these putative deuto- and tritocerebral clones did not reveal neuromere organizations, either (Fig. 4F, Supplemental Fig. S4). These suggest that much of the adult brain composition may be unrelated to its segmental origin.

Biochemical heterogeneity within clonal units

Complex computation by neural networks involves nerve cells with diverse physiological functions, such as excitatory and inhibitory neurons and modulatory monoaminergic neurons. Is such biochemical diversity also correlated with clonal units? GABAergic and monoaminergic neurons in the mammalian brain are mostly formed in distinct subregions and therefore belong to specific cell lineages (MaKay, 1997, Brown et al., 2011, Bonilla, et al., 2008). Similarly, GABAergic projection neurons and glutamatergic local neurons in the insect AL are formed by specialized clones (Okada et al., 2009, Das et al., 2011). I therefore asked whether the formation of neurons with particular transmitters would closely be correlated with clonal units.

I co-registered the brain labeled with anti-GABA antibody with those of the clones. Considering that locations of clonal cell bodies may fluctuate slightly between individuals, I identified clones that are likely to contain GABAergic neurons only when the labeled cell locations were within the possible fluctuation level, and found at least 45 such clones (Table 1A). Characteristic cell positions and projection patterns labeled with the anti-5-hydroxytryptamine (5HT), tyrosine hydroxylase (TH), and tyrosine decarboxylase 2 (TDC2) antibodies enabled us to identify seven, eight and eight clones that produce serotonin, dopamine, and octopamine, respectively (Table 1A).

In most cases the number of the GABAergic or monoaminergic cells was smaller than the average cell number of the clones that occupy that location, and the projections of monoaminergic cells cover only subsets of the entire projections of the associated clones. Registration of GABAergic or monoaminergic neurons with clonal cell clusters suggests that they may coexist in a single clone (Supplemental Fig. S5). These indicate that neurons with multiple types of transmitters are generated in many if not all the clones.

In the vertebrate brain, monoaminergic neurons form extensive projections whereas GABAergic neurons are mostly local interneurons. Consistent with this, all but one clones

featuring monoaminergic neurons have extensive projections (Table 1B). In contrast, only half of the locally-arborizing clones contain GABAergic cells.

Community analysis of neural projections

The comprehensive collection of clones serves as a useful tool for providing a systematic view on the entire neural projections in the brain, the projectome (Kasthuri and Lichtman, 2007). As discussed earlier, a clonal unit may contain several neuronal subgroups with different projection patterns. By tracing the fiber bundles arising from the cell body clusters, I identified in total 247 such projection subgroups. Although single neurons in each subgroup may further show variability in their fine projection patterns, analysis of these subgroups should provide an acceptable overview of the existing neural network.

Using these data, I first made a connection map of the cerebrum (Fig. 6A). The map evaluates the clonal variety of connections rather than the actual number of neurons connecting them. Neuropils like the SMP, SLP, SCL and ICL have a large number of connections with others, serving as the hubs, whereas those of the AL, MB and CX have much fewer connections. This is consistent with the differences in the number of clones that arborize in them (Fig. 4R-V). The number of bilateral connections was highly variable between neuropils (Fig. 6B), with abundant connections in, e.g., SMP, SIP, SLP, SCL, ICL, SPS, and AVLP, but none in, e.g., MB calyx and LH.

The network is characterized by a small average distance between pairs of neuropils and abundance of mutually connected triplets of neuropils. This indicates that the network has so called small-world property, meaning that most nodes in the network can be reached from all other nodes by a small number of connections (Watts and Strogatz, 1998, Bullmore and Sporns, 2009). The node degree (*k,* number of neuropils connected to a given neuropil, Supplemental Fig. S6A) and node strength (*s,* number of projection subgroups that mediate these connections, shown by the reddish hue in Fig. 6A) are both bimodally distributed. *s* superlineally depends on *k* (Fig. 6C), indicating that a neuropil connected to many other neuropils (i.e. large *k*) tends to be connected to each of them by a large clonal variety of connections (i.e. large *s/k*). Although the dependence of *s* on *k* has not been systematically investigated for brain networks, such superlinear dependence is commonly observed in various types of networks (Barrat et al., 2004).

To further reveal global organization of the connection map, I carried out a community analysis, i.e., partitioning the network into densely connected communities. Because synaptic contacts between neurons of different clones cannot be assumed safely at the current state, I examined only direct connections between neuropils via each projection subgroup, without assuming any interneuronal contacts. Considering the abundance of neurons that also contribute to the network of contralateral neuropils, I took into account the 494 projection subgroups of both brain sides.

Blondel's algorithm for community detection (Blondel et al., 2008) identified five communities (white boxes 1-5 in Fig. 6D). The Q value ($0 \leq Q \leq 1$, a factor to quantify the quality of the obtained partitioning) was 0.301, suggesting mild community structure of the network. Communities 1-3 contain neuropils of the ventral, dorsal-lateral, and dorsal-medial cerebrum, respectively, and communities 4 and 5 correspond to the right and left MBs (Fig. 6H-L). Though communities 1-3 contain corresponding neuropils of both brain sides, the pair of MBs is separated into distinct communities (4 and 5) because of the few commissural connections between them.

To assess the extent of inter- and intracommunity communication for each neuropil, I calculated the node strength originating from the neuropils of different communities and those within the same community (extrinsic and intrinsic node strengths, s_{ex} and s_{in}). Although s_{ex} and s_{in} are highly correlated for communities 1 and 2 ($R^2 > 0.70$; Supplemental Fig. S6G-L), community 3 has two subpopulations with high and low s_{ex}/s_{in} ratios. Interestingly, the latter subpopulation of community 3 exactly matches with the neuropils of the CX (yellow box in Fig. 6D), suggesting their limited intercommunity communication. Communities 4 and 5 (right and left MBs) also possess low s_{ex}/s_{in} ratios. Indeed, the links incident to the CX neuropils are mostly confined within community 3, and the MBs have only a limited amount of intercommunity links (Fig. 6D). Thus, in spite of their importance in higher order brain functions, the CX and MB are relatively isolated structures in the fly brain, communicating with only specific neuropils.

Discussion

Clonal organization of heterogeneous neural populations

Considering the vast number of identified clones with specific cell body locations and projection patterns, most clonal units in the fly cerebrum should be unique. Indistinguishable clonal units might be generated redundantly by more than one neuroblast. Because of the wide variance in clone induction frequency among neuroblasts, I was not able to assess the existence of redundancy. However, even the four near identical MB clones (Ito et al., 1997) are actually unique in that each clone arborizes in characteristic subregions of the calyx (Ito and Awasaki, 2008) and that early embryonic neurons show lineage-specific projections (Kunz et al., 2012), supporting the uniqueness of most clones. Alternatively, a single neuroblast might take variable fates to generate different clonal units among individuals. If this would occur, there should be a group of clonal units with cell bodies in the identical locations but arborizations in different brain parts, which I did not find. Neuroblasts in the embryonic brain are uniquely identifiable by the combination of genes they express (Urbach and Technau 2003), suggesting that the clonal identify should directly be correlated with the neuroblast identity.

As discussed previously (Ito and Awasaki, 2008), neuronal variety in a clone can be determined by two factors: birth order of neurons and fate determination between sibling neurons. Different types of neurons are generated sequentially in a time-dependent manner, as has been reported for the AL and MB (Lai et al., 2008, Lee et al., 1999). Neuroblasts change their gene expression patterns drastically during neurogenesis (Isshiki et al., 2001), some of which control the generation of specific cell types (Doe, 2006). The GMCs generated by the neuroblasts divide once more to give rise to sibling neurons with high and low Notch activities, forming two lines of hemilineages (Truman et al., 2010). Chromatin modification observed in the Notch-mediated fate determination of peripheral olfactory sensory neurons (Endo et al., 2012) might also work in the hemilineages of clonal units.

Number of the identified clones

In this study I identified 96 clonal units in the cerebrum. Extensive cross comparison

between my study and the companion study (Yu et al., in press) revealed that 77 clones were identified commonly, whereas 19 clones in my study and 18 clones in theirs are not covered in the counterparts. There was a wide variance in clone induction frequency among neuroblasts, and particular lineages tend to be labeled preferentially by certain genotypes of FRT recombination target sites, flippase, and expression drivers. For example, most of the PAN lineage clonal units I found were labeled with the genotypes featuring FRT^{G13} target and elav-GAL4 promoter. Because my study and the companion study used different genotypes for clone induction, recombination in certain neuroblasts may not have occurred at high enough frequency to be detected in the respective screening.

When combined, the two studies identified in total 114 clonal units in the cerebrum. However, only 106 neuroblasts were observed in the embryonic cerebrum (Urbach and Technau, 2003). A possible explanation for this discrepancy would be that the neuroblasts that give rise to 13 VPN clones, lying in the lateralmost part of the larval cerebrum, may have been excluded in the embryonic neuroblast count, even though their proliferation patterns are rather different from that of the optic lobe neuroblasts (Hofbauer, and Campos-Ortega, 1990). Another possibility might be that some of the embryonic neuroblasts might give rise to more than one neuroblast lineages in larvae, though such division of neuroblasts has not yet been reported.

In my study I found two potential clones, named SLPpm4* and SMPad4* with asterisks to indicate that they are identified based on the observations of reproducibly labeled two-cell GMC clones. Their projection patterns do not match with any other clonal units. Because the purpose of my study is to identify as many distinct clonally related neural projection patterns as possible, I included them in my projection analysis. However, they might belong to some other identified lineages, reducing further the discrepancy between the number of the total clonal units and the number of the reported embryonic neuroblasts. Neurons made by the late embryonic or first-born postembryonic GMCs may have different projection patterns than those in other neurons of the secondary lineages (Yu et al., in press). Clonal units DM1 and SMPad2 have their cell body clusters close to the cell bodies of these two potential clones, respectively, suggesting possible associations that are yet to be resolved.

Because of the difficulty to induce heat shock in early embryos, neurons of the primary lineages made during embryogenesis were not visualized in both studies. As mentioned above, neurons of the primary lineage, made during embryogenesis, may have different projection patterns than those of the secondary lineages. In addition, the first few neurons of the primary lineages may also form different projections than other embryonic neurons generated later, as has been reported in the ventral nerve cord (Schmit et al., 1997, Bossing et al., 1996) and the four MB neuroblasts (Kunz et al., 2012). Considering that these specific projections may persist throughout development, some of the neuronal projection patterns in the adult brain might be left undetected in my studies.

Estimation of cell counts

The total estimated number of the cells visualized in my catalogue of clones was 9,394. The companion study (Yu et al., in press) identified 10,083 cells on an average. The discrepancy is due to different cell counts of the PAN clones. The total cell counts of the commonly-identified clones except for the PAN clones were nearly identical – 7,085 and 6,988, respectively – whereas the cell counts of the eight PAN clones was 1,466 in my study but 2,177 in the companion study. This is primarily because most of the PAN clones I identified were visualized only with elav-GAL4 driver, which tend to label fewer numbers of cells than the actin-GAL4 driver. The average total cell counts of the clones identified uniquely in respective studies were 843 in my study and 917 in the companion study. If I take the larger cell counts of PAN clones in the companion study and add up the cell counts of unique clones, the total cell count of the clonal units identified by both studies is estimated to be about 11,000.

The total number of embryonic neurons in the cerebrum is not yet known. The number of MB neurons in the first-instar larval brain is estimated to be 250 (Hinke, 1961); about 62 per one of the four MB neuroblasts. If I assume that (1) the other continuously-proliferating neuroblast of the ALl1 lineage would generate the same number of neurons, and (2) the remaining 101 neuroblasts in the embryonic cerebrum would proliferate at the same rate but only for half the period during early to mid embryonic stages, producing about 30 neurons per each, the total count of embryonic neurons in the cerebrum is estimated to be about 3,300. This would be an over estimation, because most

neuroblasts other than the MB lineages produce much fewer cells during postembryonic periods, suggesting their slower proliferation rate (Ito and Hotta, 1992).

Three reasons are conceivable to fill the remaining discrepancy between the above-estimated cell counts of embryonic and postembryonic neurons and the estimated 15,000 neurons in the adult cerebrum. First, the latter cell counts, based on the automated detection of nuclear labeling (Shimada, Kato et al., in preparation), could be over estimation. Second, there would be several clonal units that are yet to be identified. And third, GAL4 drivers used for expressing reporter genes may not be active in all the neurons of the clone, as has been shown for the elav drivers in PAN lineages. Also in other clonal units, some of the arborizations observed in my clone samples were not visualized in the corresponding clones of the companion study and vice versa, possibly because of the different expression drivers used in the respective studies.

Cell migration and clonal units with multiple cell body clusters

In this study I identified 96 clonal units including two potential ones. Although most clonal units arise from a single cluster of cell bodies, there were 14 clonal units with two or three detached clusters (Fig. 2J, R, X). Neurons of discrete clusters tend to project differently. Although type-II neuroblasts form multiple intermediate neural precursors, 11 out of the 14 multi-cluster clones derive from type-I neuroblasts. It is therefore likely that the subpopulation of neuronal progeny would migrate during development as a group. It is not yet known whether they migrate actively or are pushed away passively from original locations during pupal development, when thick cell body rind of the larval brain is thinned as the underlying neuropil volume increases. I found several other clones in which the single cell body cluster has fused but distinguishable masses of cell bodies with distinct fiber bundles (Supplemental Fig. S3D-I). Such clones may represent an intermediate organization between clonal units with single and multiple cell body clusters.

Analysis of small-world property

The small-world property posits that most real networks have small average path length L and large clustering coefficient C (Newman, 2010, Watts and Strogatz, 1998). L is defined as the number of hops needed to travel from a node (i.e., neuropil) to another, averaged

over all the node pairs. C represents the density of triangles in the network and is given by

$$C = \frac{1}{N}\sum_{i=1}^{N} \frac{\text{number of triangles containing node } i}{\frac{k_i(k_i-1)}{2}}$$

where N is the number of nodes, and k_i is the degree of node i. I discarded the link weight to binarize the network, as is usually done for investigating the small-world property of brain networks (Bullmore and Sporns, 2009), and obtained L=1.788 and C=0.706.

Next, for comparison, I generated randomized networks on the same set of nodes. I randomly placed the same number of links as that of the original network such that the degree of each node is equal to that of the original network. Usually, such a randomized network has small L, as is comparable with real networks and a C value much smaller than for real networks (Newman, 2010). The mean and the standard deviation of the two quantities on the basis of 100 randomly generated networks are equal to L=1.685 ± 0.003 and C=0.632 ± 0.007. Even though L for the original network is significantly larger than that for the randomized networks, I judge that L of the original network is sufficiently small (Newman, 2010, Watts and Strogatz, 1998); node pairs are connected within two hops on an average. C of the original network is significantly larger than that of the randomized networks. It should be noted that C of the randomized networks is large because the networks are denser (i.e., relatively more links) than many other networks investigated so far (Newman, 2010).

Structural properties of the *Drosophila* brain network

The network of the *Drosophila* brain obtained in this study has the small-world property, heterogeneous distributions of the node degree (k) and node strength (s), and community structure. These are consistent with the properties of structural and functional brain networks of mammals including humans (Bullmore and Sporns, 2009) as well as those of the *C. elegans* neural network (Watts and Strogatz, 1998, Sohn et al., 2011, Pan et al., 2010).

The detected communities show interesting functional correlation with sensory pathways. The three major secondary visual centers (PVLP, PLP, and AOTU) are separated in communities 1, 2, and 3, respectively, because they are connected with other neuropils with rather different preferences. The neuropils having extensive connections

with the primary auditory center (AMMC) are all categorized in community 1. In the olfactory system, the AL/LH, MB, and the so called MB-associated neuropils (SMP, SIP and CRE) which feature extensive connections with the MB lobes (Tanaka et al., 2008), are categorized into different communities (2, 4/5, and 3, respectively), because of the limited variety of connections of the MB and differently preferential connections of the AL/LH and MB-associated neuropils with other neuropils. These suggest that the visual information sent to the three secondary centers would be processed in different manners, among which that sent to community 1 is most likely to be integrated with the auditory information and those sent to communities 2 and 3 would be integrated with different types of olfactory information.

These results were not consistent with the cluster analysis based on randomly labeled single neurons (Chiang et al. 2011), which categorized all the visual centers and olfactory centers respectively into single groups. This is because my analysis is more sensitive to the different varieties of connections between neuropils than the amount of parallel fibers connecting the primary and secondary sensory centers of each modality.

Connections between neuropils can be categorized into three types. First, 67% of connections are mediated by the projection neurons with no apparent asymmetric distribution of presynaptic sites (Fig. 6E). These may mediate bidirectional or unidirectional communication depending on the asymmetric distribution of postsynaptic sites, which I did not analyze because of technical complexity. Second, 26% of connections showed presynaptic sites only at one end, which should play important roles in the directed information flow (Fig. 6F). And third, the remaining 7% of connections are mediated by local arborizations spanning neighboring neuropils (Fig. 6G). They contribute only to specific connections, notably between communities 1 and 2 as well as 2 and 3, but hardly between 1 and 3.

Comparison between node degree and node strength

As explained in the main text, the node degree k (number of neuropils connected with a given neuropil) obeys a bimodal distribution (Supplemental Fig. S6A). For each neuropil k is the sum of the number of intrinsic (i.e., intracommunity) links and that of extrinsic (i.e., intercommunity) links, denoted by k_{in} and k_{ex}, respectively. Distributions of Both k_{in} and k_{ex}

(Supplemental Fig. S6B, C) feature two peaks, one at small k_{in} or k_{ex} values (up to 5) and the other at large values (about 15-25). These suggest that the neuropils have two subpopulations, with abundant and scarce connections with others.

The intrinsic and extrinsic node strengths (s_{in} and s_{ex}) are linearly correlated with the total node strength (s, Supplemental Fig. S6D, E), suggesting that neuropils tend to be connected with the same community and different communities with a similar proportion. For each neuropil s_{in} tends to be larger than s_{ex}, which is consistent with the concept of community detection; a community is by definition a collection of nodes with dense links within the community and sparse links connecting different communities. When s_{in} and s_{ex} are separately compared for each community (Supplemental Fig. S6G-L), the two quantities are more strongly correlated (i.e., larger coefficient of correlation R^2) than when the entire brain network is considered (Supplemental Fig. S6F). (Note that R^2 is small for Fig. S6J-L at least partly because of the small numbers of neuropils.) The fact that all the neuropils of communities 1 and 2 and the non-CX neuropils in community 3 show similar s_{ex}/s_{in} ratio suggests that these neuropils participate in inter- and intracommunity communication at similar rates regardless of the number of connections they have.

The average number of associated projection subgroups of a node is represented by node strength over node degree (s/k). I examined mean s/k of inter and intra communities (Supplemental Fig. S6M-O). Intrinsic mean s/k of each community is higher than extrinsic mean s/k. It is natural because a community on the network should have dense connections for inside and sparse connection for outside. Respectively, intrinsic mean s/k in community 4, 5 and CX part of community 3 are much higher than extrinsic mean s/k. This suggests that central complex and mushroom body have much connection density inside the community but less connection density with the other communities. This suggestion matches the limited intercommunity links of central complex and mushroom body in Fig.6D.

Comparison between node strength and betweenness centrality

Betweenness centrality (*BC*) quantifies the role of a neuropil in intercommunity connections (Bullmore and Sporns, 2009, Freeman, 1979). Because k and s are strongly correlated, neuropils with large s can be regarded as hubs (i.e., neuropils with large k). In the human

brain, hubs tend to have large *s* and large *BC* (Hagmann et al., 2008). In the *Drosophila* brain network, *BC* of the hub neuropils varied depending on whether or not the neuropil is directly connected with the relatively isolated neuropils such as the MB and CX. Neuropils such as SLP, SMP, SIP, PLP and LAL have both large *s* and large *BC* (Supplemental Table S4). These neuropils are connected extensively with other neuropils including MB and CX (Fig. 6D). Neuropils like SCL, ICL, ATL and GOR have large *s* but relatively small *BC*. Though these neuropils are also extensively connected with others, they have few if any connections with the MB and CX. The VL and ML have large *BC* compared to relatively small *s* values; they are the only neuropils within the MB with extensive connections with communities 1-3. As discussed in the main text, MB and CX are relatively isolated from other neuropils in communities 1-3. The *BC* value of a neuropil tends to be large when the neuropil is directly connected with MB or CX.

Comparison with a previous work

Chiang et al. constructed an anatomical brain network of *Drosophila* based on a group of single neurons they identified (Chiang et al., 2011), and revealed four densely connected clusters. However, conventional hierarchical clustering is not an effective method for identifying clusters in networks (Fortunato, 2010). I therefore relied on the Blondel's algorithm for graph clustering, which is an acknowledged method for this purpose.

When I translate the different definitions of neuropils used in the study (The Insect Brain Name Working Group, submitted), both analyses are consistent in that the CX and the surrounding neuropils (e.g. LAL, CRE, SMP) fall into the same group, so do the auditory centers of AMMC and WED. On the other hand, their study put the olfactory-associated AL, LH and MB into a single group, whereas my analysis isolated the MB reflecting the fact that the AL and LH have much larger variety of connections between each other and with other brain regions than with the MB (Tanaka et al., 2008, Tanaka et al., 2012). In addition, their study put the two secondary visual centers (OG and AOTU) into a single group, whereas I put three visual centers into three different communities. This is because my analysis is more sensitive to the different varieties of connections within the cerebrum than the amount of parallel fibers connecting with the optic lobe, and because they did not distinguish PVLP and PLP despite their structural differences (Fig. 3H, I).

Chiang et al. also showed that the node degree obeys a long tailed distribution. Roughly consistent with this, the node degree in the current network is widely distributed (Fig. S6A). As discussed above, I further decomposed the node degree into intracommunity and intercommunity node degrees and also considered the node strength to examine their characteristic properties (Fig. S6B-L).

Functional significance of clonal units

Because the *Drosophila* brain is an assembly of clonal units, there seem to be some advantages in clone-dependent organization of the brain. If each neuron independently projects its neurite to various parts of the brain, a large variety of guidance signals would be required. On the other hand, if a group of neurons form neural fiber bundles and project to the same areas of the brain, the guidance signal is required only for the pioneer neuron and the follower neurons are simply trace the same trajectory. Most of the clonal units have only a few projection subgroups which make fiber bundles and innervate the same area. Clone-dependent neural path finding is an efficient way for organizing the systematic neural projections in the brain.

Organizing the brain structure by the clone-dependent composition may be an efficient way for developing new functional neural circuits during evolution. Just like duplication of genes on the genome sometimes happened, duplication of clonal units might occur during evolution. Because the mushroom body in the *Drosophila* is composed by homogenous four clonal units, duplication of clonal units might occur during evolution. There is another possibility to obtain new functional neural circuits. Just like a mutation of gene changes a translated amino acid and therefore obtain new function or loss of function, a change of guidance cue of the pioneer neuron may lead to a drastic change of the innervation target of the clonal unit. Duplication and change of the innervation target of a clonal unit may be an efficient way to obtain new functional neural circuits during evolution.

Clonal units across species

Central body (fan-shaped body and ellipsoid body) is evolutionally conserved structure among Arthropoda (Strausfeld, 2009). In the palaeoptera and neoptera, central body is a symmetric layered module which is connected with protocerebral bridge and noduli.

Malacostracan and entomostracan crustaceans also have a central body, though this is much less prominent than in the palaeoptera and neoptera. Most malacostracans have no obvious layered module in the central body, although these structures connected to bridge-like neuropils. Layered modules of the central body are derived from a set of clonal units in the *Drosophila* brain. (Fig. 3B, E). Studies in locusts also revealed similar clonally-organized structures in the central body (Boyan and Williams, 2011) suggesting that the clonal units should be evolutionarily conserved organization across insecta. The number of stem cells is rather similar between diverse species like locusts and flies (Broadus and Doe, 1995), suggesting the existence of similar variety of clonal units. Identification of clonal units in other insects, especially in their diffuse neuropils, should provide an organized view about the consensus structure of the insect brain.

Mammalian excitatory and inhibitory neurons are mostly made by different stem cells (Brown et al., 2011) except for a few reported exceptions (Letinic et al., 2002), whereas many *Drosophila* stem cells produce neurons with different transmitters. Recent clonal studies in the mammalian cortex show, however, important similarities between mammals and insects. Specific visual characteristics are processed by the clonally associated neurons in the mammalian visual cortex (Othsuki et al., 2012, Li et al., 2012) and clonally organized layers in the fly FB (Mu et al., 2012). Neuronal and glial lineages are mixed in the mammalian brain (Alvarez-Buylla et al., 2011), and at least some *Drosophila* lineages produce both neurons and glia (Yu et al., in press, Bossing et al., 1996). As in the fly brain, a clone in the mammalian cortex contains a variety of neural types that are generated sequentially during neurogenesis (Molyneaux et al., 2007). Although many insect neurons do not migrate whereas mammalian neurons migrate extensively, the former form dendritic arborization not in their cell bodies but in distant parts of their neurites. Thus, both in mammals and insects dendrites of clonally associated neurons may often be detached from their birthplace.

Evolutionary clades leading to mammals and insects diverged more than 550 million years ago, and the mammalian neocortex is a recent structure that is absent in other vertebrates. Analysis of clonal organization in more conventional regions of the mammalian brain may reveal further similarities across species.

Conclusions

Through extensive clonal identification and comparison I show here that the basic concept of the clonal units – that the progeny of a single neuroblast form distinct structural subtypes of neurons that contribute to specific parts of the insect brain (Ito et al., 1997, Ito and Awasaki, 2008) – is broadly applicable to all the neuroblast lineages. Many clones are heterogeneous both in terms of projection patterns and biochemical transmitter properties. Gene expression patterns are also heterogeneous, as has been shown in the clusters of *fruitless*-expressing cells scattered in numerous clones (Cachero et al., 2010). Neuropils are composed synergistically by multiple clones. The degree of clonal overlap varies greatly depending on neuropils. The entire brain neural network consists of several neuropil communities connected with varying degree of clonal projections. Fiber bundles are also organized clonally. Asymmetric distributions of presynaptic sites showed that clonal units propagate information not only from proximal to distal but also in the opposite direction in various cases. Analysis of clonal units thus provides an overarching view of the organized architecture of brain neuropils as well as crucial aspects of what cell arrangements characterize a neural network.

Identification of most of the clonally associated units in the *Drosophila* brain revealed organized architecture both in the well-known and hardly-investigated neuropils. Because of the relatively small number of units to be analyzed and their importance in developmental and evolutionary aspects, understanding the brain from the clonal point of view should be an efficient way to reveal its neural network architecture.

Acknowledgements

I am deeply grateful to K. Ito for supervision. I am grateful to N. Masuda for collaboration of network analysis, K. Endo and K. Shinomiya for technical advices. I thank N. Strausfeld, K. Hanashima for discussion; T. Awasaki and T. Lee for communicating results prior to publication; B. Dickson, M. Ramaswami, and the Bloomington Stock Center for fly strains; I thank all my lab members, especially J. Tanimura for sharing antibody labeling data, and S. Shuto, K. Yamashita, and H. Hirose for technical assistance. This work was supported by a CREST/JST grant to K.I. and Grant-in-Aid for Scientific Research from the Ministry of Education, Culture, Sports, Science and Technology of Japan to K.I. and N. M.

Reference

Alvarez-Buylla, A., Garcia-Verdugo, J.M., and Tramontin, A.D. (2001). A unified hypothesis on the lineage of neural stem cells. Nat Rev Neurosci 2, 287-293.

Barrat, A., Barthélemy, M., Pastor-Satorras, R., and Vespignani, A. (2004). The architecture of complex weighted networks. Proc Natl Acad Sci U S A 101, 3747-3752.

Bello, B.C., Izergina, N., Caussinus, E., and Reichert, H. (2008). Amplification of neural stem cell proliferation by intermediate progenitor cells in *Drosophila* brain development. Neural Dev 3, 5.

Blondel, V.D., Guillaume, J.-L., Lambiotte, R., and Lefebvre, E. (2008). Fast unfolding of communities in large networks. J. Stat. Mech., P10008.

Bonilla, S., Hall, A.C., Pinto, L., Attardo, A., Gotz, M., Huttner, W.B., and Arenas, E. (2008). Identification of midbrain floor plate radial glia-like cells as dopaminergic progenitors. Glia 56, 809-820.

Boone, J.Q., and Doe, C.Q. (2008). Identification of *Drosophila* type II neuroblast lineages containing transit amplifying ganglion mother cells. Dev Neurobiol 68, 1185-1195.

Bossing, T., Udolph, G., Doe, C.Q., and Technau, G.M. (1996). The embryonic central nervous system lineages of *Drosophila melanogaster*. I. Neuroblast lineages derived from the ventral half of the neuroectoderm. Dev Biol 179, 41-64.

Boyan, G., and Williams, L. (2011). Embryonic development of the insect central complex: insights from lineages in the grasshopper and *Drosophila*. Arthropod Struct Dev 40, 334-348.

Broadus, J., and Doe, C.Q. (1995). Evolution of neuroblast identity: *seven-up* and *prospero* expression reveal homologous and divergent neuroblast fates in *Drosophila* and *Schistocerca*. Development 121, 3989-3996.

Brown, K.N., Chen, S., Han, Z., Lu, C.H., Tan, X., Zhang, X.J., Ding, L., Lopez-Cruz, A., Saur, D., Anderson, S.A., et al. (2011). Clonal production and organization of inhibitory interneurons in the neocortex. Science 334, 480-486.

Bullmore, E., and Sporns, O. (2009). Complex brain networks: graph theoretical analysis of structural and functional systems. Nat Rev Neurosci 10, 186-198.

Cachero, S., Ostrovsky, A.D., Yu, J.Y., Dickson, B.J., and Jefferis, G.S. (2010). Sexual dimorphism in the fly brain. Curr Biol 20, 1589-1601.

Chiang, A.S., Lin, C.Y., Chuang, C.C., Chang, H.M., Hsieh, C.H., Yeh, C.W., Shih, C.T., Wu, J.J., Wang, G.T., Chen, Y.C., et al. (2011). Three-dimensional reconstruction of brain-wide wiring networks in *Drosophila* at single-cell resolution. Curr Biol 21, 1-11.

Costa, M.R., and Hedin-Pereira, C. (2010). Does cell lineage in the developing cerebral cortex contribute to its columnar organization? Front Neuroanat 4, 26.

Das, A., Chiang, A., Davla, S., Priya, R., Reichert, H., Vijayraghavan, K., and Rodrigues, V. (2011). Identification and analysis of a glutamatergic local interneuron lineage in the adult *Drosophila* olfactory system. Neural Syst Circuits 1, 4.

Das, A., Gupta, T., Davla, S., Prieto-Godino, L.L., Diegelmann, S., Reddy, O.V., Raghavan, K.V., Reichert, H., Lovick, J., and Hartenstein, V. (2013). Neuroblast lineage-specific

origin of the neurons of the Drosophila larval olfactory system. Dev Biol 373, 322-337.

Doe, C.Q. (2006). Chinmo and neuroblast temporal identity. Cell 127, 254-256.

Endo, K., Karim, M.R., Taniguchi, H., Krejci, A., Kinameri, E., Siebert, M., Ito, K., Bray, S.J., and Moore, A.W. (2012). Chromatin modification of Notch targets in olfactory receptor neuron diversification. Nat Neurosci 15, 224-233.

Fortunato, S. (2010). Community detection in graphs. Physics Reports 486, 75-174.

Freeman, L.C. (1979). Centrality of networks. Soc. Netw. 1, 215-239.

Hagmann, P., Cammoun, L., Gigandet, X., Meuli, R., Honey, C.J., Wedeen, V.J., and Sporns, O. (2008). Mapping the structural core of human cerebral cortex. PLoS Biol 6,

Hampel, S., Chung, P., McKellar, C.E., Hall, D., Looger, L.L., and Simpson, J.H. (2011). *Drosophila* Brainbow: a recombinase-based fluorescence labeling technique to subdivide neural expression patterns. Nat Methods 8, 253-259.

Hanesch, U., Fischbach, K.F., and Heisenberg, M. (1989). Neuronal architecture of the central complex in *Drosophila melanogaster*. Cell Tissue Res. 257, 343-366.

Hinke, W. (1961). Das relative postembryonale Wachstum der Hirnteile von Culex pipiens, Drosophila melanogaster und Drosophila-mutanten. Z. Morph. Ökol. Tiere 50, 81-118.

Hofbauer, A., and Campos-Ortega, J.A. (1990). Proliferation pattern and early differentiation of the optic lobes in Drosophila melanogaster. Roux Arch. devel. Biol. 198, 264-274.

Ito, K., and Awasaki, T. (2008). Clonal unit architecture of the adult fly brain. Adv Exp Med Biol 628, 137-158.

Ito, K., and Hotta, Y. (1992). Proliferation pattern of postembryonic neuroblasts in the brain of *Drosophila melanogaster*. Dev Biol 149, 134-148.

Ito, K., Awano, W., Suzuki, K., Hiromi, Y., and Yamamoto, D. (1997). The *Drosophila* mushroom body is a quadruple structure of clonal units each of which contains a virtually identical set of neurones and glial cells. Development 124, 761-771.

Isshiki, T., Pearson, B., Holbrook, S., and Doe, C.Q. (2001). *Drosophila* neuroblasts sequentially express transcription factors which specify the temporal identity of their neuronal progeny. Cell 106, 511-521.

Izergina, N., Balmer, J., Bello, B., and Reichert, H. (2009). Postembryonic development of transit amplifying neuroblast lineages in the *Drosophila* brain. Neural Dev 4, 44.

Jefferis, G.S., Marin, E.C., Stocker, R.F., and Luo, L. (2001). Target neuron prespecification in the olfactory map of *Drosophila*. Nature 414, 204-208.

Kamikouchi, A., Shimada, T., and Ito, K. (2006). Comprehensive classification of the auditory sensory projections in the brain of the fruit fly *Drosophila melanogaster*. J Comp Neurol 499, 317-356.

Kasthuri, N., and Lichtman, J.W. (2007). The rise of the 'projectome'. Nat Methods 4, 307-308.

Kimura, K., Hachiya, T., Koganezawa, M., Tazawa, T., and Yamamoto, D. (2008). Fruitless and doublesex coordinate to generate male-specific neurons that can initiate courtship. Neuron 59, 759-769.

Kunz, T., Kraft, K.F., Technau, G.M., and Urbach, R. (2012). Origin of *Drosophila* mushroom body neuroblasts and generation of divergent embryonic lineages. Development 139, 2510-2522.

Lai, S.L., Awasaki, T., Ito, K., and Lee, T. (2008). Clonal analysis of *Drosophila* antennal lobe neurons: diverse neuronal architectures in the lateral neuroblast lineage. Development 135, 2883-2893.

Larsen, C., Shy, D., Spindler, S.R., Fung, S., Pereanu, W., Younossi-Hartenstein, A., and Hartenstein, V. (2009). Patterns of growth, axonal extension and axonal arborization of neuronal lineages in the developing Drosophila brain. Dev Biol 335, 289-304.

Lee, T., and Luo, L. (1999). Mosaic analysis with a repressible cell marker for studies of gene function in neuronal morphogenesis. Neuron 22, 451-461.

Lee, T., Lee, A., and Luo, L. (1999). Development of the *Drosophila* mushroom bodies: sequential generation of three distinct types of neurons from a neuroblast. Development 126, 4065-4076.

Letinic, K., Zoncu, R., and Rakic, P. (2002). Origin of GABAergic neurons in the human neocortex. Nature 417, 645-649.

Li, Y., Lu, H., Cheng, P.L., Ge, S., Xu, H., Shi, S.H., and Dan, Y. (2012). Clonally related visual cortical neurons show similar stimulus feature selectivity. Nature 486, 118-121.

Lichtneckert, R., Bello, B., and Reichert, H. (2007). Cell lineage-specific expression and function of the empty spiracles gene in adult brain development of Drosophila melanogaster. Development 134, 1291-1300.

Liu, G., Seiler, H., Wen, A., Zars, T., Ito, K., Wolf, R., Heisenberg, M., and Liu, L. (2006). Distinct memory traces for two visual features in the *Drosophila* brain. Nature 439, 551-556.

McKay, R. (1997). Stem cells in the central nervous system. Science 276, 66-71.

Miyazaki, T., and Ito, K. (2010). Neural architecture of the primary gustatory center of *Drosophila melanogaster* visualized with GAL4 and LexA enhancerrap systems. J Comp Neurol 518, 4147-4181.

Molyneaux, B.J., Arlotta, P., Menezes, J.R., and Macklis, J.D. (2007). Neuronal subtype specification in the cerebral cortex. Nat Rev Neurosci 8, 427-437.

Mu, L., Ito, K., Bacon, J.P., and Strausfeld, N.J. (2012). Optic glomeruli and their inputs in *Drosophila* share an organizational ground pattern with the antennal lobes. J Neurosci 32, 6061-6071.

Newman, M.E.J. (2010). Networks – An Introduction, (Oxford: Oxford University Press).

Newman, M.E.J., and Girvan, M. (2004). Finding and evaluating community structure in networks. Phys Rev E Stat Nonlin Soft Matter Phys 69, 026113.

Nicholas James Strausfeld (2009) Brain organization and the origin of insects:an assessment *Proc. R. Soc. B* 2009 276 1929-37

Ohtsuki, G., Nishiyama, M., Yoshida, T., Murakami, T., Histed, M., Lois, C., and Ohki, K. (2012). Similarity of visual selectivity among clonally related neurons in visual cortex. Neuron 75, 65-72.

Okada, R., Awasaki, T., and Ito, K. (2009). Gamma-aminobutyric acid (GABA)-mediated

neural connections in the *Drosophila* antennal lobe. J Comp Neurol 514, 74-91.

Otsuna, H., and Ito, K. (2006). Systematic analysis of the visual projection neurons of *Drosophila melanogaster*. I. Lobula-specific pathways. J Comp Neurol 497, 928-958.

Pan, R.K., Chatterjee, N., and Sinha, S. (2010). Mesoscopic organization reveals the constraints governing *Caenorhabditis elegans* nervous system. PLoS One 5, e9240.

Peng, H., Chung, P., Long, F., Qu, L., Jenett, A., Seeds, A.M., Myers, E.W., and Simpson, J.H. (2011). BrainAligner: 3D registration atlases of *Drosophila* brains. Nat Methods 8, 493-500.

Prokop, A., and Technau, G.M. (1991). The origin of postembryonic neuroblasts in the ventral nerve cord of *Drosophila melanogaster*. Development 111, 79-88.

Ramon y Cajal, S. (1909). Histology of the nervous system of man and vertebrates (English translation by Swanson, N. and Swanson, L.W. in 1995), (New York, Oxford.: Oxford Univ. Press).

Sawa, H. (2010). Specification of neurons through asymmetric cell divisions. Curr Opin Neurobiol 20, 44-49.

Schindelin, J., Arganda-Carreras, I., Frise, E., Kaynig, V., Longair, M., Pietzsch, T., Preibisch, S., Rueden, C., Saalfeld, S., Schmid, B., et al. (2012). Fiji: an open-source platform for biological-image analysis. Nat Methods 9, 676-682.

Schmidt, H., Rickert, C., Bossing, T., Vef, O., Urban, J., and Technau, G.M. (1997). The embryonic central nervous system lineages of Drosophila melanogaster. II. Neuroblast lineages derived from the dorsal part of the neuroectoderm. Dev Biol 189, 186-204.

Sohn, Y., Choi, M.-K., Ahn, Y.-Y., Lee, J., and Jeong, J. (2011). Topological cluster analysis reveals the systemic organization of the *Caenorhabditis elegans* connectome. PLoS Comp Biol 7, e1001139.

Spindler, S.R., and Hartenstein, V. (2011). Bazooka mediates secondary axon morphology in Drosophila brain lineages. Neural Dev 6, 16.

Strausfeld, N.J. (2012). Arthropod brains. Evolution, functional elegance, and historical significance. , (Harvard, London.: Belknap Press, Harvard University Press).

Tanaka, N.K., Endo, K., and Ito, K. (2012). The organization of antennal lobe-associated neurons in the adult Drosophila melanogaster brain. J Comp Neurol.

Tanaka, N.K., Tanimoto, H., and Ito, K. (2008). Neuronal assemblies of the Drosophila mushroom body. J Comp Neurol 508, 711-755.

The Insect Brain Name Working Group: Ito, K., Shinomiya, K., Ito, M., Armstrong, J.D., Boyan, G., Hartenstein, V., Harzsch, S., Heisenberg, M., Homberg, U., Jenett, A., Keshishian. H., Restifo, L.L., Rössler, W., Simpson, J.H., Strausfeld, N.J., Strauss, R., and Vosshall, L.B. A coordinated nomenclature system for the insect brain. submitted.

Truman, J.W., Moats, W., Altman, J., Marin, E.C., and Williams, D.W. (2010). Role of Notch signaling in establishing the hemilineages of secondary neurons in *Drosophila melanogaster*. Development 137, 53-61.

Urbach, R., and Technau, G.M. (2003). Molecular markers for identified neuroblasts in the developing brain of *Drosophila*. Development 130, 3621-3637.

Wan, Y., Otsuna, H., Chien, C.-B., and Hansen, C. (2009). An interactive visualization tool

for multi-channel confocal microscopy data in neurobiology research. IEEE Transactions on Visualization and Computer Graphics 15, 1489-1496.

Watts, D.J., and Strogatz, S.H. (1998). Collective dynamics of 'small-world' networks. Nature 393, 440-442.

Viktorin, G., Riebli, N., Popkova, A., Giangrande, A., and Reichert, H. (2011). Multipotent neural stem cells generate glial cells of the central complex through transit amplifying intermediate progenitors in Drosophila brain development. Dev Biol 356, 553-565.

Yu, J.Y., Kanai, M.I., Demir, E., Jefferis, G.S., and Dickson, B.J. (2010). Cellular organization of the neural circuit that drives *Drosophila* courtship behavior. Curr Biol 20, 1602-1614.

Yu, H.-H., Awasaki, T., Schroeder, M.D., Long, F., Yang, J.S., He, Y., Ding, P., Kao, J.-C., Jenett, A., Wu, G.Y.-Y., et al. Clonal development and organization of the adult *Drosophila* central brain. in press.

Zheng, X., Zugates, C.T., Lu, Z., Shi, L., Bai, J.M., and Lee, T. (2006). Baboon/dSmad2 TGF-beta signaling is required during late larval stage for development of adult-specific neurons. Embo J 25, 615-627.

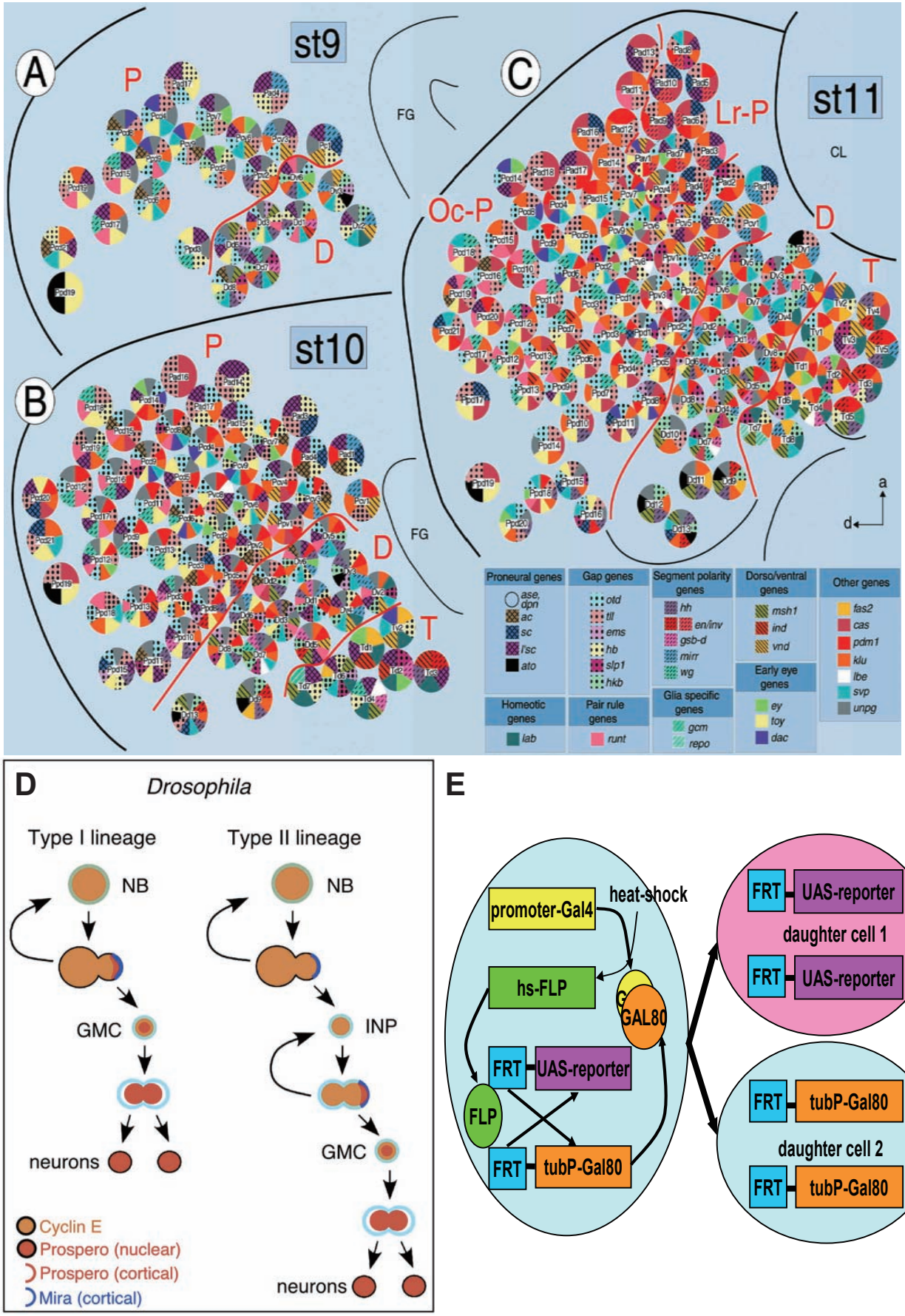

Fig.1 Molecular markers expressed in brain neuroblasts and clone labeling technique

Figure 1 Molecular markers expressed in brain neuroblasts and clone labeling technique. (A-C) Summary diagram of molecular markers expressed in brain NBs at different stages of embryonic development. Color code indicates the expression of more than 40 different molecular markers in individual brain NBs. Each brain NB expresses a specific combination of molecular markers. Accordingly, each NB can be uniquely identified at stage 9 (A; st9), stage 10 (B; st10) and stage 11 (C; st11, which is when the entire population of brain NBs is established). Red lines indicate the neuromeric boundaries between the trito- (T) and deutocerebrum (D), and the ocular (Oc-P) and labral protocerebrum (Lr-P). Anterior (a) is towards the top; dorsal (d) is towards the left. CL, clypeolabrum; FG, foregut. (Urbach and Technau, 2003) (E) Proliferation pattern of type I and type II neuroblast. NSC: neural stem cell, GMC: ganglion mother cell, INP: intermediate neural progenitor. (E) Concept figure of the MARCM system. GAL4:transcription factor, UAS : target sequence of GAL4, FLP : recombination protein, FRT : target sequence of FLP GAL80 : antagonist of GAL4, tubP: tubulin promoter.

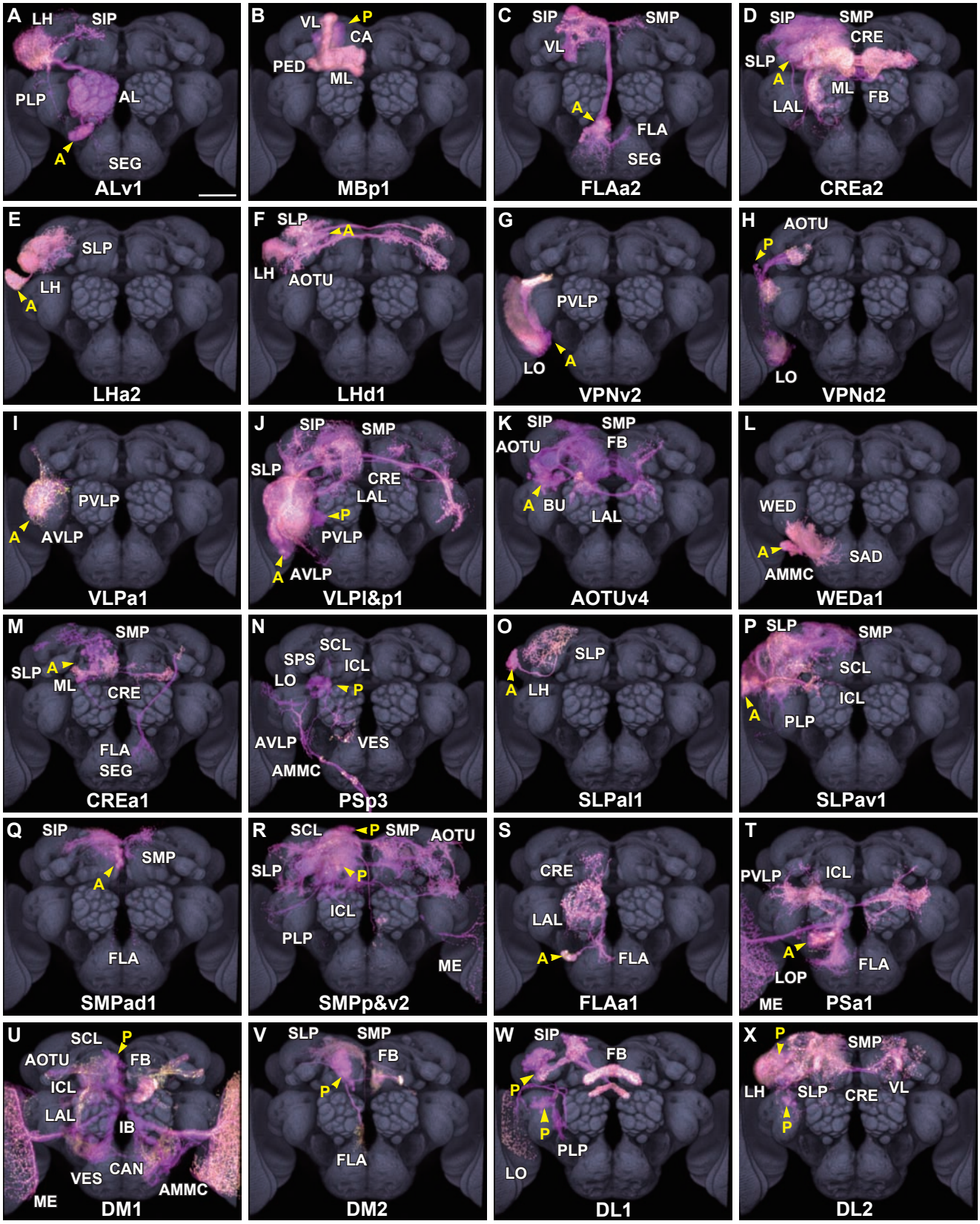

Figure 2 Examples of clonal units in the adult *Drosophila* brain.

Figure 2 Examples of clonal units in the adult *Drosophila* brain. Anterior views of 3D reconstructions. Cell bodies and neuronal fibers (magenta), distributions of presynaptic sites (white), and the entire neuropil of the template brain (grey) are shown. Arrowheads indicate the location of cell body clusters. Characters A and P denote their positions in the anterior or posterior brain, respectively. Images of the entire set of the identified clones are shown in Supplemental Fig. S1. See Supplemental Table S2A for the names of neuropils. Scale bar equals to 50 μm. Genotypes: *elav^{c155}-Gal4 hs-FLP/ UAS-DsRed; FRT^{G13} tub-GAL80/ FRT^{G13}; UAS-nSyb::GFP, elav^{c155}-Gal4 hs-FLP/ UAS-Syt::HA; FRT^{G13} tub-GAL80/ FRT^{G13} UAS-GFP*; *UAS*-mCD8::GFP/+, *hs-FLP tub-GAL80 FRT^{19A}/ UAS-DsRed FRT^{19A}; actin-Gal4/ +; UAS-n-Syb::GFP/*+.

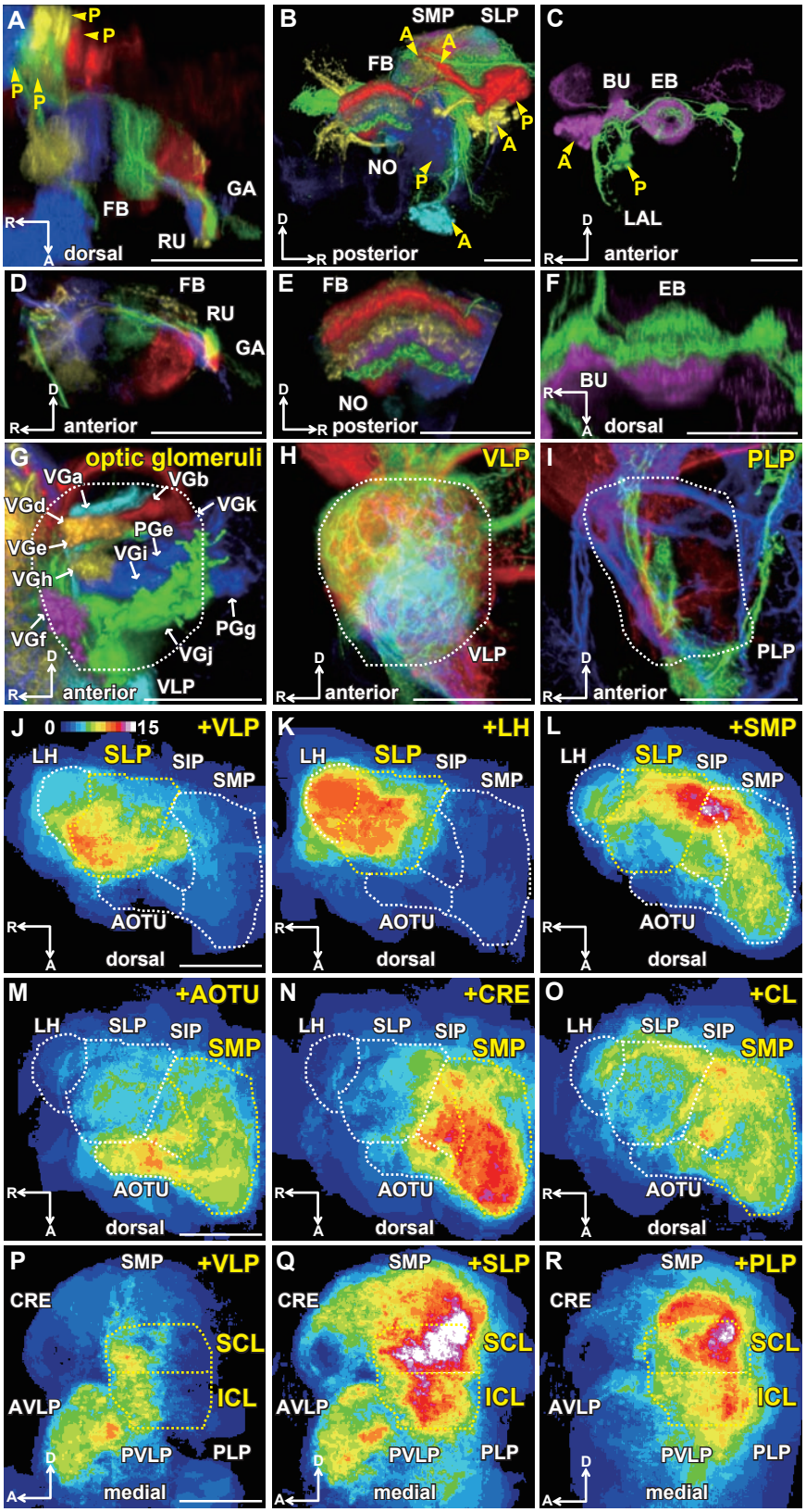

Figure 3 Clonally organized structures in the brain.

Figure 3 Clonally organized structures in the brain. 3D reconstruction of selective clones viewed from the directions indicated in each panel. (A-F) Clones of the central complex (CX). Those deriving from one side of brain are shown. (A) Clones that contain small-field neurons of the CX. (B) Clones containing large-field CX neurons. (C) Two clones that preferentially project to the ellipsoid body (EB). (D) Anterior close up view of (A), showing the output terminals in the rubus (RB) and gall (GA) with overlapping projections from the four clones. (E) Posterior close up view of (B), showing discrete six layers of clonal arborizations in the fan-shaped body (FB). (F) Anterior-dorsal close up view of (C), showing antero-posterior layers in the EB. (G) Terminals of the VPN clones in the VLP and PLP, shown in different colors. Arrows indicate the optic glomeruli. (H, I) Close up view of the VLP and PLP, showing characteristic arborization patterns of the cerebral clonal units. (J-R) Cross section view of the dorsal brain, showing the overlay of arborizations of the clones associated with particular neuropils (indicated with yellow dotted lines). Color code in (J) denotes the degree of overlap of the clones. Horizontal cross-sections of the SLP (J-L). Horizontal cross-sections of the SMP (M-O) and sagittal cross sections of the SCL and ICL (P-R). A: anterior, R: right, D: dorsal (body axis). Scale bar equals to 50 μm. Clones shown in the overlay: DM1, 2, 3 and 4 (A, D); DM6, DL1, AOTUv4, CREa2, LALv1 and SMPad4 (B, E); EBa1 and EBp1 (C, F); VPNd1, 3, VPNp2, 3, VPNv1, 2 and 3 (G); VLPl2, VLPl&p1 and 2 (H); SLPp&v1, WEDa2 and SLPa&l1 (I).

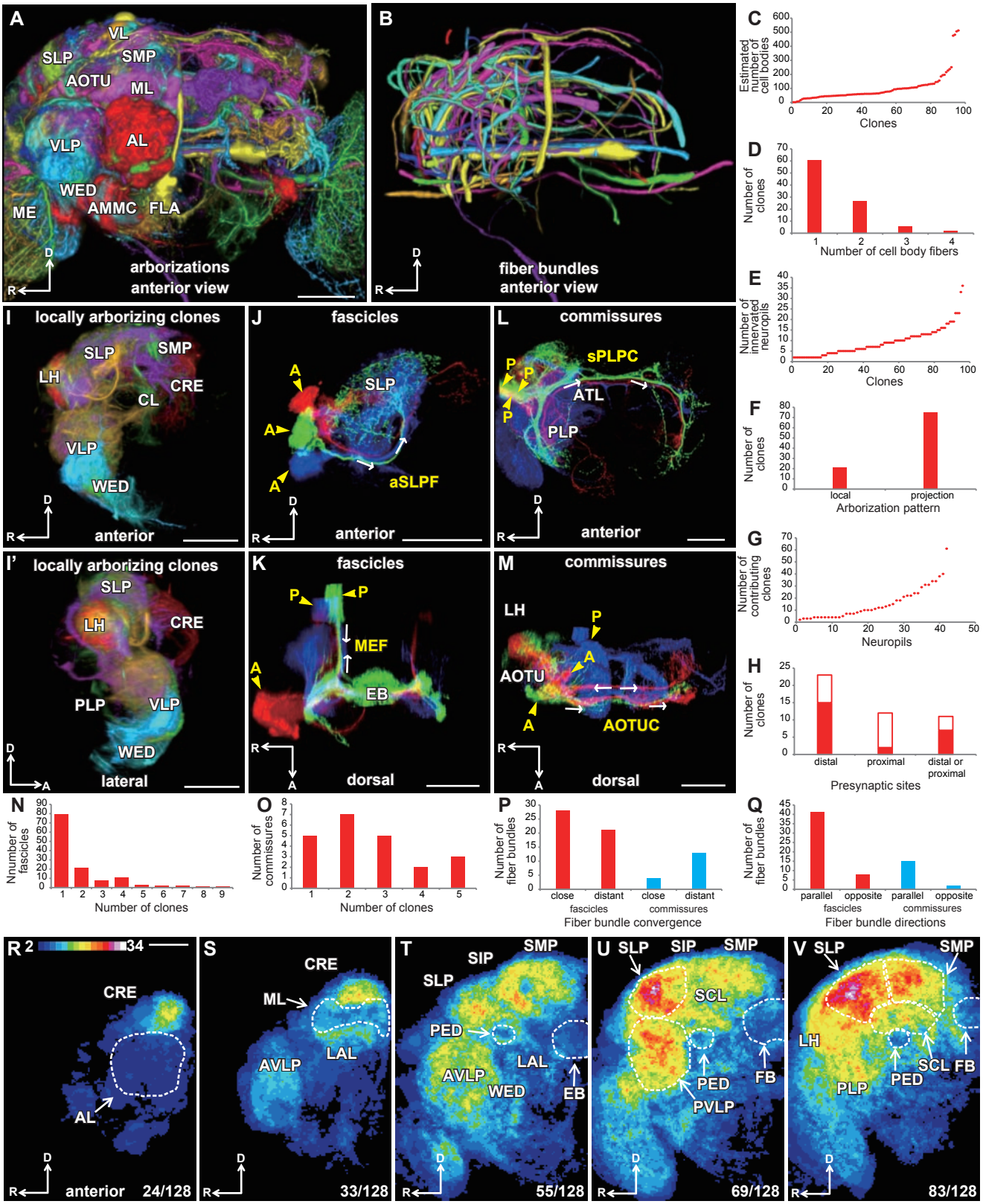

Figure 4 Spatial association of the identified clones.

Figure 4 Spatial association of the identified clones. (A) Overlay of all the identified clones, anterior view. (B) Distribution of the identified neuronal fiber bundles, anterior view. Signals of cell bodies are removed to visualize the underlying neural projections. (C-H) Quantitative characterization of clonal attributes. For (H), red bars indicate the number of clones that exclusively contain projections with asymmetric distribution of presynaptic sites, and white bars indicate the number of clones that contain mixed projections with either symmetric or asymmetric distribution of presynaptic sites. The rightmost bar indicates the number of clones that contain mixed projections with presynaptic sites either in their distal or proximal parts. (I) Distribution of the clones with locally confined arborizations within a single or neighboring neuropils. Anterior (I) and lateral (I') views of the arborizations. (J-M) Fiber bundles formed by multiple clones. Three clones that contribute to a bundle are shown in different colors. Arrowheads indicate the cell body clusters. Arrows indicate directions of fiber bundles from proximal to distal (from the cell bodies) parts of neurites. (N-Q) Quantitative characterization of fiber bundles. aSLPF: anterior SLP fascicle, MEF: medial equatorial fascicle, sPLPC: superior PLP commissure, AOTUC: AOTU commissure. Scale bar equals to 50 μm. Clones shown in the overlay: SLPpl4, SLPal1 and 2 (J); AOTUv3, EBp1 and DM5 (K); SLPp&v1, LHp2 and VPNp&v1 (L); LHd1, AOTUv2 and SMPp&v1 (M). (R-V) Number of clones contributing to neuropils. Frontal sections of the cerebrum (from anterior to posterior) showing the color-coded number of clones that arborize in each small region of the brain. Color code shown at the top margin of panel R. White dotted lines indicate neuropils with high or low clonal overlap. Bottom right numbers denote the number of sections counted from the anterior. ML, PED and CA are parts of the MB, and EB and FB are parts of the CX. A: anterior, R: right, D: dorsal (body axis). Scale bar equals to 50 μm.

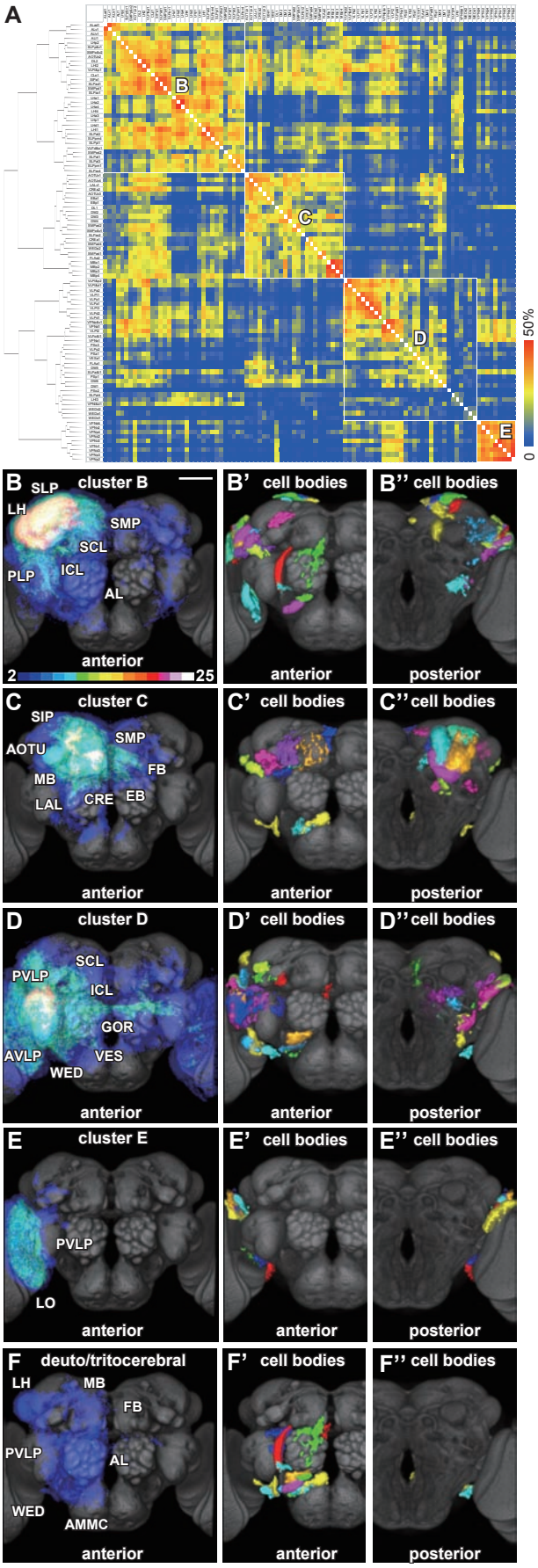

Figure 5 Overlap between clonal arborizations.

Figure 5 Overlap between clonal arborizations. (A) Cluster analysis of the clones with spatial overlap. Color code denotes the number of overlapping voxels between each combination of clones. Boxes B-E framed in white show the four clusters of clones with high spatial overlap. A larger image of the diagram is provided in Supplemental Fig. S4. (B-E) Overlay images of the clones that form the four clusters indicated in (A). Leftmost panels show the overlay of arborizations. Color code denotes the number of overlapping clones. Middle (') and right ('') panels show the distribution of cell bodies of these clones (shown in different colors) in the anterior (middle, ') and posterior (right, '') brains. (F) Overlay images of putative deuto- and tritocerebral clones. Scale bar equals to 50 μm.

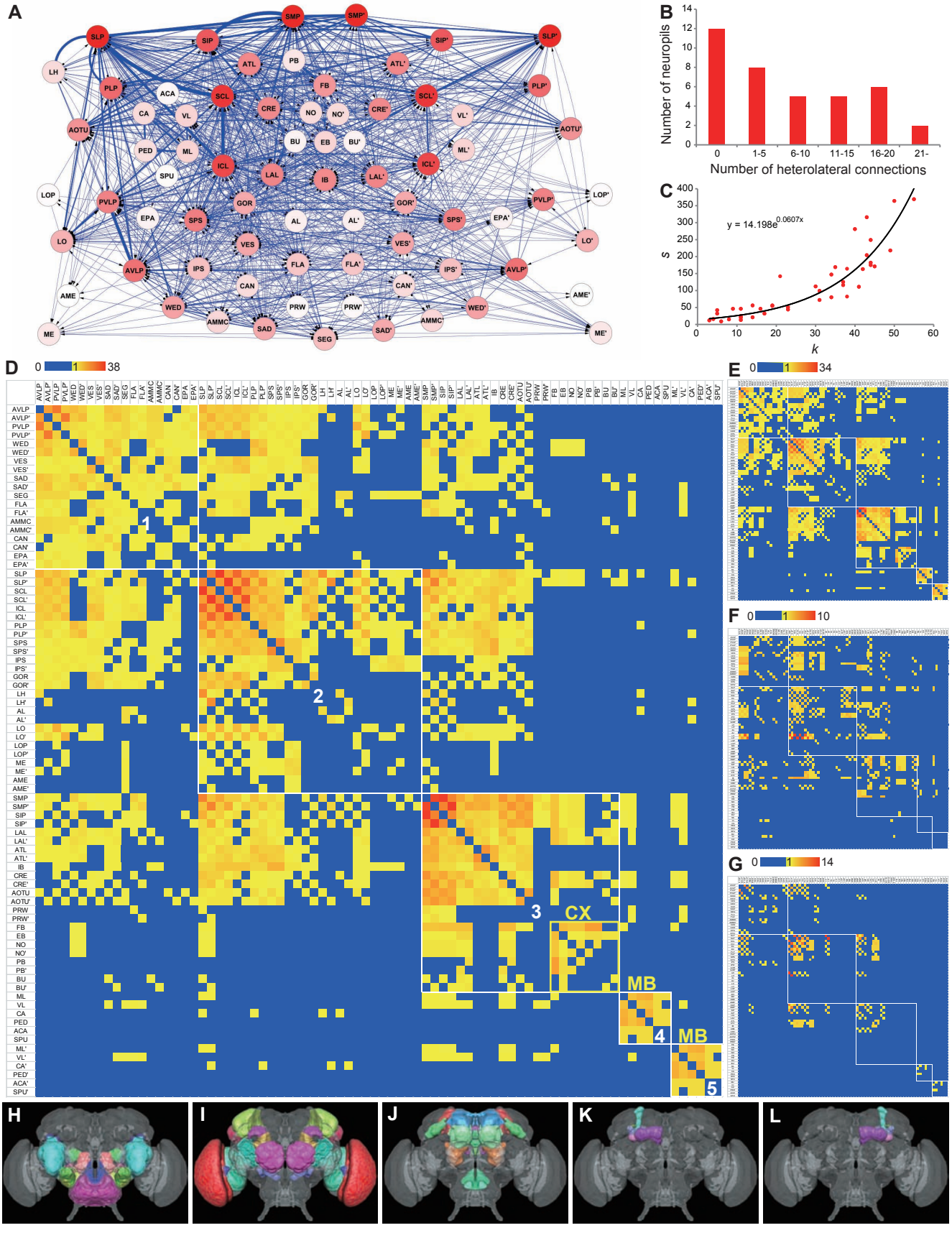

Figure 6 Network analysis of the clonal projections.

Figure 6 Network analysis of the clonal projections.

(A) Network diagram of the connections between neuropils. Neuropil names with apostrophe (’) indicate those in the contralateral brain side. Thickness of the lines indicates the number of projection subgroups that contribute to the link between two neuropils. Reddish hue at each neuropil indicates the total number of connections associated with it. Arrows indicate the estimated direction of information, polarizing the direction from the arborization lacking presynaptic sites to that with presynaptic sites. Neuropils in the ventral cerebrum have fewer connections than in the dorsal cerebrum, in part because connections made by the clones in the SEG were not analyzed in the current study. (B) Number of bilateral connections for each neuropil. (C) Scatter diagram of node degree (*k*, number of neuropils directly connected to a given neuropil) and node strength (*s,* number of projection subgroups that mediate these connections). (D) Matrix diagram of connections between neuropils. Color code represents the number of clonal connections. White frames indicate the five communities of closely associated neuropils. Yellow frame indicates the neuropils that compose the CX. (E-G) Connections mediated by specific types of clonal arborizations. (E) Connections of projection neurons without asymmetric distribution of presynaptic sites. (F) Connections of projection neurons with asymmetric presynaptic sites. Rows denoted along the ordinates (left sides) indicate the input neuropils lacking presynaptic sites; rows denoted along the top of the diagram indicate the output neuropils with presynaptic sites. Such connections are found from the optic lobe to the cerebrum, from lower auditory centers to AVLP and PVLP, from the anterior ventral cerebrum to the VLP and SCL/ICL, from dorsal cerebrum to the CX and MB lobes, from the FB to dorsal and ventral cerebrum, and from the IB to various neuropils. (G) Connections mediated by locally arborizing clones. Larger image of diagrams A and D-G are provided in Supplemental Fig. S6. (H-L) The five groups of neuropils indicated in (D), anterior view.

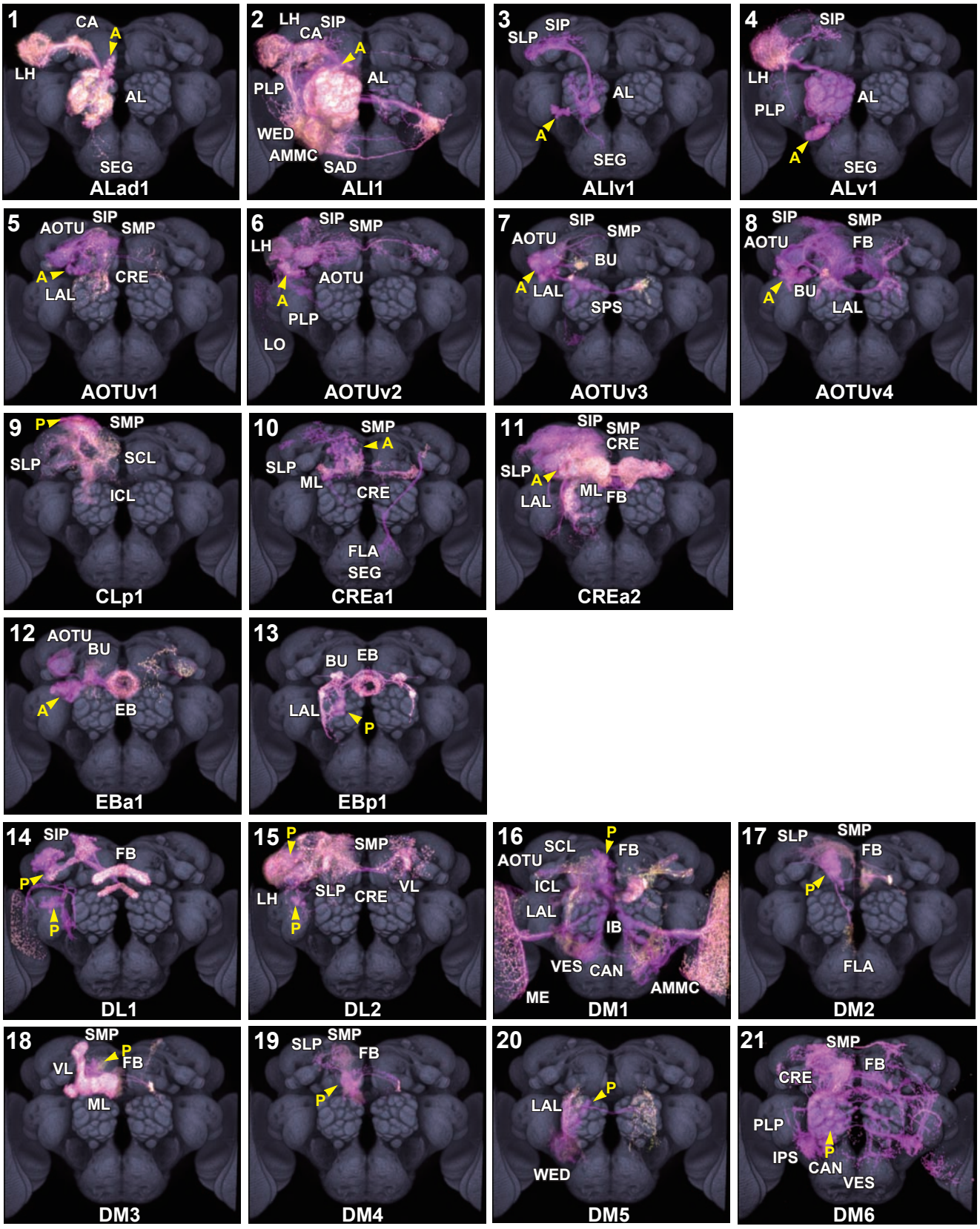

Figure S1 (part 1) Identified clonal units in the adult Drosophila brain.

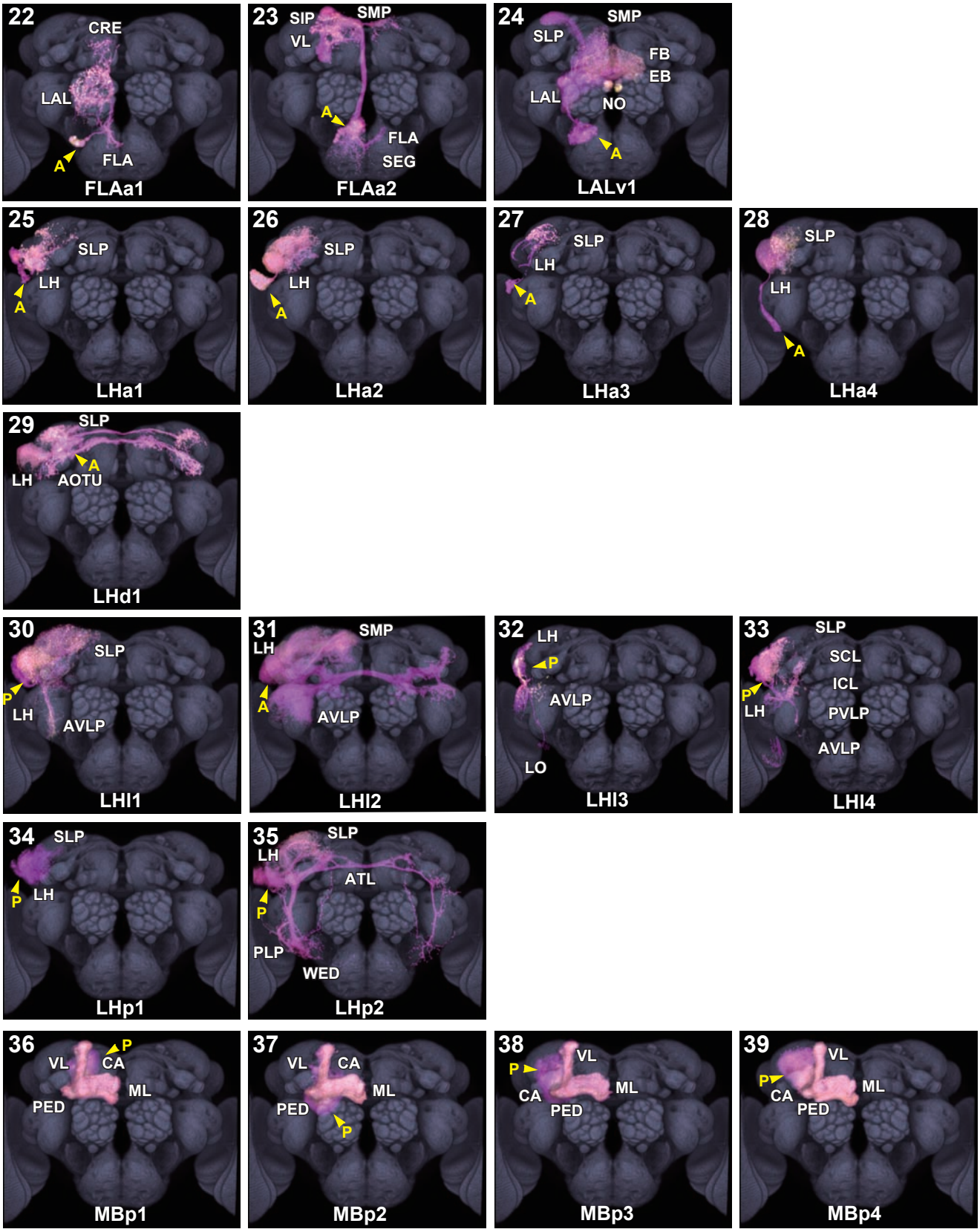

Figure S1 (part 2) Identified clonal units in the adult Drosophila brain.

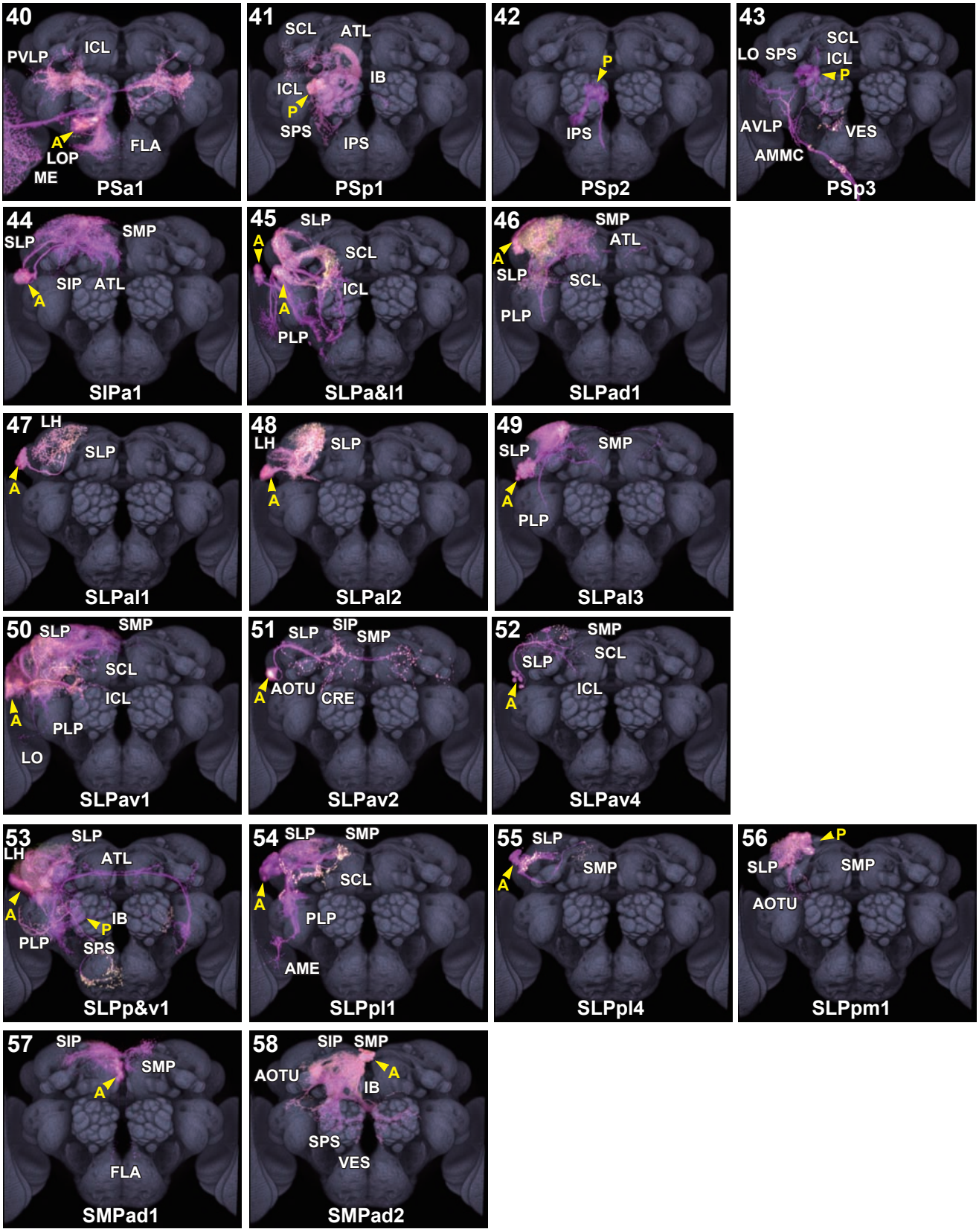

Figure S1 (part 3) Identified clonal units in the adult Drosophila brain.

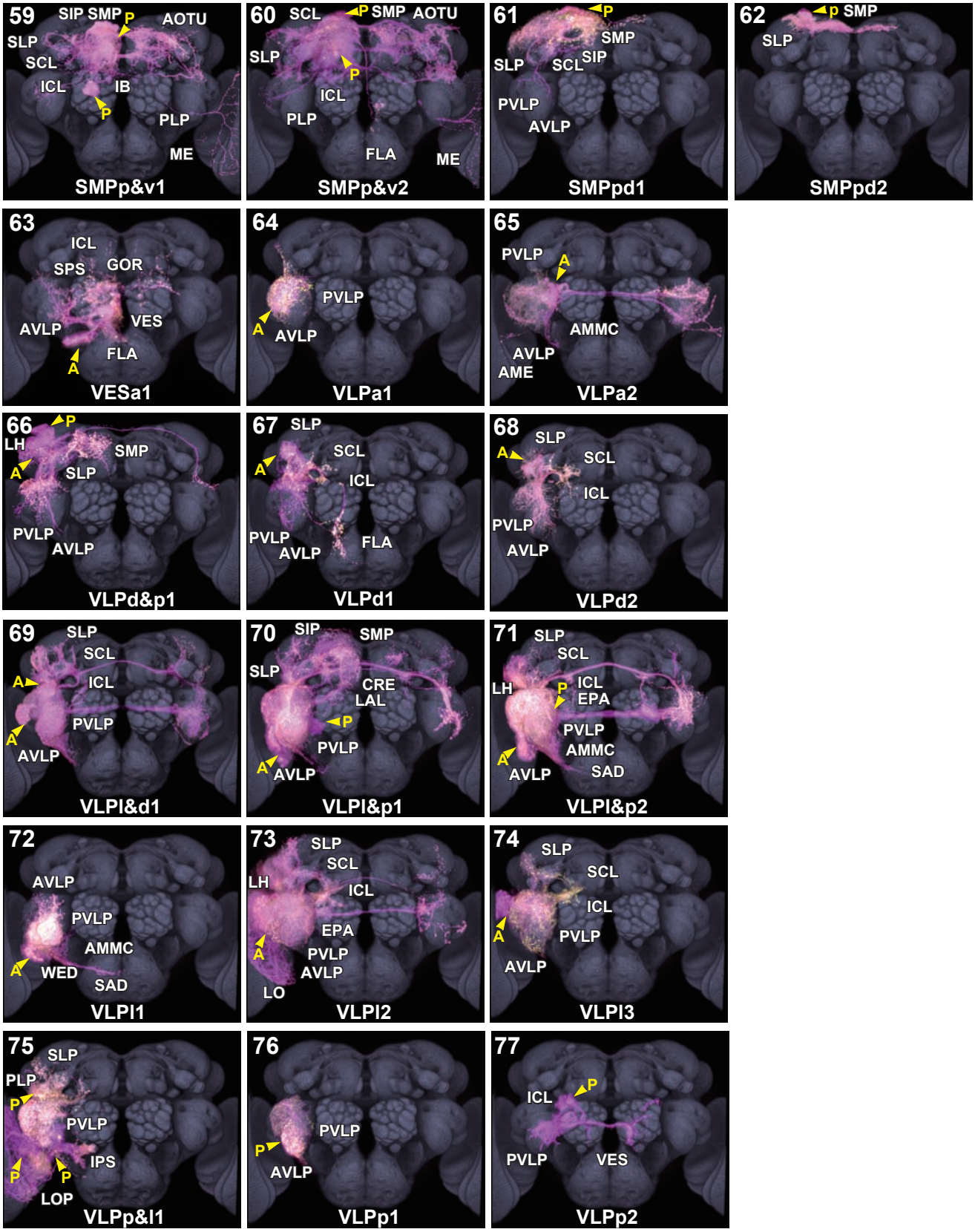

Figure S1 (part 4) Identified clonal units in the adult Drosophila brain.

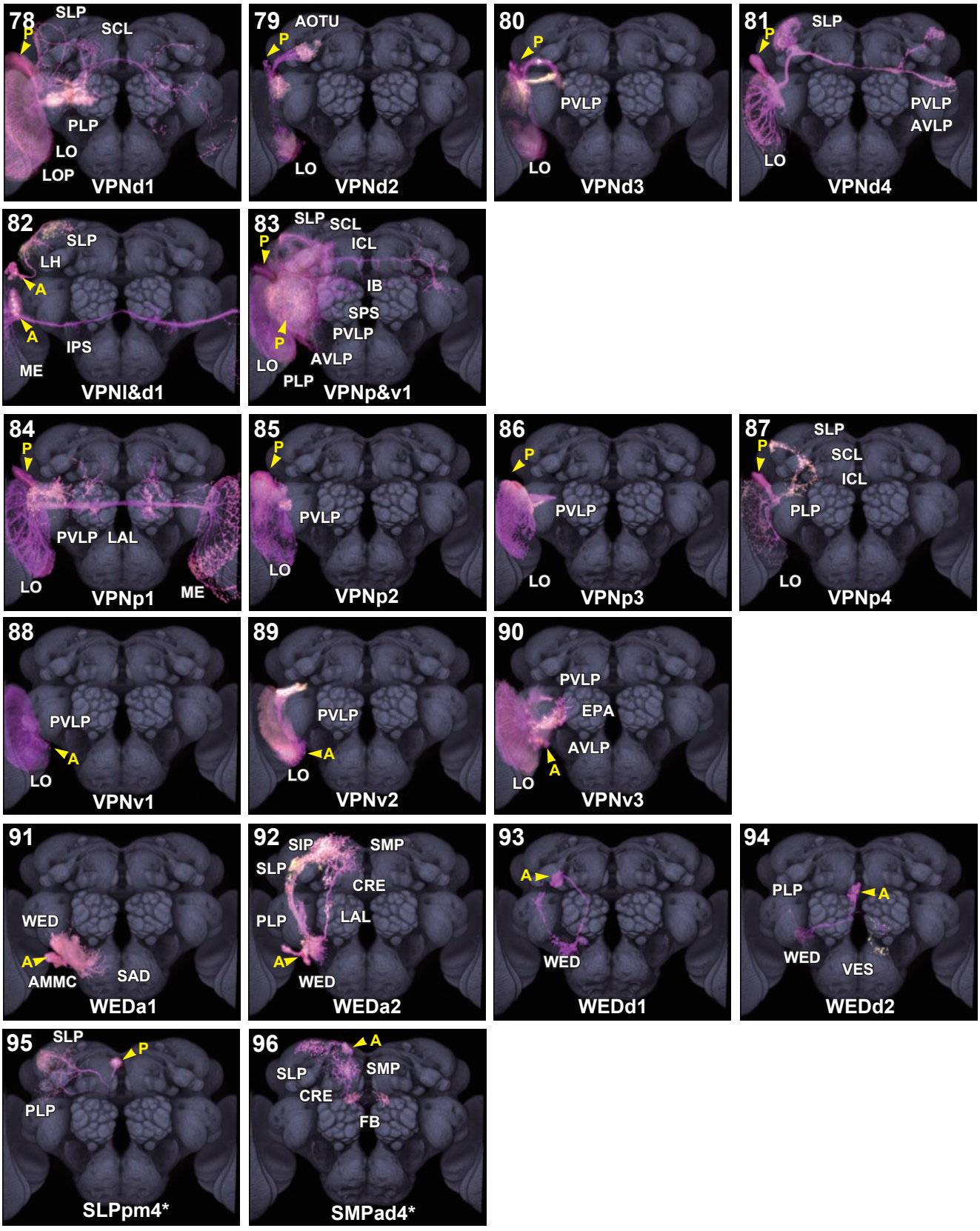

Figure S1 (part 5) Identified clonal units in the adult Drosophila brain.

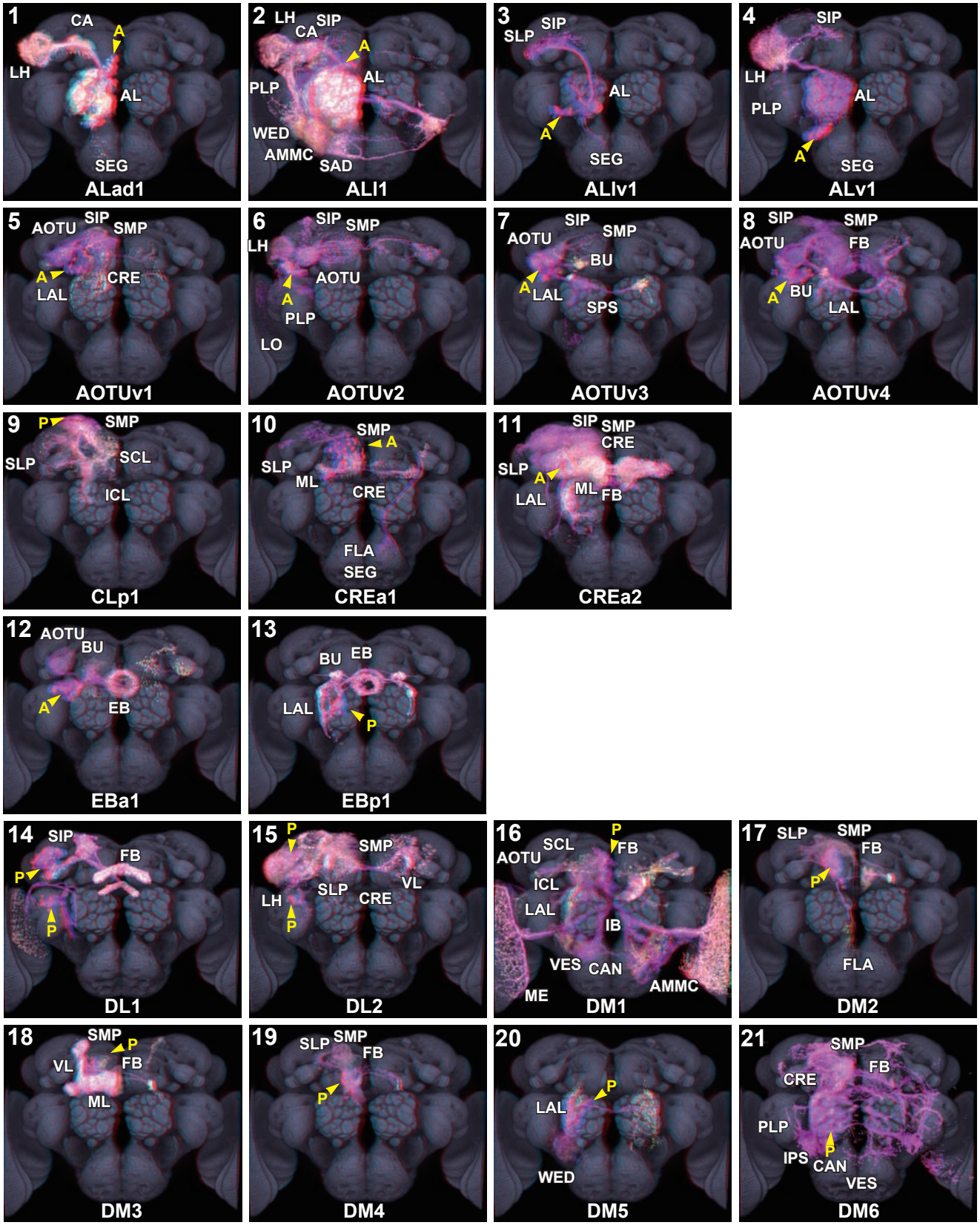

Figure S1 (part 6) Identified clonal units in the adult Drosophila brain (3D stereograms).

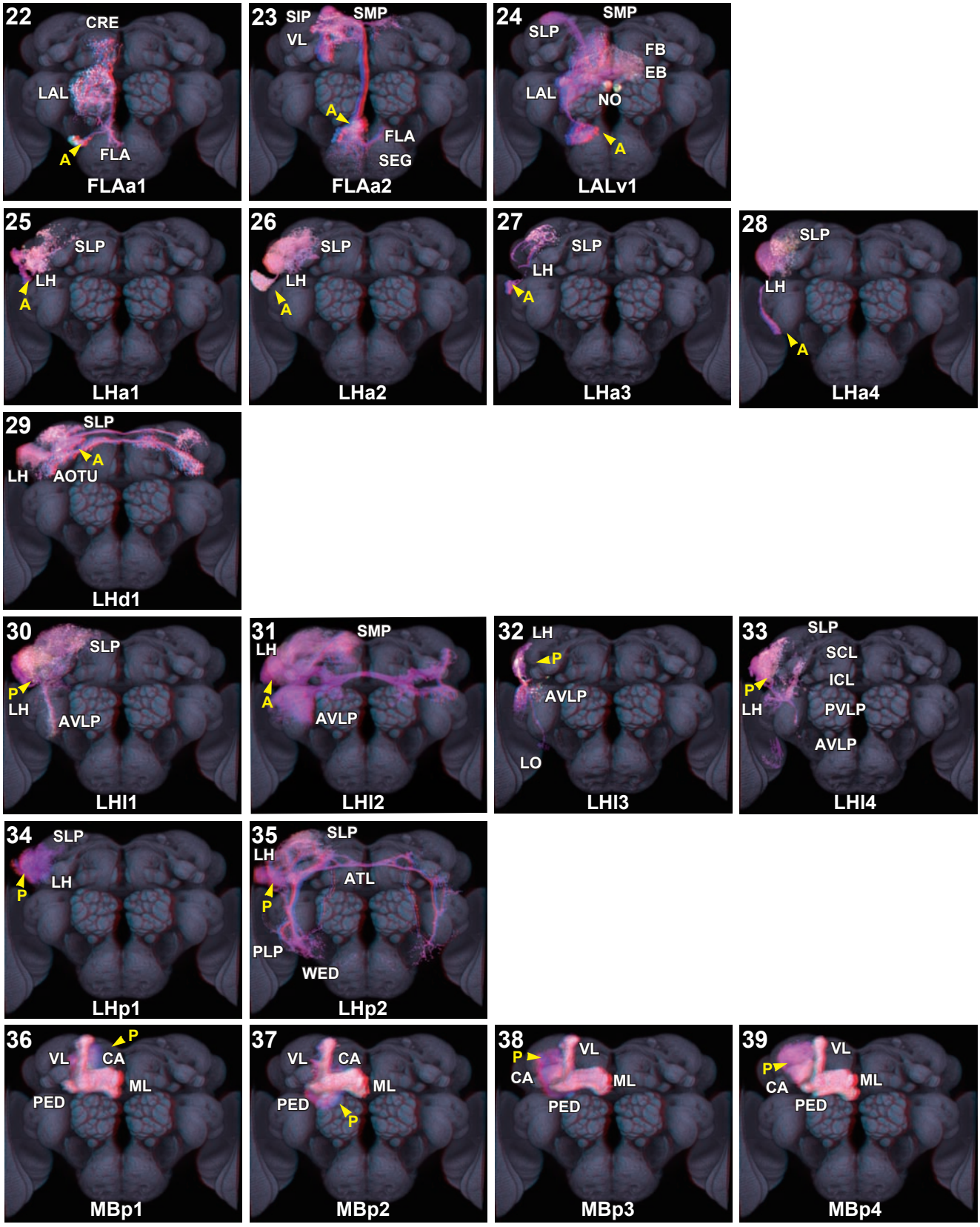

Figure S1 (part 7) Identified clonal units in the adult Drosophila brain (3D stereograms).

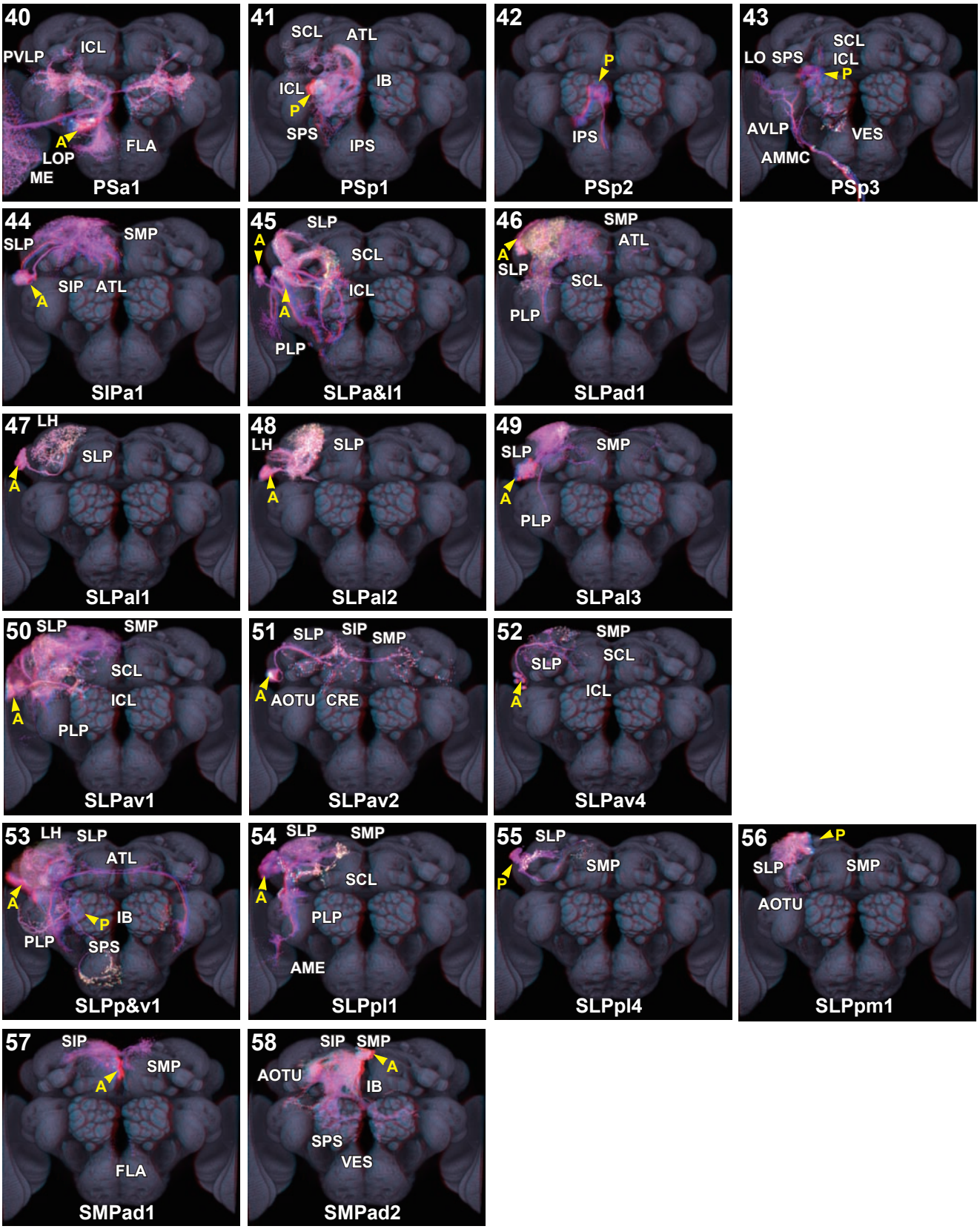

Figure S1 (part 8) Identified clonal units in the adult Drosophila brain (3D stereograms).

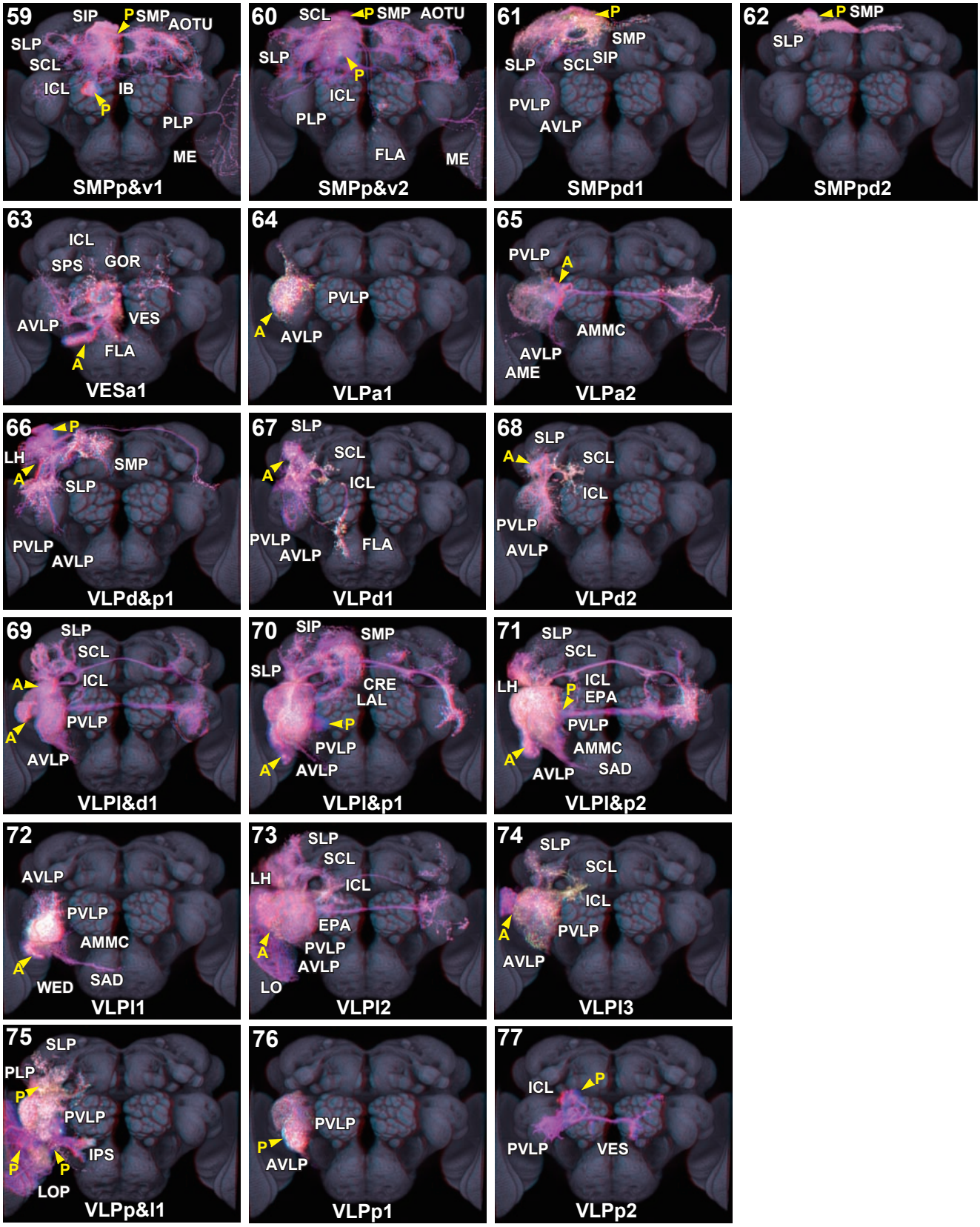

Figure S1 (part 9) Identified clonal units in the adult Drosophila brain (3D stereograms).

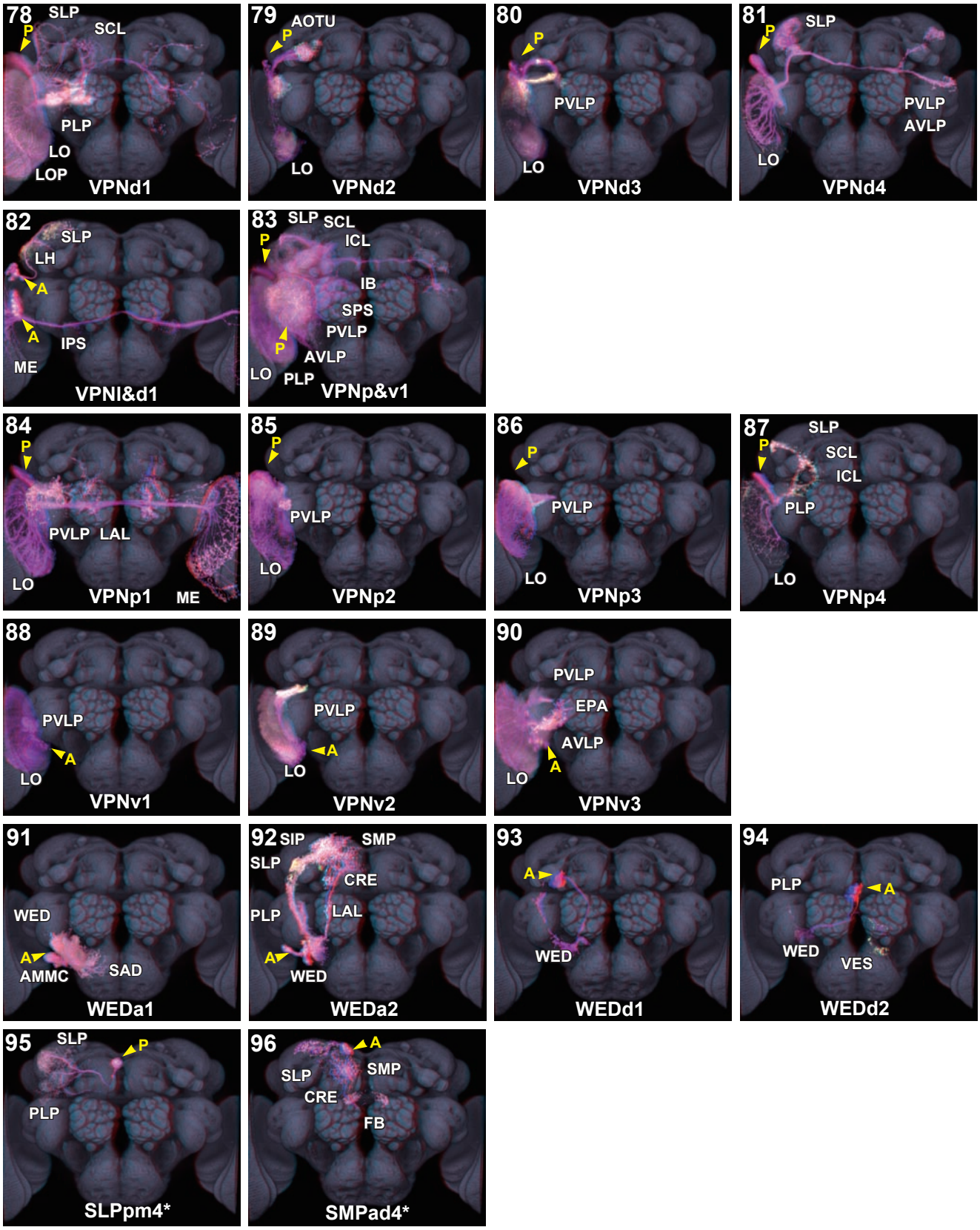

Figure S1 (part 10) Identified clonal units in the adult Drosophila brain (3D stereograms).

Figure S1 (part 1-10) Identified clonal units in the adult *Drosophila* brain. (related to Fig. 1) Frontal views of 3D reconstructions as in Fig. 1. Part 1-5 shows flat reconstruction views. Part 6-10 shows 3D stereogram version of the same images; depth information can be obtained when the images are viewed through red-cyan stereo glasses (red: left eye, cyan: right eye). Cell bodies and neuronal fibers (magenta), distributions of presynaptic sites (white), and the entire neuropil of the template brain (grey) are shown. Arrowheads indicate the location of cell body clusters. Characters A and P denote their positions in the anterior or posterior brain, respectively. Note that the intensity of the labeling may not represent the number of neurons contributing to the structure. For example, massive labeling of the MB in the DM3 clone (No. 18) is actually formed by the extensive branches of a single cell, which is likely to be the dorsal paired medial (DPM) neuron. Scale bar equals to 50 μm. Genotypes: *elav^{c155}-Gal4 hs-FLP/ UAS-DsRed; FRT^{G13} tub-GAL80/ FRT^{G13}; UAS-nSyb::GFP, elav^{c155}-Gal4 hs-FLP/ UAS-Syt::HA; FRT^{G13} tub-GAL80/ FRT^{G13} UAS-GFP*; *UAS*-mCD8::GFP, *hs-FLP tub-GAL80 FRT^{19A}/ UAS-DsRed FRT^{19A}; actin-Gal4/ +; UAS-n-Syb::GFP*, *hs-FLP tub-GAL80 FRT^{19A}/FRT^{19A}; actin-Gal4/ UAS-GFP.*

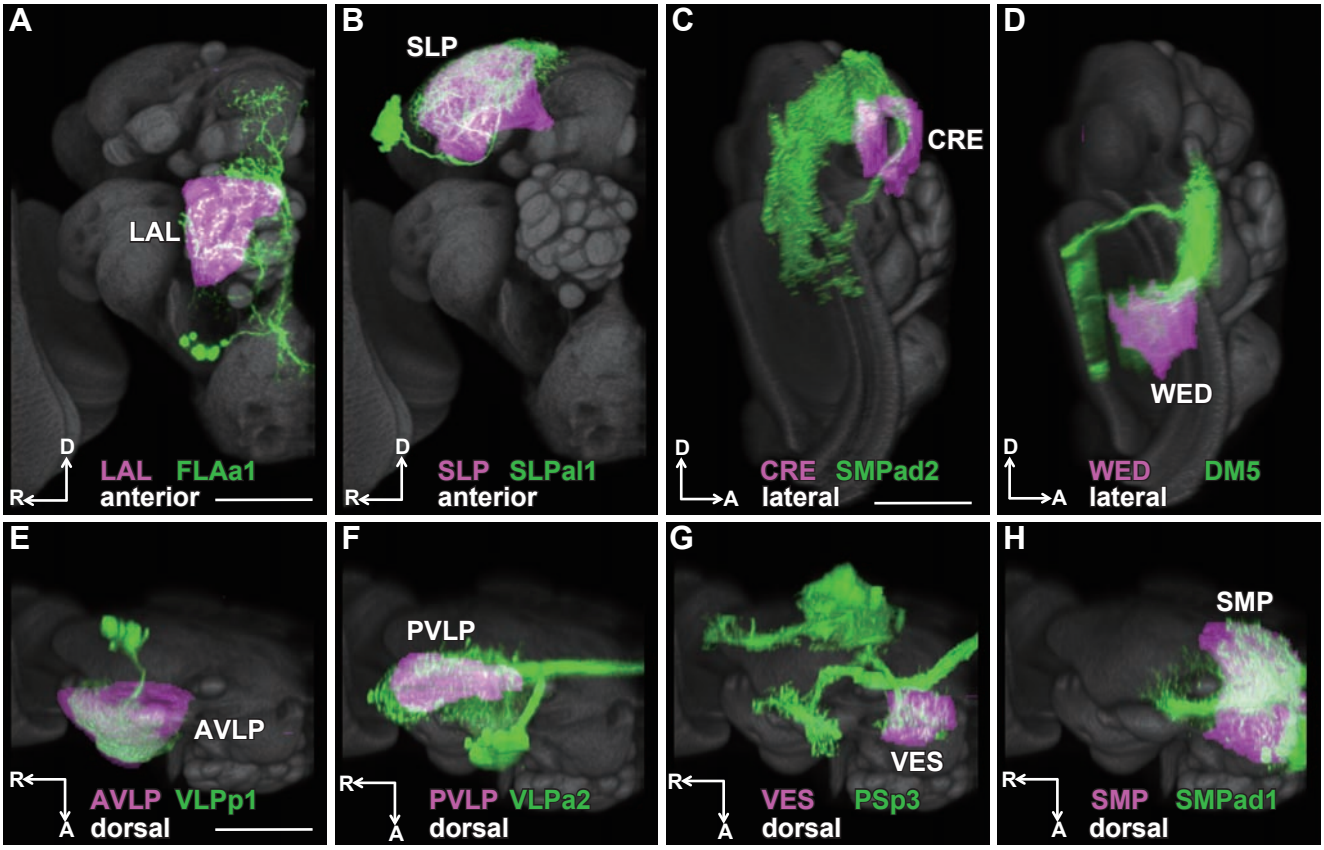

Figure S2 Correlation between clonal units and neuropil boundaries.

Figure S2 Correlation between clonal units and neuropil boundaries. (related to Fig. 2)
(A-H) Overlay of the 3D reconstruction of boundaries of neuropils (magenta) and the clonal units arborizing in these neuropils (green). (A) LAL, anterior view; (B) SLP, anterior view; (C) CRE, lateral view; (D) WED, lateral view; (E) AVLP, dorsal view; (F) PVLP, dorsal view; (G) VES, dorsal view; (H) SMP, dorsal view. A: anterior, R: right, D: dorsal (body axis). Scale bar equals to 50 μm. Genotypes: *elav^{c155}-Gal4 hs-FLP/ UAS-DsRed; FRT^{G13} tub-GAL80/ FRT^{G13}; UAS-nSyb::GFP, elav^{c155}-Gal4 hs-FLP/ UAS-Syt::HA; FRT^{G13} tub-GAL80/ FRT^{G13} UAS-GFP*; *UAS*-mCD8::GFP, *hs-FLP tub-GAL80 FRT^{19A}/ UAS-DsRed FRT^{19A}; actin-Gal4/ +; UAS-n-Syb::GFP*.

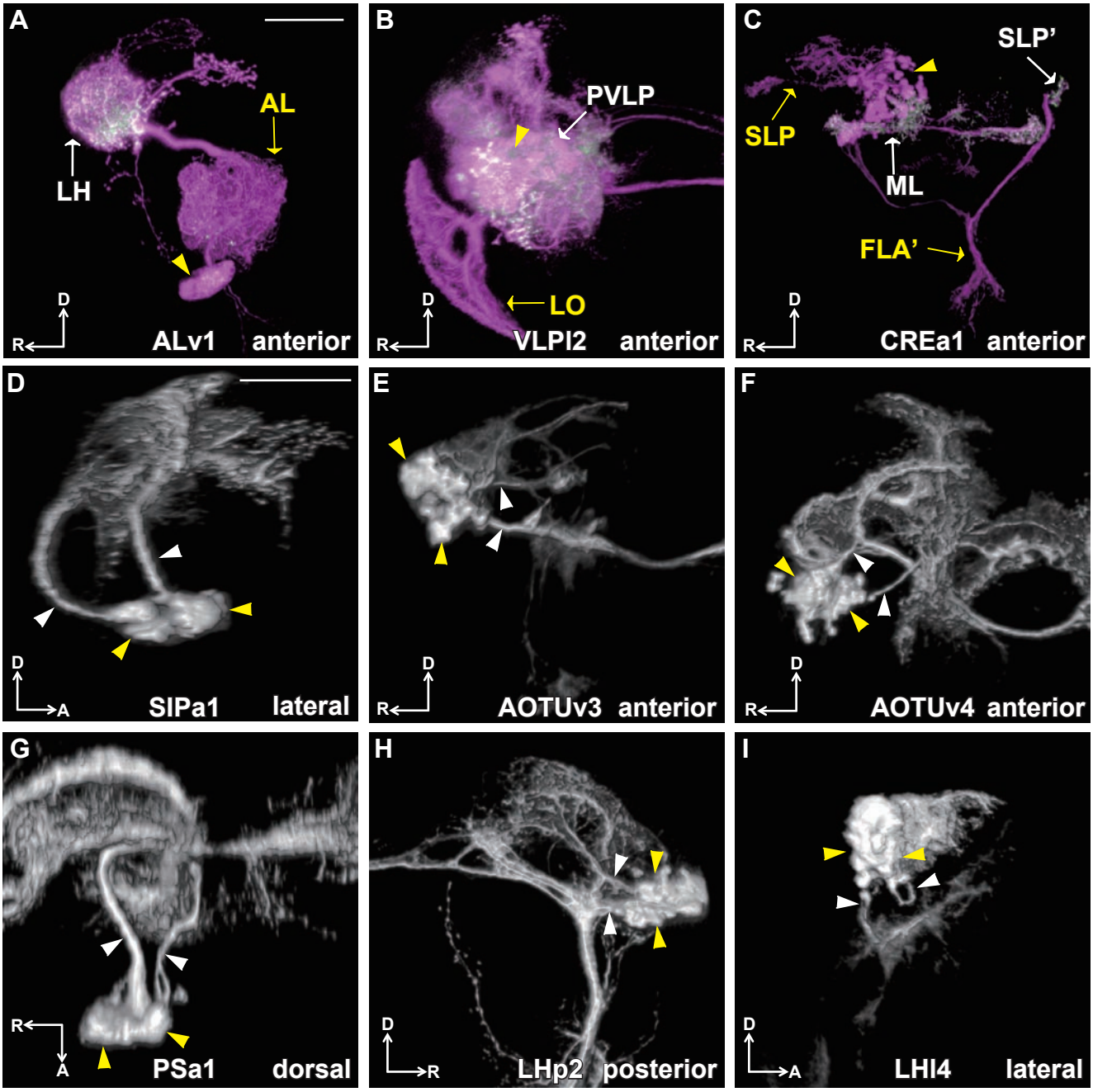

Figure S3 Detailed aspects of clonal units.

Figure S3 Detailed aspects of clonal units (related to Fig. 3)

(A-C) Clonal units with polarized distribution of presynaptic sites. Cell bodies and neuronal fibers (magenta), distributions of presynaptic sites (white). Yellow arrowheads indicate the cell body cluster. White and yellow arrows indicate the arborization with and without presynaptic sites, respectively. (A) A clonal unit with presynaptic sites mainly on the distal part of neurites, anterior view. (B) A clonal unit with presynaptic sites mainly on the proximal part of neurites, anterior view. (C) A clonal unit with presynaptic sites either on the distal or proximal part of neurites depending on branches, anterior view. (D-I) Clonal units with fused but distinguishable masses of cell body clusters. Yellow arrowheads indicate two masses of cell bodies in the cluster. White arrowheads indicate the fiber bundles arising from them; (D) lateral view, (E, F) anterior view, (G) dorsal view, (H) posterior view, (I) lateral view. A: anterior, R: right, D: dorsal (body axis). Scale bar equals to 50 μm. Genotypes: *elav^{c155}-Gal4 hs-FLP/ UAS-DsRed; FRT^{G13} tub-GAL80/ FRT^{G13}; UAS-nSyb::GFP, elav^{c155}-Gal4 hs-FLP/ UAS-Syt::HA; FRT^{G13} tub-GAL80/ FRT^{G13} UAS-GFP*; *UAS*-mCD8::GFP, *hs-FLP tub-GAL80 FRT^{19A}/ UAS-DsRed FRT^{19A}; actin-Gal4/ +; UAS-n-Syb::GFP*.

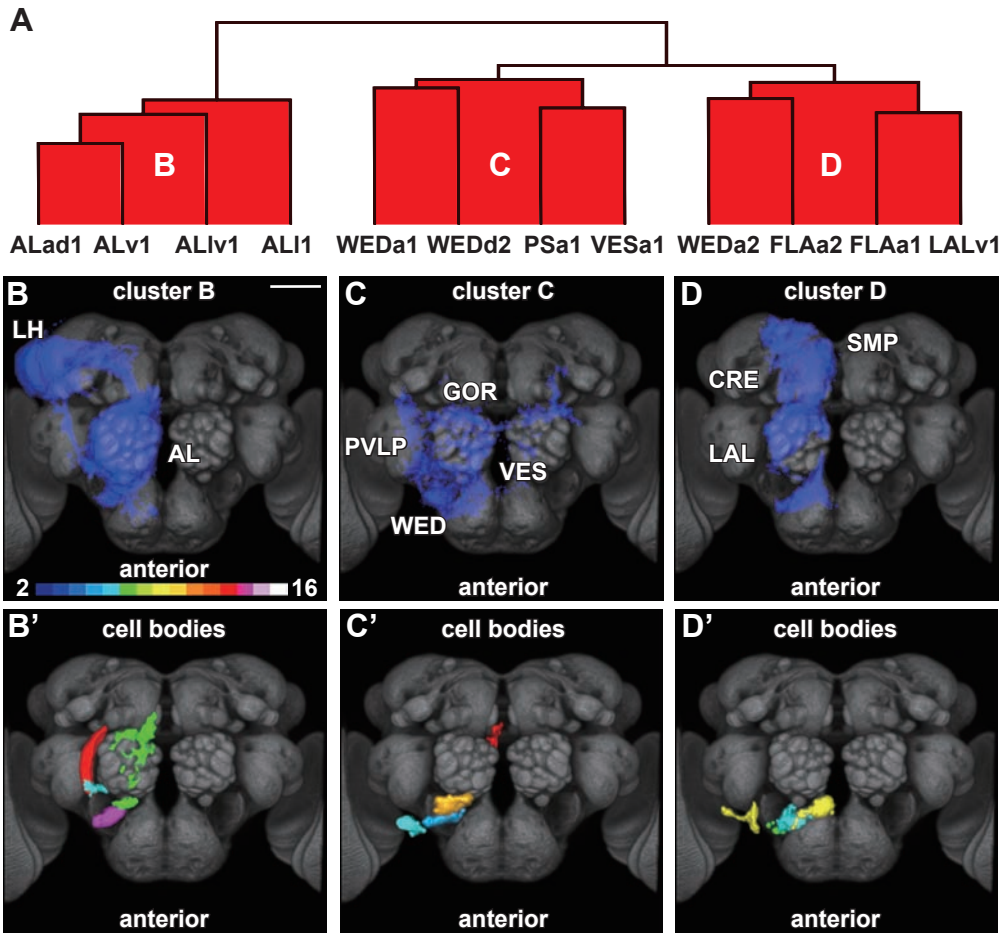

Figure S4 (part 1) Overlap between putative deuto- and tritocerebral clonal units.

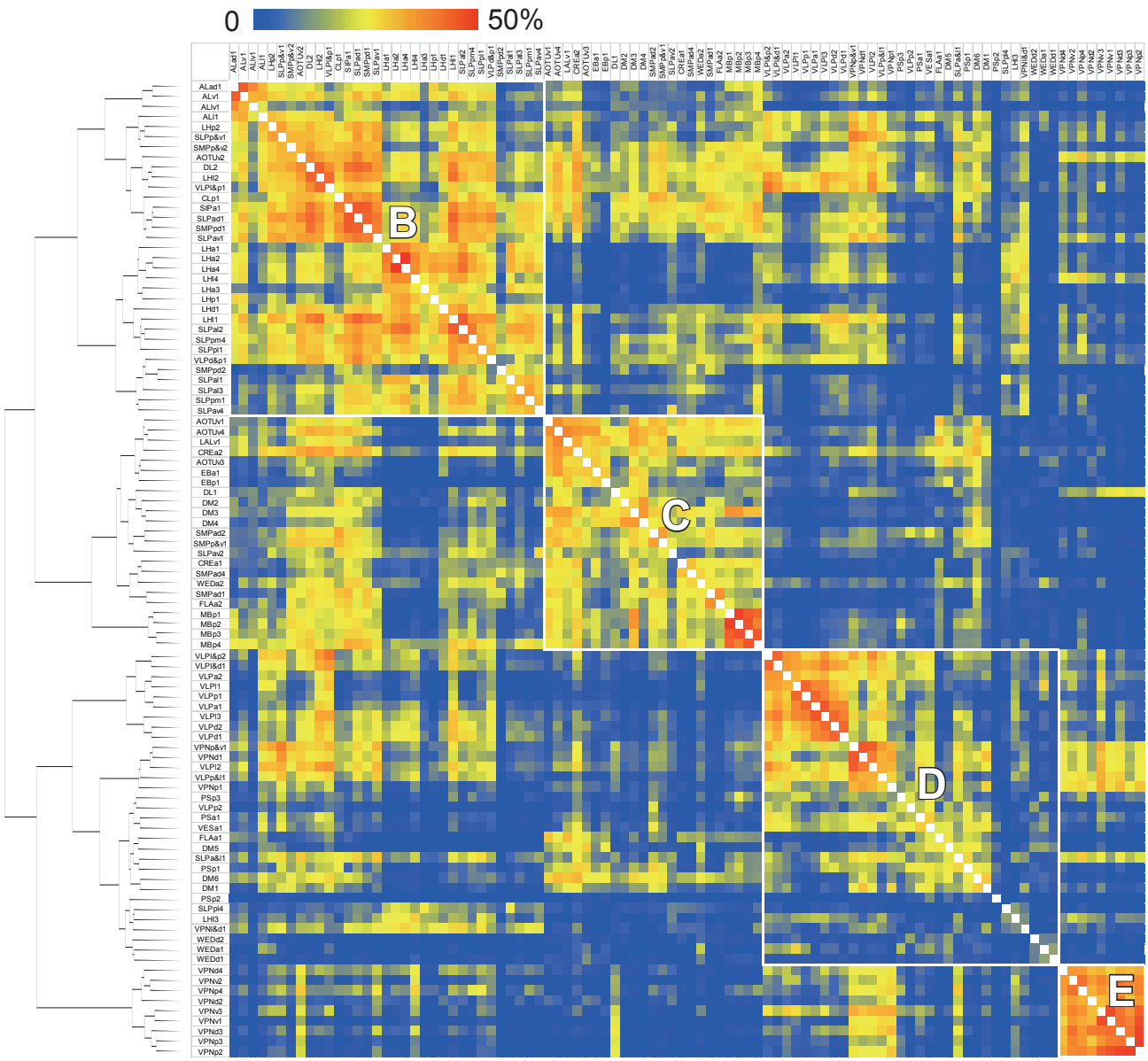

Figure S4 (part 2) Large version of the matrix diagram shown in Fig. 4A.

Figure S4 Overlap between putative deuto- and tritocerebral clonal units (related to Fig. 4)
Part1: (A) Cluster analysis of the clones with spatial overlap. Only clonal units that are unambiguously deuto- or tritocerebral were examined. Their cell bodies reside in the anterior brain at the level around and below the deutocerebral AL neuropil. Clonal units with their cell bodies in the lateral and posterior ventral parts of the cerebrum were not included, because neuromere boundaries remain ambiguous in these sides. (B-D) Overlay images of the clones that form the three clusters indicated in (A). Upper panels show the overlay of arborizations (color code denotes the number of overlapping clones). Major neuropils contributed by these clonal units are indicated in each panel. Lower panels show the distribution of cell bodies of these clones (shown in different colors). Scale bar equals to 50 μm.
Part 2 (Large version of Fig. 4A): Cluster analysis of the clones with spatial overlap. Color code denotes the number of overlapping voxels between each combination of clones. Boxes B-E framed in white show the four clusters of clones with high spatial overlap.

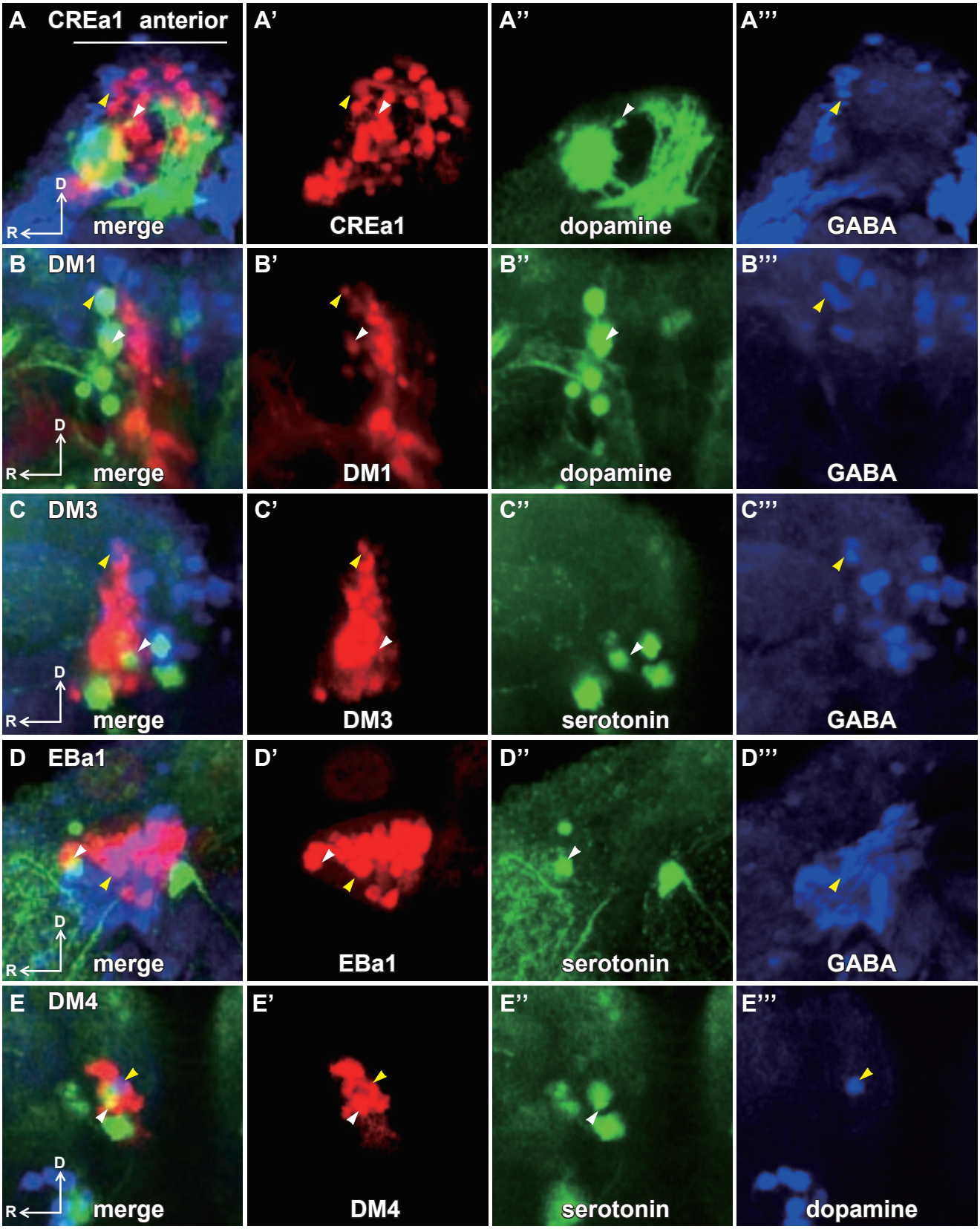

Figure S5 Spatial correlation between clones and transmitters.

Figure S5 Spatial correlation between clones and transmitters. (related to Table 1)

Overlay of the sections of different samples registered to the template volume. For each row of panels (A-E), the first panel indicates the merged image, the second panel (’) indicates the cell body cluster of the clonal units (red), and the third (’’) and fourth (’’’) panels show the cell bodies of the neurons with different transmitters (green and blue). White and yellow arrowheads indicate the cell bodies whose positions overlap with that of the indicated clonal units. Note that, because they are registered images of different samples, registration error of up to 10 μm may exist, anterior view. Scale bar equals to 50 μm. Genotypes: *elav^{c155}-Gal4 hs-FLP/ UAS-DsRed; FRT^{G13} tub-GAL80/ FRT^{G13}; UAS-nSyb::GFP, elav^{c155}-Gal4 hs-FLP/ UAS-Syt::HA; FRT^{G13} tub-GAL80/ FRT^{G13} UAS-GFP*; *UAS*-mCD8::GFP, *hs-FLP tub-GAL80 FRT^{19A}/ UAS-DsRed FRT^{19A}; actin-Gal4/ +; UAS-n-Syb::GFP*.

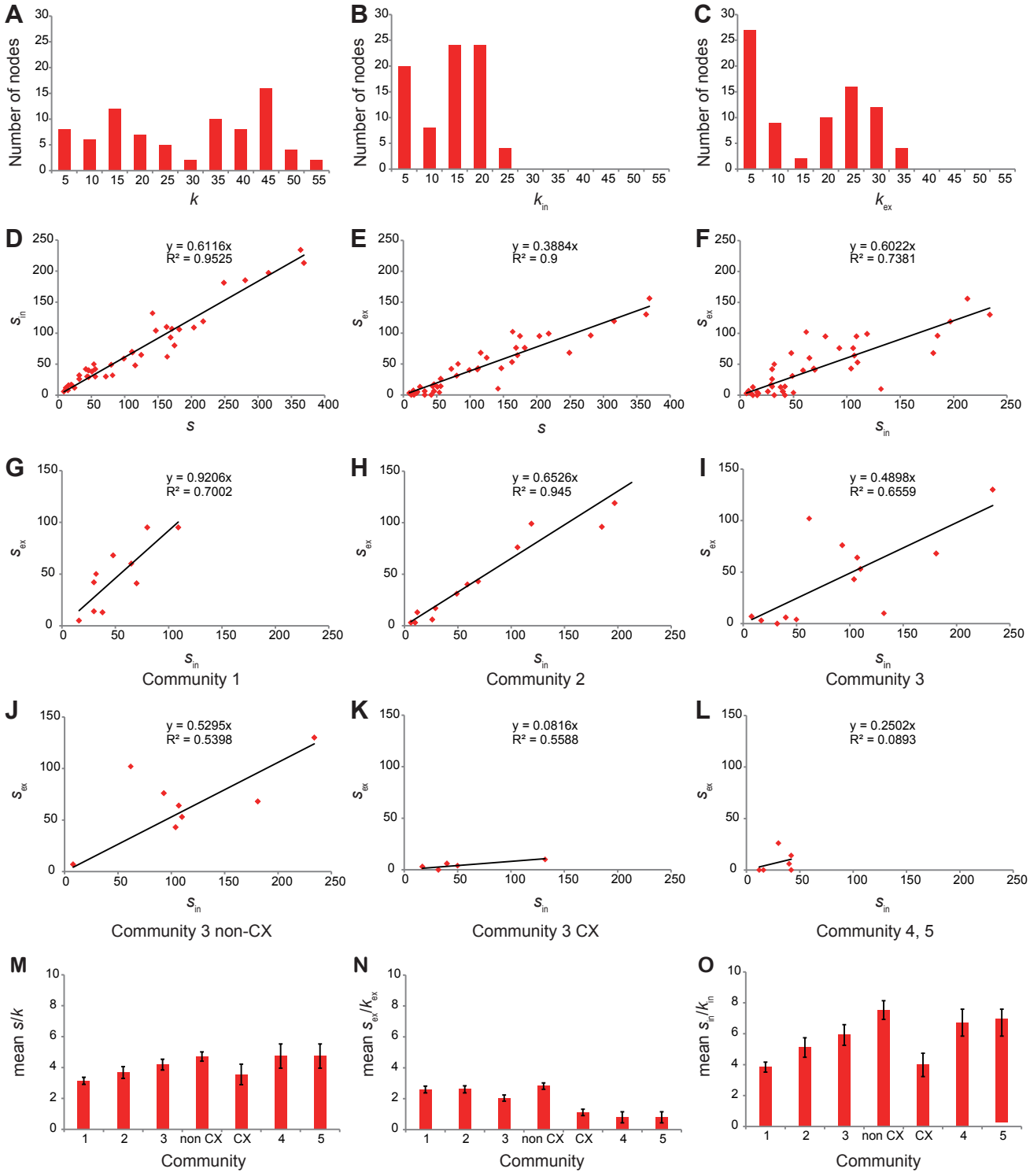

Figure S6 (part 1) Distribution and correlation of node degree and node strength.

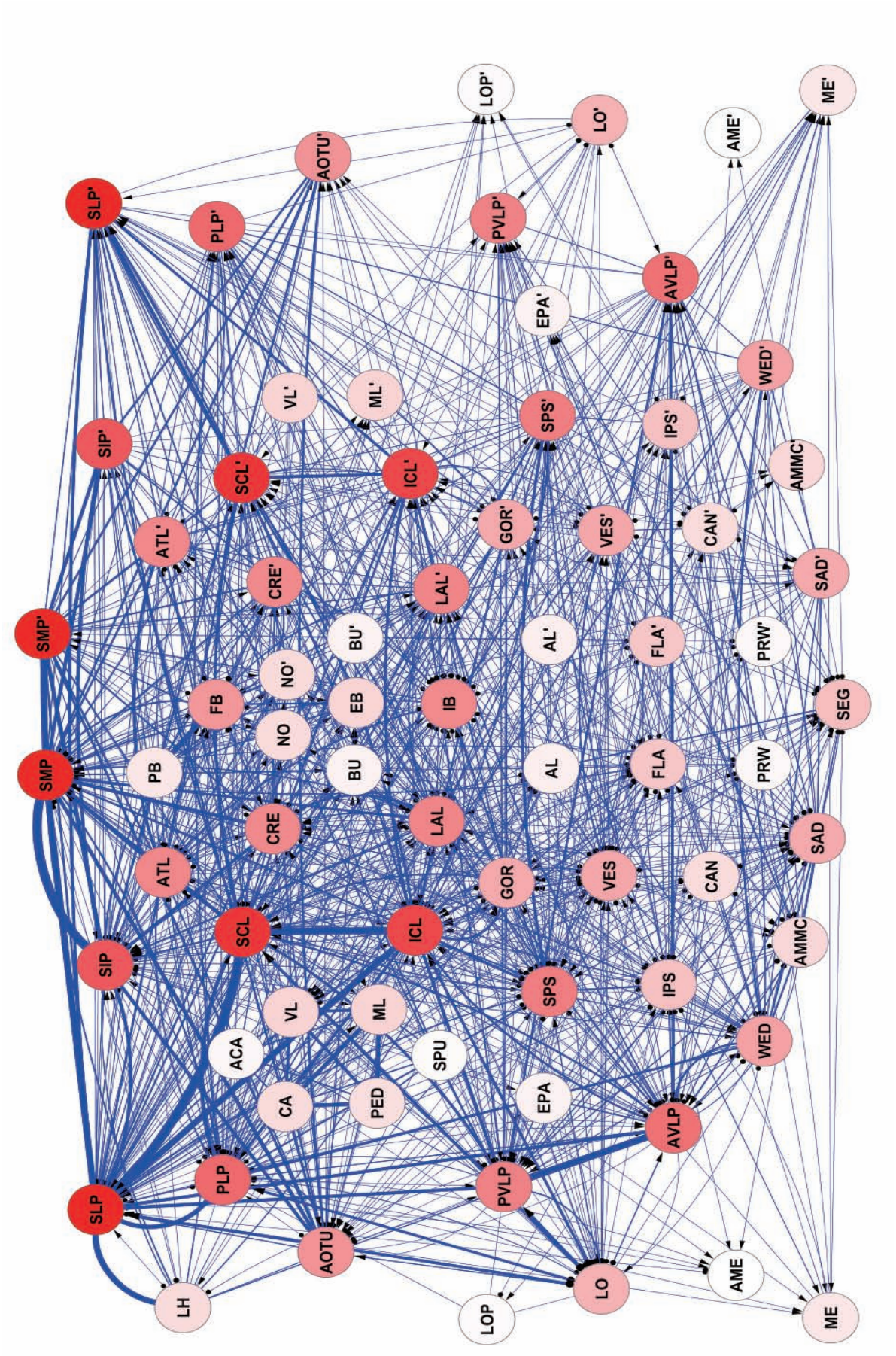

Figure S6 (part 2) Large version of the network diagram shown in Fig. 5A.

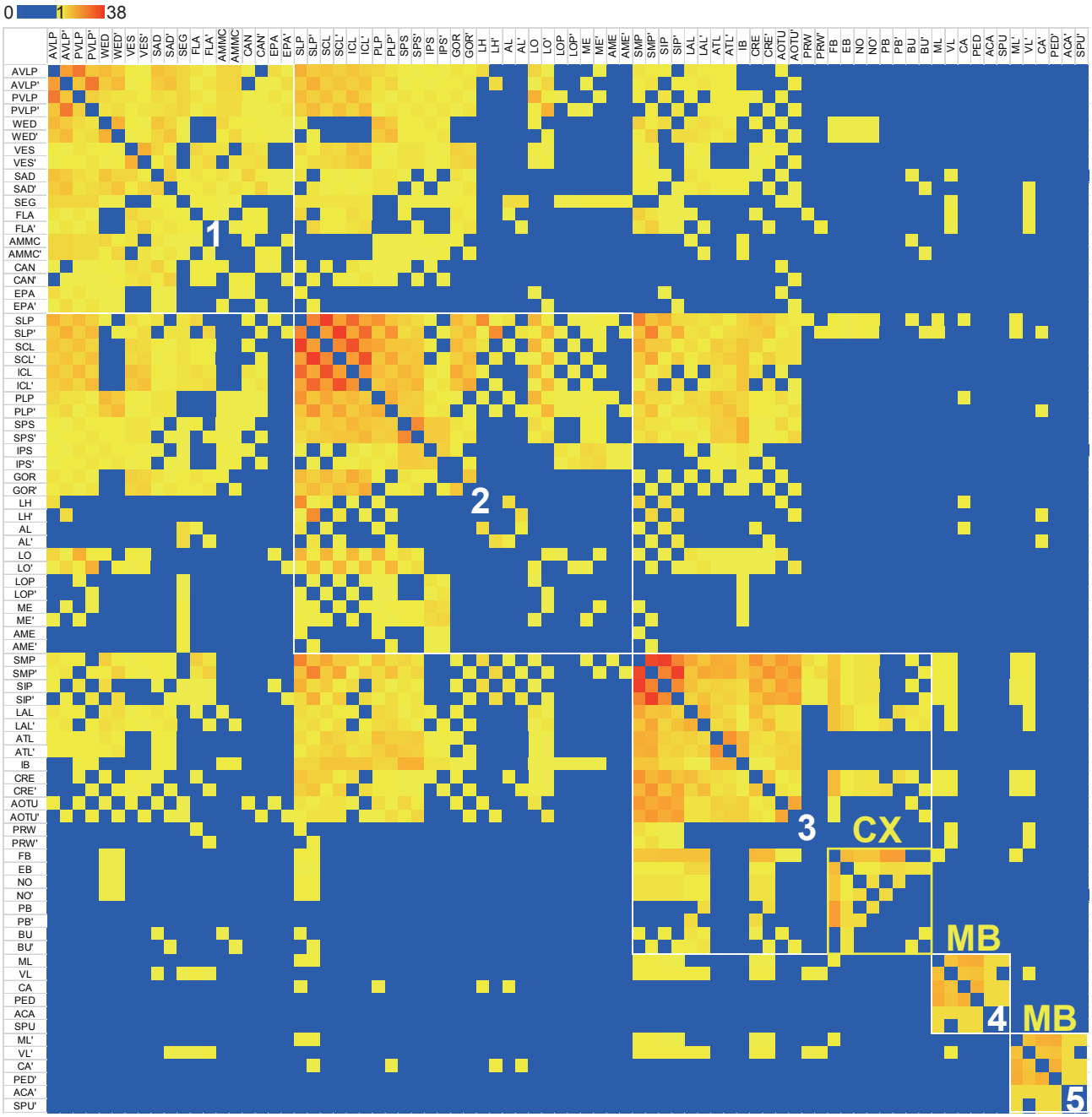

Figure S6 (part 3) Large version of the matrix diagram shown in Fig. 5D.

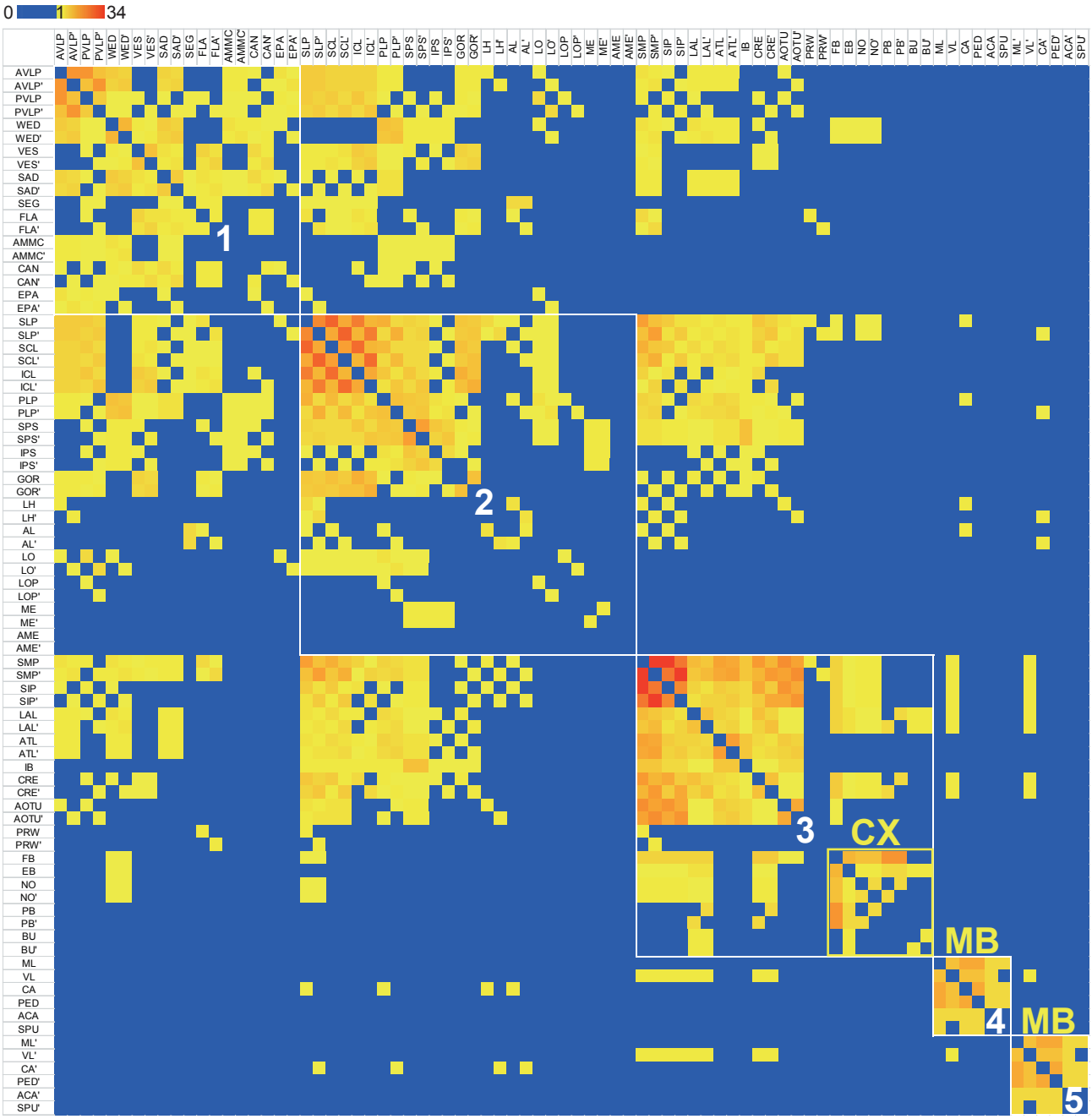

Figure S6 (part 4) Large version of the matrix diagram shown in Fig. 5E.

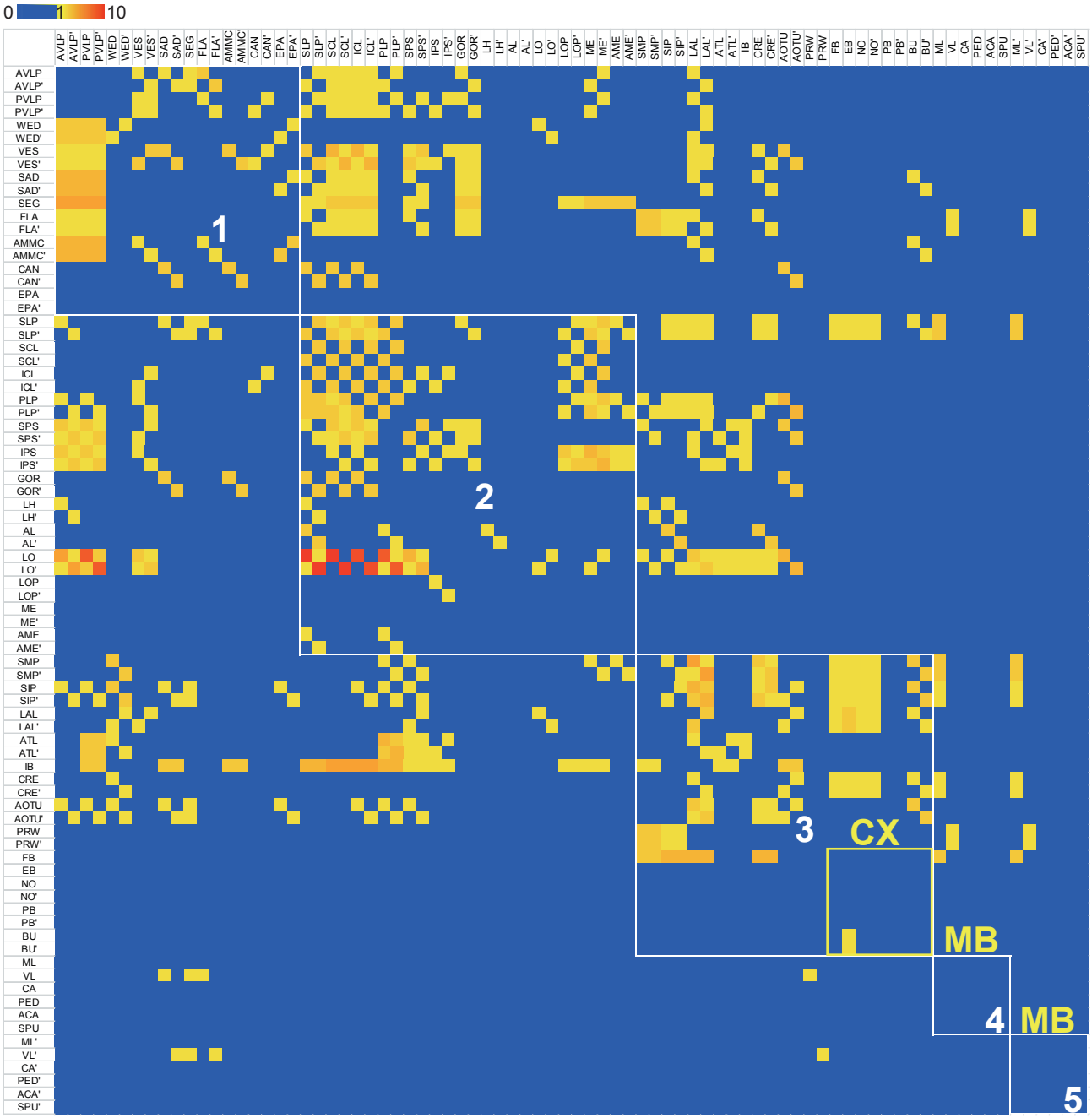

Figure S6 (part 5) Large version of the matrix diagram shown in Fig. 5F.

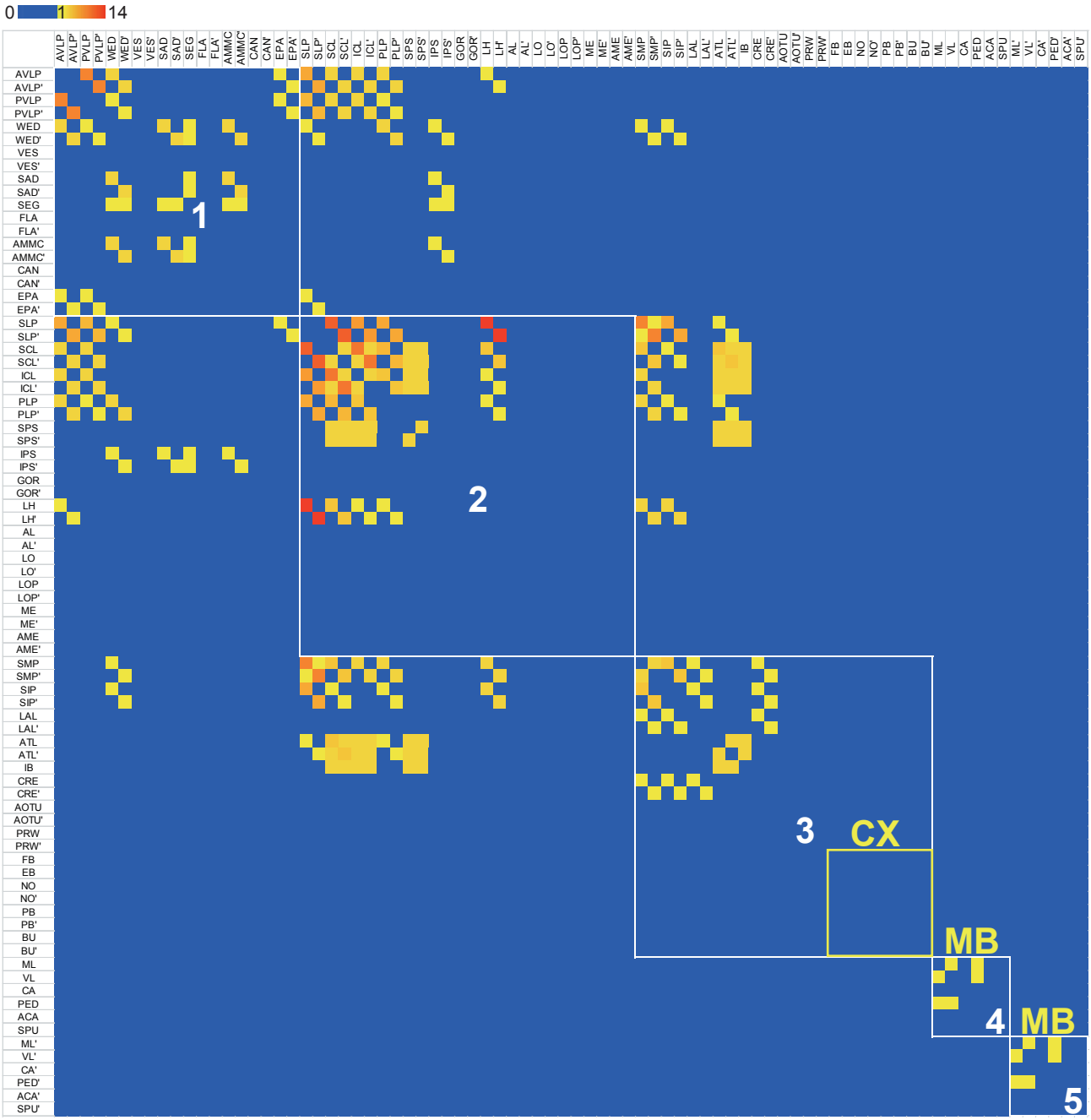

Figure S6 (part 6) Large version of the matrix diagram shown in Fig. 5G.

Figure S6 (part1-6) Distribution and correlation of node degree and node strength. (related to Fig. 5)

Part1: (A) Histogram of node degree (k), showing bimodal distribution. (B) Histogram of the intrinsic node degree (k_{in}), i.e., number of nodes within the same community to which a node is directly connected. (C) Histogram of the extrinsic node degree (k_{ex}), i.e., the number of nodes in different communities to which a node is directly connected. (D-F). Scatter diagrams between node strength (s), intrinsic node strength (s_{in}), i.e., the sum of the link weights (number of connections by projection subgroups) of the k_{in} intracommunity links for the node, and the extrinsic node strength (s_{ex}), i.e., the sum of the link weights of the k_{ex} intercommunity links for the node. y indicates the regression line, and R^2 denotes the coefficient of correlation. (G-L) Scatter diagrams between s_{in} and s_{ex} for communities 1-5. Each diagram is based on a subset of the data used in (F). (I) shows the s_{in} and s_{ex} values of all the neuropils in community 3, (J) shows those of the neuropils in community 3 with the central complex (CX) excluded, and (K) shows those of the central complex neuropils. (M-O) Mean value of s/k, s_{ex}/k_{ex} and s_{in}/k_{in} for each community including central complex and those of regions except central complex in community 3.

Part 2 (Fig. 5A): Network diagram of the connections between neuropils. Neuropil names with apostrophe (’) indicate those in the contralateral side of the brain. Thickness of the lines indicates the number of projection subgroups that contribute to the link between two neuropils. Reddish hue at each neuropil indicates the total number of connections associated with it. Arrows indicate the estimated direction of information, polarizing the direction from the arborization lacking presynaptic sites to that with presynaptic sites. Neuropils in the ventral cerebrum have fewer connections than in the dorsal cerebrum, in part because connections made by the clones in the SEG were not analyzed in the current study.

Part 3 (Fig. 5D): Matrix diagram of connections between neuropils. Color code represents the number of clonal connections. Boxes outlined by white frames indicate the five communities of closely associated neuropils. Box outlined by the yellow frame and denoted CX indicates those neuropils that compose the central complex.

Part 4 (Fig. 5E): Connections of the projection neurons without asymmetric distribution of presynaptic sites.

Part 5 (Fig. 5F): Connections of the projection neurons with asymmetric presynaptic sites. Rows denoted along the ordinates (left sides) indicate the input regions lacking presynaptic sites; rows denoted along the top of the diagram indicate the output regions with presynaptic sites.

Part 6 (Fig. 5G): Connections mediated by locally arborizing clones.

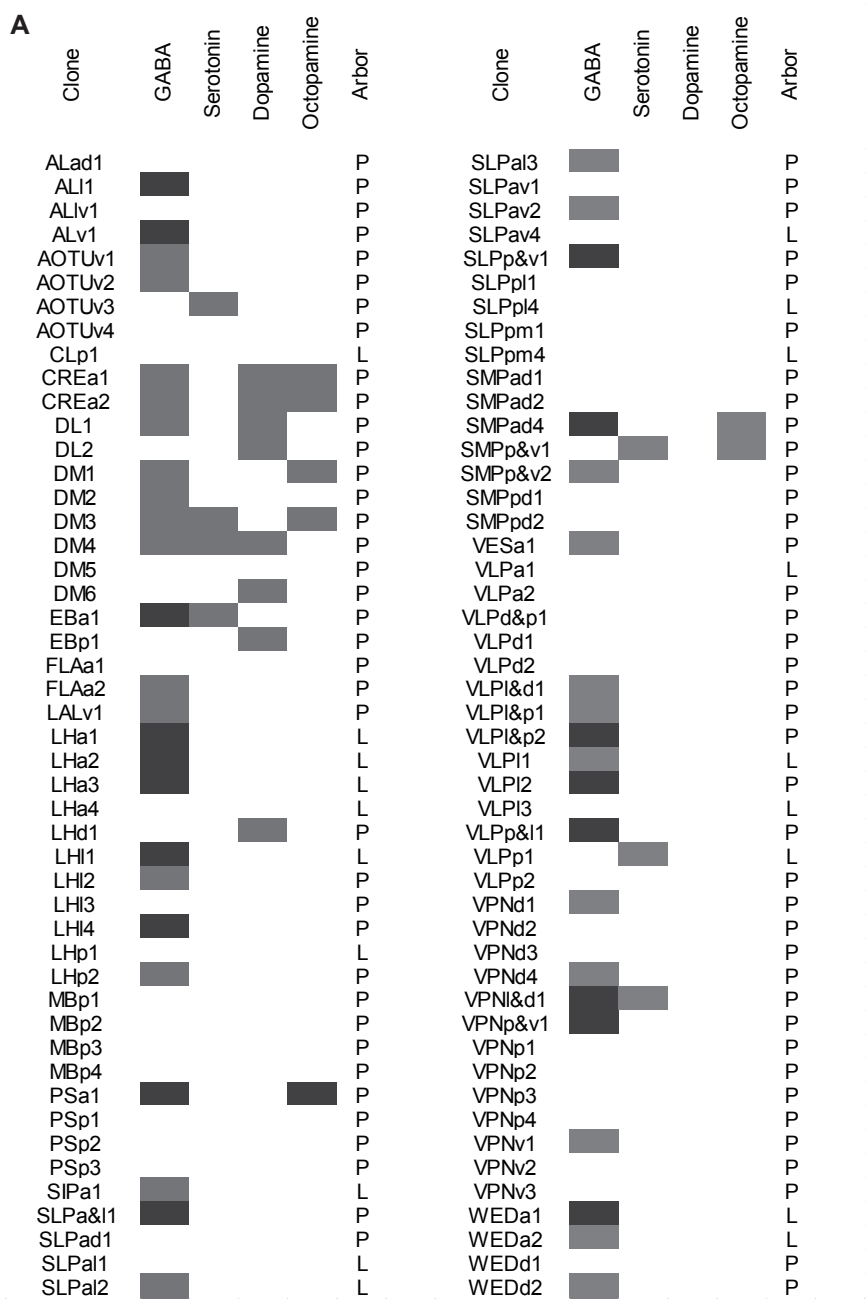

B

	GABA	Serotonin	Dopamine	Octopamine
Local	9	1	0	0
Projection	36	6	8	7

Table 1 Correlation between clones and transmitters.

Table 1 Correlation between clones and transmitters.

(A) Clones that contain neurons with GABA, serotonin, dopamine and octopamine transmitters. Gray and black boxes indicate that a small or large, respectively, subsets of the neurons in the clonal cell cluster are labeled to feature these transmitters. Letters P and L in the column of “Arbor” indicate whether the clone has only local arborizations (L) or contain projection neurons (P). (B) Correlation between transmitters and arborization types of the clones.

Clone name	Number of samples	Number of cell body clusters	Estimated number of cell bodies	Number of cell body fibers	Number of innervated neuropils	Arborization pattern	Distribution of presynaptic sites	fru clones			AL clones			Others
								Cachero et. al. 2010 [1]	Yu et. al. 2010 [2]	Kimura et. al. 2008 [3]	Das et. al. 2013 [4]	Lai et. al. 2008 [5]	Jefferis et. al. 2001 [6]	Previous reported clones
ALad1	7	1	63	1	4	P	B	aDT-a			BAmv3	adPN	adNB	
ALl1	26	1	196	4	16	P	D + B	aDT-e	aDT3	AL3	BAlc	lAL	lNB	
ALlv1	1	1	54	1	7	P	B				BAlp4			
ALv1	17	1	61	1	7	P	D + B	aDT-f			BAla1	vPN		BAla1[7,8]
AOTUv1	2	1	57	2	7	P	D							
AOTUv2	5	1	48	2	13	P	P + B							
AOTUv3	9	1	80	2	19	P	D + P + B	aSP-i	aSP11	AL5a				
AOTUv4	9	1	99	2	12	P	D	aSP-j						
CLp1	15	1	105	1	12	L	L							
CREa1	15	1	107	2	10	P	D + P	aDT-b	aDT2	mAL				
CREa2	11	1	118	2	13	P	D + P	aSP-d		AL4				
DL1	11	2	137 & 48	3	7	P	D + P + B							
DL2	14	2	114 & 18	2	23	P	B							
DM1	26	1	237	4	36	P	D + P + B	pMP-a		pSP1a				DM1[9]
DM2	11	1	215	3	10	P	B	pMP-b		pSP2-2				DM2[9]
DM3	19	1	227	2	16	P	B							DM3[9]
DM4	10	2	96 & 20	2	12	P	B							DM4[9]
DM5	17	1	103	1	4	P	D	pIP-g						DM5[9]
DM6	22	1	251	3	33	P	P + B	pMP-f	pMP4	P2e				DM6[9]
EBa1	19	1	86	2	11	P	D							DALv2[7,8], EB[10]
EBp1	4	1	6	1	5	P	B							
FLAa1	1	1	8	1	5	P	D							
FLAa2	3	1	60	1	10	P	D + P							EM lineage?[11]
LALv1	11	1	105	1	9	P	D							BAmv1[7,8]
LHa1	2	1	58	1	2	L	L							
LHa2	7	1	55	1	2	L	L							
LHa3	2	1	47	1	2	L	L							
LHa4	2	1	50	1	2	L	L							
LHd1	1	1	55	2	11	P	P + B			aSP3a				
LHl1	20	1	49	1	5	L	L							
LHl2	4	1	97	1	13	P	B	aSP-h						
LHl3	1	1	46	1	5	P	D + P							
LHl4	13	1	107	2	7	P	P + B							
LHp1	3	1	30	1	2	L	L							
LHp2	8	1	100	2	16	P	B							
MBp1	21	1	475	1	6	P	B	MB	MB	MB				MB[12,13]
MBp2	12	1	482	1	6	P	B	MB	MB	MB				MB[12,13]
MBp3	10	1	512	1	6	P	B	MB	MB	MB				MB[12,13]
MBp4	27	1	506	1	6	P	B	MB	MB	MB				MB[12,13]
PSa1	23	1	64	2	18	P	D	aDT-g	aDT5 + aDT7					
PSp1	1	1	28	1	12	P	B							
PSp2	5	1	33	1	2	P	B			P2d				
PSp3	8	1	45	2	15	P	P	pIP-a	pIP1	P2b				
SIPa1	5	1	70	2	6	L	L							
SLPa&l1	8	2	86 & 70	2	8	P	D + B	aSP-m						
SLPad1	15	1	147	2	12	P	D + B							
SLPal1	3	1	64	1	3	L	L							
SLPal2	6	1	61	1	3	L	L							
SLPal3	6	1	61	1	10	P	D + B							
SLPav1	7	1	60	1	9	P	P + B							
SLPav2	20	1	37	1	14	P	B	aSP-l	aSP7					
SLPav4	5	1	29	1	4	L	L							
SLPp&v1	6	2	56 & 5	3	19	P	D + P + B							
SLPpl1	5	1	62	1	9	P	D + P	pSP-b						
SLPpl4	3	1	45	1	2	L	L							
SLPpm1	2	1	72	1	4	L	L							
SLPpm4	3	1	2	1	3	L	L							
SMPad1	8	1	28	1	5	P	B	aSP-a	aSP2	aSP2				
SMPad2	13	1	50	1	13	P	B	aSP-b		aSP1				
SMPad4	4	1	2	1	7	P	B	aSP-c						
SMPp&v1	19	2	63 & 34	2	23	P	D + B							
SMPp&v2	1	2	55 & 12	2	23	P	D + P							
SMPpd1	9	1	59	2	9	P	B	pSP-a						
SMPpd2	4	1	17	1	4	P	B							
VESa1	3	1	29	1	13	P	B							BAla3[7]
VLPa1	9	1	94	1	2	L	L	aIP-b						
VLPa2	6	1	77	1	11	P	P	aIP-a						
VLPd&p1	12	2	51 & 50	2	10	P	P + B							
VLPd1	2	1	57	1	9	P	D + P							
VLPd2	8	1	50	1	6	P	D							
VLPl&d1	18	2	63 & 66	2	12	P	B	aIP-c		AL5b + AL6b				
VLPl&p1	17	2	78 & 43	3	18	P	B	aIP-g						
VLPl&p2	26	2	92 & 40	2	14	P	P + B							
VLPl1	15	1	100	1	5	L	L							
VLPl2	6	1	194	1	15	P	P + B	aIP-e	aSP9					
VLPl3	2	1	125	1	5	L	L							
VLPp&l1	8	3	53 & 27 & 18	3	9	P	D + B							
VLPp1	7	1	34	1	2	L	L	pIP-c	pIP7?					
VLPp2	3	1	47	1	10	P	D + B							
VPNd1	9	1	123	1	14	P	B							
VPNd2	40	1	44	1	2	P	D			Lv1 + Ld				
VPNd3	22	1	42	1	2	P	B							
VPNd4	1	1	93	1	5	P	D							
VPNl&d1	16	2	106 & 18	2	8	P	P + B	aIP-f						
VPNp&v1	28	2	87 & 44	2	19	P	P + B							
VPNp1	16	1	145	1	13	P	D	pIP-b	pIP8	Lv2				BLD5[8], DC[9]
VPNp2	5	1	34	1	2	P	D							
VPNp3	7	1	40	1	2	P	D							
VPNp4	11	1	45	1	5	P	D							
VPNv1	4	1	51	1	2	P	B							
VPNv2	26	1	59	1	2	P	D							
VPNv3	15	1	42	1	4	P	B							
WEDa1	1	1	67	1	5	L	L							
WEDa2	7	1	75	2	7	L	L							
WEDd1	3	1	62	1	2	P	B							
WEDd2	1	1	24	1	7	P	B							

Table S1 Characteristics of identified clones.

Table S1 Characteristics of identified clones.

“Estimated number of cell bodies” indicates the average cell count estimation of up to three clone samples, counted separately by two individuals. For the clones with multiple cell body clusters, estimated cell count of each cluster is shown separated by “&”. For “Number of Innervated neuropils”, see Table S2B for the detailed neuropils list. “Arborization pattern” is classified as L (Local, which form a single mass of arborization) and P (Projection, which form multiple volumes of arborizations connected with fiber bundles). “Distribution of presynaptic sites” is classified as D (presynaptic sites only on the Distal parts of neurites), P (presynaptic sites only on the Proximal parts of neurites), B (presynaptic sites in Both distal and proximal parts), L (presynaptic sites distributed in the Locally-arborizing clonal units). Clones with multiple subgroups of neurons that form separate projections (i.e. projection subgroups) tend to have different distribution of presynaptic sites depending on subgroups, which are indicated by multiple symbols connected with “+”.

“Comparison of the clone names” is shown for the following studies: Cachero et. al. 2010 [1], Yu et. al. 2010 [2], Kimura et. al. 2008 [3], Das et. al. 2013 [4], Lai et. al. 2008 [5], Jefferis et. al. 2001 [6], Larsen et. al. 2009 [7], Spindler and Hartenstein 2011 [8], Viktorin et. al. 2011 [9], Zheng et al. 2006 [10], Lichtneckert et. al. 2007 [11], Lee et. al. 1999 [12], and Ito et. al. 1997 [13]. Among the clones reported in these studies, only those with convincing identity are listed here in order to avoid confusion by possible misspeculation. Because of the large structural differences between the clones identified in the larval brain and those identified in the adults, for the larval clone studies we compared only lineages for which information in the adult brain is provided [25, 26]. It was not possible to compare with the studies of embryonic clones, because we visualized only postembryonic neurons, whose projection patterns might be different from the embryonic neurons of the same lineage. Question mark (?) is added for the EM lineage, because the reported projection pattern does not match completely with FLAa2. It might correspond either FLAa2, FLAa3 reported in the companion study [1], or a clone that is yet to be identified.

LA	lamina
ALA	accessory lamina
ME	medulla
AME	accessory medulla
LO	lobula
LOP	lobula plate
MB	mushroom body
CA	calyx
ACA	accessory calyx
PED	pedunculus
SPU	spur
VL	vertical lobe
ML	medial lobe
CX	central complex
FB	fan-shaped body
EB	ellipsoid body
PB	protocerebral bridge
NO	noduli
BU	bulb
LAL	lateral accessory lobe
AOTU	anterior optic tubercle
VLP	ventrolateral protocerebrum
AVLP	anterior VLP
PVLP	posterior VLP
PLP	posteriorlateral protocerebrum
WED	wedge
LH	lateral horn
SLP	superior lateral protocerebrum
SIP	superior intermediate protocerebrum
SMP	superior medial protocerebrum
CRE	crepine
CL	clamp
SCL	superior clamp
ICL	inferior clamp
IB	inferior bridge
ATL	antler
AL	antennal lobe
VES	vest
GOR	gorget
EPA	epaulette
PS	posterior slope
SPS	superior posterior slope
IPS	inferior posterior slope
SAD	saddle
AMMC	antennal mechanosensory and motor center
FLA	flange
CAN	cantle
PRW	prow
SEG	subesophageal ganglion

Table S2A (part 1) Abbreviations of the neuropil and fiber bundle names.

aAOTUF	anterior AOTU fascicle
AL-FLAF	AL-FLA fascicle
AL-GCF	AL-great commissure fascicle
AL-IFSF	AL-inferior fiber system fascicle
AL-LALF	AL-LAL fascicle
AL-SLPF	AL-SLP fascicle
AL-VESF	AL-VES fascicle
AMMC-IFSF	AMMC-inferior fiber system fascicle
AOT	anterior optic tract *
AOTU-BUF	AOTU-BU fascicle
AOTU-IFSF	AOTU-inferior fiber system fascicle
AOTU-LALF	AOTU-LAL fascicle
AOTU-PLPF	AOTU-PLP fascicle
AOTU-SLPF	AOTU-SLP fascicle
AOTU-SPSF	AOTU-SPS fascicle
aSEC-AOTUF	anterior superior ellipsoid commissure-AOTU fascicle
aSLPF	anterior SLP fascicle
AST	anntenal lobe-subesophageal ganglion tract
ATL-PLPF	ATL-PLP fascicle
ATL-SLPF	ATL-SLP fascicle
AVLP-FLAF	AVLP-FLA fascicle
BU-EBF	BU-EB fascicle
BU-GAF	BU-gall fascicle
CA-PEDF	CA-PED fascicle
CA-STJF	CA-superior fiber system fascicle
CRE-AOTUF	CRE-AOTU fascicle
CRE-FBF	CRE-FB fascicle
CRE-MLF	CRE-ML fascicle
CRE-SMPF	CRE-SMP fascicle
EB-BUF	EB-BU fascicle
EPA-PVLPF	EPA-PVLP fascicle
EPA-SADF	EPA-SAD fascicle
EPA-SCLF	EPA-SCL fascicle
EPA-SIPF	EPA-SIP fascicle
FB-EBF	FB-EB fascicle
FB-GAF	FB-gall fascicle
FB-NOF	FB-NO fascicle
FB-RUF	FB-rubus fascicle
FLA-AVLPF	FLA-AVLP fascicle
FLA-IFSF	FLA-inferior fiber system fascicle
FLA-IPSF	FLA-IPS fascicle
FLA-LALF	FLA-LAL fascicle
GA-BUF	gall-BU fascicle
GC-AVLPF	great commissure-AVLP fascicle
GC-CVF	great commissure-cervical connective fascicle
GC-IPSF	great commissure-IPS fascicle
GC-VESF	great commissure-VES fascicle
GC-WEDF	great commissure-WED fascicle
hVLPF	horizontal VLP fascicle
IB-PLPF	IB-PLP fascicle
IB-SCLF	IB-SCL fascicle
IB-SMPF	IB-SMP fascicle
ICCF	inferior cerebro-cervical fascicle
ICL-SLPF	ICL-SLP fascicle
IFS-AMMCF	inferior fiber system-AMMC fascicle
IFS-AOTF	inferior fiber system-anterior optic tract fascicle
IFS-LALF	inferior fiber system-LAL fascicle
IFS-VESF	inferior fiber system-VES fascicle
IFS-WEDF	inferior fiber system-WED fascicle
iSLPF	inferior SLP fascicle
iVLPF	inferior VLP fascicle
LAL-ALF	LAL-AL fascicle
LAL-AOTUF	LAL-AOTU fascicle
LAL-aSECF	LAL-anterior superior ellipsoid commissure fascicle
LAL-FBF	LAL-FB fascicle
LAL-FLAF	LAL-FLA fascicle
LAL-IFSF	LAL-inferior fiber system fascicle
lALT	lateral antennal lobe tract
LEF	lateral equatorial fascicle
LHF	LH fascicle
LO-IPSF	LO-IPS fascicle
LO-PLPF	LO-PLP fascicle
LO-PVLPF	LO-PVLP fascicle
lSLPF	lateral SLP fascicle
LVF	lateral ventral fascicle
lVLPF	laveral VLP fascicle
mALT	medial antennal lobe tract *
MBDL	median bundle *
MEF	medial equatorial fascicle *
MEF-EBF	medial equatorial fascicle-EB fascicle
MEF-FBF	medial equatorial fascicle-FB fascicle
MEF-GAF	medial equatorial fascicle-gall fascicle
MEF-IFS	medial equatorial fascicle-inferior fiber system fascicle
MEF-LALF	medial equatorial fascicle-LAL fascicle
MEF-VESF	medial equatorial fascicle-VES fascicle
mlALT	mediolateral antennal lobe fascicle *
ML-FBF	ML-FB fascicle
PB-FBF	PB-FB fascicle
PB-LALF	PB-LAL fascicle
PB-SFSF	PB-superior fiber system fascicle
PB-SMPF	PB-SMP fascicle
PLF	posterior lateral fascicle *
pLHF	posterior LH fascicle
PLP-AMEF	PLP-AME fascicle
PLP-CAF	PLP-CA fascicle
PLP-CREF	PLP-CRE fascicle
PLP-EPAF	PLP-EPA fascicle
PLP-ICLF	PLP-ICL fascicle
PLP-LALF	PLP-LAL fascicle
PLP-LOF	PLP-LO fascicle
PLP-PVLPF	PLP-PVLP fascicle
PLP-SPSF	PLP-SPS fascicle
pSLPF	posterior SLP fascicle
PVLP-AMMCF	PVLP-AMMC fascicle
PVLP-LOF	PVLP-LO fascicle
PVLP-MEF	PVLP-ME fascicle
PVLP-WEDF	PVLP-WED fascicle
PYF	pyriform fascicle *
SCL-PVLPF	SCL-PVLP fascicle
SFS-PVLPF	superior fiber system-PVLP fascicle
SFS-SLPF	superior fiber system-SLP fascicle
SFS-SPSF	superior fiber system-SPS fascicle
SFS-VLF	superior fiber system-VL fascicle
SLP-LOF	SLP-LO fascicle
SLP-PLPF	SLP-PLP fascicle
SMP-FBF	SMP-FB fascicle
SMP-LALF	SMP-LAL fascicle
SMP-SFSF	SMP-superior fiber system fascicle
SPS-GCF	SPS-great commissure fascicle
SPS-IBF	SPS-IB fascicle
SPS-LALF	SPS-LAL fascicle
vALF	vertical AL fascicle
VES-GORF	VES-GOR fascicle
VES-WEDF	VES-WED fascicle
VLP-ICLF	VLP-ICL fascicle
VLP-SCLF	VLP-SCL fascicle
vSMPF	vertical SMP fascicle
vVLPF	vertical VLP fascicle *
ADC	anterior dorsal commissure
AOTUC	AOTU commissure *
aSEC	anterior superior ellipsoid commissure
ATLC	ATL commissure
GC	great commissure
GORC	GOR commissure
iALC	inferior AL commissure
IBC	IB commissure
iEBC	inferior EB commissure
LALC	LAL commissure
MDC	middle dorsal commissure
MLC	medial lobe commissure
POC	posterior optic commissure *
pSEC	posterior superior ellipsoid commissure
SAC	superior arch commissure
sAMMCC	superior AMMC commissure
SLP-ICL'C	SLP-contralateral ICL commissure
SMPC	SMP commissure
sPLPC	superior PLP commissure
SPS-ICL'C	SPS-contralateral ICL commissure
VESC	VES commissure
WEDC	WED commissure

Table S2A (part 2) Abbreviations of the neuropil and fiber bundle names.

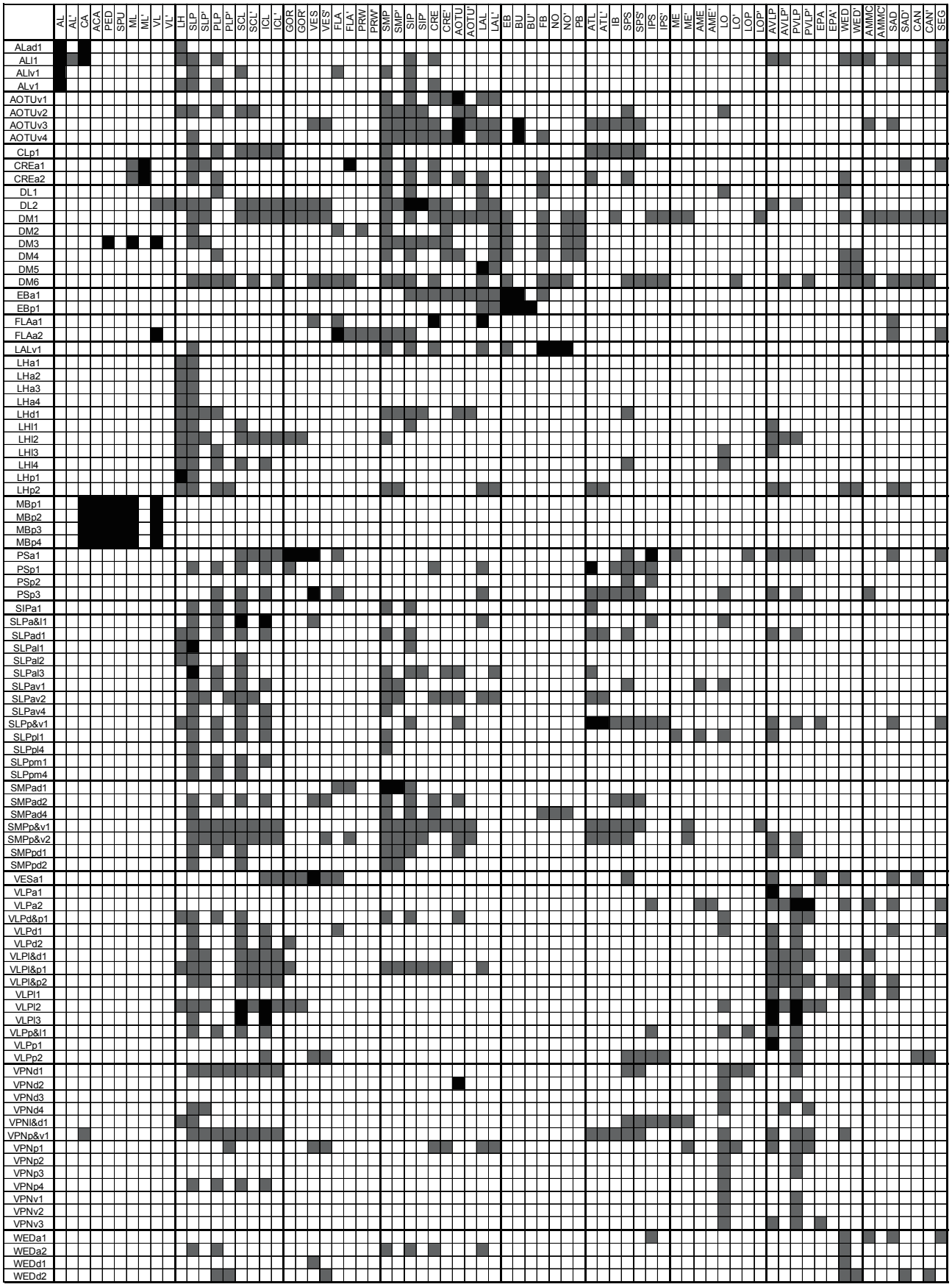

Table S2B List of the neuropils contributed by each clonal unit.

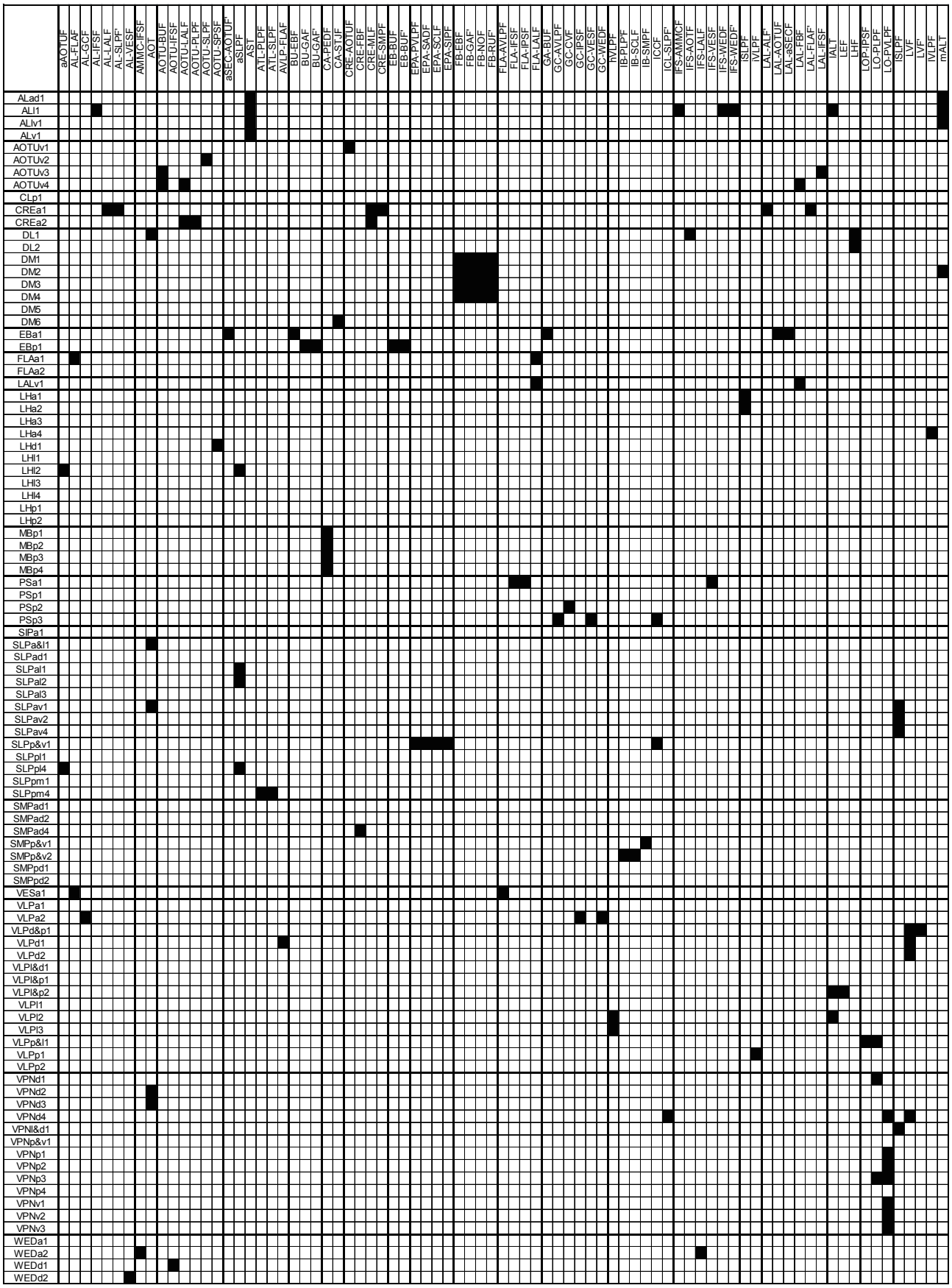

Table S2C (part 1) List of the fiber bundles contributed by each clonal unit.

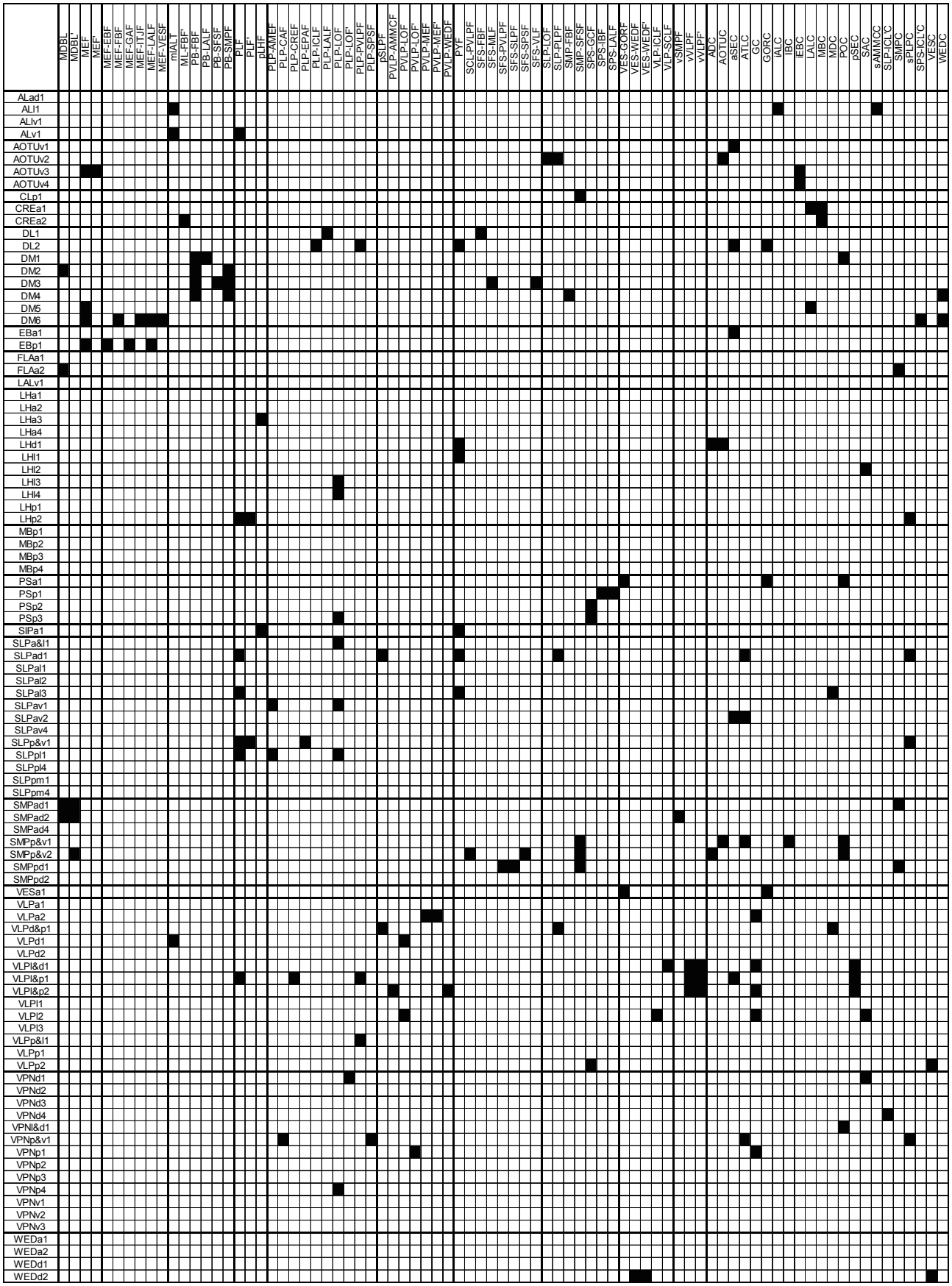

Table S2C (part 2) List of the fiber bundles contributed by each clonal unit.

Table S2 Abbreviations and list of the neuropils and fiber bundles contributed by each clonal unit.

(A) Abbreviations of the neuropil and fiber bundle names. Neuropils names and their abbreviations are according to the proposal of the Insect Brain Name Working Group. Among the 44 proposed neuropils, the clones we identified arborize in 42 neuropils, except for the lamina and the accessory lamina of the optic lobe, the latter of which does not exist in the *Drosophila* brain. For the names of fiber bundles, I used already existing names for known bundles. For newly identified bundles, I named them either with the names of the two neuropils they connect or the name of the neuropil in which the bundle runs through, following the naming scheme of the Insect Brain Name Working Group. The order in which the two neuropils appear in the fiber bundle name is determined from proximal to distal parts of the projections measured from the cell bodies. Occasionally there are two bundles with the same set of neuropil names in the reversed order. They are not identical bundles, as they take different trajectories. There are eight fascicles and two commissures in which projections of different clonal units run in the opposite directions (Fig. 3Q). Asterisks (*) in the list indicate these bundles. The clonal units I identified contributed to 120 unique fascicles in the same side of the cerebrum as their cell body clusters. They also contributed to 20 fascicles in the contralateral side, among which 12 were observed also in the ipsilateral side but eight were found only in the contralateral side. Thus, 128 unique fascicles were identified in the cerebrum. I also found 22 commissures. In total 150 types of fiber bundles were therefore documented.

(B) List of neuropils contributed by each clonal unit. Rows indicate the clonal units, and columns indicate the neuropils. Grey boxes indicate that the neurons of the clone arborize in some parts of the neuropil. Black boxes indicate that the neurons of the clone form broad arborization that matches with the extent of that neuropil.

(C) List of fiber bundles contributed by each clonal unit. Rows denoted along the ordinates (left sides) indicate the clonal units; and rows denoted along the top of the diagram indicate the identified fiber bundles (fascicles: F, or commissures: C). Fascicle names with apostrophe (’) indicate those in the contralateral side of the brain.

ALad1

```
rsAL-<rsAL>{
    -<AL>{
        -o[AL]/
        -|vALF|-o[SEG]}/
    -<AL>{
        -o[AL]/
        -|mALT|-<CA>{
            -o[CA]/
            -|mALT|-o[LH]}}}
```

ALl1

```
rlAL-<rlAL>{
    -o[AL]/
    -o[AL]-|iALC|-o[AL']/
    -<AL>{
        -o[AL]/
        -|vALF|-o[SEG]}/
    -<AL>{
        -o[AL]/
        -|mALT|-<CA>{
            -o[CA]/
            -o[LH]}}/
     -<AL>{
        -o[AL]/
        -|mlALT|-o[PLP]}/
    -<AL>{
        -o[AL]/
        -|lALT|-o[LH]}/
    -<AL>{
        -[AL]/
        -|lALT|-o[SLP+SIP+CRE]}/
    -|AL-IFSF|-<IFS>{
        -|IFS-AMMCF|-o[AMMC+SAD+SAD']/
        -|IFS-WEDF|-o[WED+AVLP]/
        -|sAMMCC|-|IFS-WEDF'|-o[WED'+AVLP']}}
```

ALlv1

```
rilAL-<rilAL>{
    -<AL>{
        -[AL]/
        -|vALF|-[FLA+SEG]}/
    -<AL>{
        -[AL]/
        -|mALT|-[SCL+SLP]}/
    -<AL>{
        -[AL]/
        -|mALT|-[SIP+SMP]}}
```

ALv1

```
riAL-<riAL>{
    -[AL]-|vALF|-[SEG]/
    -<AL>{
        -[AL]/
        -|mlALT|-o[LH]}/
    -<AL>{
        -[AL]/
        -|mlALT|-<PLP>{
            -|PLF|-o[PLP]/
            -|PLF|-o[SLP+SIP+CRE]}}}
```

AOTUv1

```
raCRE-<raCRE>{
    -|CRE-AOTUF|-[AOTU+SIP+SMP]-o[CRE+LAL]/
    -|CRE-AOTUF|-[AOTU+SIP+SMP]-|aSEC|-o[CRE'+LAL']}
```

AOTUv2

```
riAOTU-<riAOTU>{
    -o[AOTU+SIP+SCL+SMP]-|AOTUC|-o[SMP'+SCL'+SIP'+AOTU']/
    -o[AOTU+SLP+LH]/
    -o[AOTU]-|AOTU-SLP|-|SLP-PLPF|-[PLP+SPS]/
    -o[AOTU]-|AOTU-SLP|-|SLP-LOF|-[LO]}
```

AOTUv3

```
riAOTU-<riAOTU>{
    -<AOTU>{
        -|AOTU-BUF|-o[BU]/
        -[AOTU+SIP+SMP+CRE+LAL]-|LAL-IFSF|-[AMMC+SAD]}/
    -[AOTU+SIP+SMP+ATL+IB]-[IB+ATL'+SMP'+SIP'+AOTU']/
    -<LAL>{
        -[LAL+VES]/
        -|MEF|-[SPS]/
        -|iEBC|-<LAL'>{
            -o[LAL'+VES']/
            -|MEF'|-o[SPS']}}}
```

AOTUv4

```
riAOTU-<riAOTU>{
    -[AOTU+SIP+SMP+SLP]-|AOTU-BUF|-o[BU]/
    -|AOTU-LALF|-<LAL>{
        -|LAL-FBF|-[FB]/
        -o[LAL+CRE+SMP+SIP]/
        -|iEBC|-o[LAL'+CRE'+SMP'+SIP']}}
```

CLp1

```
rpSMP-<rpSMP>{
     -|SMP-SFSF|-o[SMP+SCL+ICL+SLP+PLP]/
     -|SMP-SFSF|-o[SCL+SPS+ATL+IB+ATL'+SPS'+SCL']}
```

CREa1

```
raCRE-<raCRE>{
    -<CRE>{
        -|CRE-MLF|-o[ML]-|MLC|-o[ML']/
        -|CRE-SMPF|-<SMP>{
            -[CRE+SIP+SMP+SLP]/
            -[SMP+SLP]}}/
    -|AL-LALF|-|LALC|-<LAL'>{
        -|LAL-FLAF'|-[FLA'+SAD'+SEG]/
        -|LAL-ALF'|-|AL-SLPF'|-o[SLP']}}
```

CREa2

```
raSIP-<raSIP>{
    -|CRE-MLF|-o[ML]-|MLC|-<ML'>{
        -o[ML']/
        -|ML'-FBF|-[FB]}/
    -<SIP>{
        -[SIP+SMP+SLP]/
        -o[ML]-|MBC|-o[ML']}/
    -<SIP>{
        -[SMP+SLP]/
        -o[SIP+CRE+LAL]}/
    -[AOTU+SIP+SMP+ATL]-<AOTU>{
        -|AOTU-PLPF|-o[PLP+SPS]/
        -|AOTU-LALF|-o[LAL+WED]}}
```

Table S3 (part 1) Arborization patterns of clonal units.

EBa1

```
rslAL-<rslAL>{
    -[LAL(GA)]-|GA-BUF|-[BU]-|BU-EBF|-o[EB]/
    -<LAL>{
        -|LAL-AOTUF|-[AOTU]/
        -[LAL+CRE+SIP]-|LAL-aSECF|-|aSEC|-
         |aSEC-AOTUF'|-o[AOTU']}/
     -|LAL-aSECF|-<aSEC>{
         -[FB]/
         -|aSEC|-o[CRE'+SIP'+LAL']}}
```

EBp1

```
rpSPS-|MEF|-<MEF>{
    -|MEF-LALF|-o[LAL]/
    -|MEF-GAF|-o[LAL(GA)]/
    -|MEF-EBF|-o[EB]-<EB>{
       -|EB-BUF|-o[BU]-|BU-GAF|-o[LAL(GA)]/
       -|EB-BUF'|-o[BU']-|BU-GAF'|-o[LAL'(GA)]}}
```

DL1

```
rpLH-<rpLH>{
    -|LHF|-<SFS>{
        -o[SIP+SMP]/
        -|SFS-FBF|-o[FB]}/
    -|LHF|-<SFS>{
        -o[SIP+SMP]/
        -|SFS-FBF|-o[FB]}}

rpPLP-<rpPLP>{
    -o[PLP+WED]-|IFS-AOTF|-|AOT|-o[LO]/
    -|PLP-LAL|-[LAL+AVLP]-|IFS-AOTF|-|AOT|-o[LO]}
```

DL2

```
rpLH-<rpLH>{
    -<LH>{
        -o[LH]/
        -|PYF|-o[SLP+SIP+SMP]}/
    -|LHF|-<SFS>{
        -o[SIP+SMP+VL(α')+CRE+LAL]/
        -|aSEC|-o[SIP'+SMP'+VL'(α')+CRE'+LAL']}}

rpPLP-<rpPLP>{
    -|PLP-PVLPF|-o[PVLP+AVLP+SLP]/
    -|PLP-ICLF|-o[SCL+SLP+ICL+VES+GOR]-|GORC|-
    o[GOR'+VES'+ICL'+SCL'+SLP']}
```

DM1

```
rpPB-<rpPB>{
    -o[PB]-|PB-FBF|-o[FB]-|FB-EBF|-o[EB]/
    -o[PB]-|PB-FBF|-o[FB]-|FB-NOF|-o[NO']/
    -o[PB]-|PB-FBF|-o[FB]-|FB-RUF'|-o[CRE'(RU)]/
    -o[PB]-|PB-FBF|-o[FB]-|FB-GAF'|-o[LAL'(GA)]/
    -|PB-LALF|-<LAL>{
        -o[LAL+WED]/
        -[CRE+SMP+SIP]}/
    -[IB+VES+GOR+CAN]-o[SAD+AMMC]/
    -[IB+VES+GOR+CAN]-o[ICL+SCL+SLP+AOTU]/
    -[IB+VES'+GOR'+CAN']-o[SAD'+AMMC']/
    -[IB+VES'+GOR'+CAN']-o[ICL'+SCL'+SLP'+AOTU']/
    -<IB>{
        -[IPS+SEG]/
        -[IPS']/
        -|POC|-o[ME]}/
    -<IB>{
        -[IPS'+SEG]/
        -[IPS]/
        -|POC|-o[LOP']}/
    -<IB>{
        -[IPS'+SEG']/
        -[IPS]/
        -|POC|-o[ME']}}
```

DM2

```
rpPB-<rpPB>{
    -o[PB]-|PB-FBF|-o[FB]-|FB-EBF|-o[EB]/
    -o[PB]-|PB-FBF|-o[FB]-|FB-NOF|-o[NO']/
    -o[PB]-|PB-FBF|-o[FB]-|FB-RUF'|-o[CRE'(RU)]/
    -o[PB]-|PB-FBF|-o[FB]-|FB-GAF'|-o[LAL'(GA)]/
    -|PB-SMPF|-<SMP>{
        -o[SLP+SMP]-|mALT|-o[FLA+PRW]/
        -o[SLP+SMP]-|MBDL|-o[FLA+PRW]}}
```

DM3

```
rpPB-<rpPB>{
    -o[PB]-|PB-FBF|-o[FB]-|FB-EBF|-o[EB]/
    -o[PB]-|PB-FBF|-o[FB]-|FB-NOF|-o[NO']/
    -o[PB]-|PB-FBF|-o[FB]-|FB-RUF'|-o[CRE'(RU)]/
    -o[PB]-|PB-FBF|-o[FB]-|FB-GAF'|-o[LAL'(GA)]/
    -|PB-SFSF|-<SFS>{
        -|SFS-VLF|-o[VL(A+A')+PED]/
        -|SFS-MLF|-o[ML(B+B'+C)+PED]}/
    -|PB-SMPF|-<SMP>{
        -o[SMP+SIP+CRE+SLP]/
        -o[SMP'+SIP'+CRE'+SLP']}}
```

DM4

```
rpPB-<rpPB>{
    -o[PB]-|PB-FBF|-o[FB]-|FB-EBF|-o[EB]/
    -o[PB]-|PB-FBF|-o[FB]-|FB-NOF|-o[NO']/
    -o[PB]-|PB-FBF|-o[FB]-|FB-RUF'|-o[CRE'(RU)]/
    -o[PB]-|PB-FBF|-o[FB]-|FB-GAF'|-o[LAL'(GA)]/
    -|PB-SMPF|-<SMP>{
        -|SMP-FBF|-o[FB]/
        -o[SMP+SIP+AOTU]}}

rpIPS-<IPS>{
    -o[WED+PLP]/
    -|WEDC|-o[WED']}
```

DM5

```
rpSPS-|MEF|-<LAL>{
    -[LAL+WED]/
    -|LALC|-o[LAL'+WED']}
```

DM6

```
rpSPS-<rpSPS>{
    -|MEF|-<MEF>{
        -|MEF-FBF|-|o[FB+EB+NO+NO']/
        -|MEF-LALF|-o[LAL+WED]/
        -|MEF-LALF|-o[LAL+CRE+SMP+SIP]}/
    -|CA-STJF|-[SMP+SLP+SIP+CRE]-|MDC|-[SMP'+SLP']/
    -|SPS-ICL'C|-<ICL'>{
        -o[ICL'+SCL'+SLP'+PVLP'+AVLP']/
        -|ICL-LOF'|-[LO']}/
    -|MEF|-|MEF-VESF|-<VES>{
        -[VES+CAN+SAD+FLA]/
        -[VES'+CAN'+SAD'+FLA']}/
    -|MEF|-|MEF-ITJF|-<ITJ>{
        -o[WED+AMMC]/
        -o[WED+PLP+SPS+IPS]/
        -|WEDC|-o[WED'+PLP'+SPS'+IPS']}}
```

Table S3 (part 2) Arborization patterns of clonal units.

FLAa1

```
rimAMMC-|AL-FLAF|-<FLA>{
    -[FLA+VES+SAD]/
    -|FLA-LALF|-o[LAL+CRE]}
```

FLAa2

```
riAL-<riAL>{
    -<FLA>{
       -[PRW+FLA+PRW'+FLA']/
       -|MBDL|-<SMP>{
           -o[SMP+SIP]/
           -|pSMPC|-o[SMP']}}/
    -<FLA>{
       -[PRW+FLA+PRW'+FLA']/
       -|MBDL|-o[VL(α)]}/
    -<FLA>{
       -o[PRW+FLA+SAD+SEG]/
       -|MBDL|-[VL(α')]}}
```

LALv1

```
riAL-|FLA-LALF|-[LAL]-<LAL>{
    -|LAL-FBF|-o[FB+EB+NO+NO']/
    -<LAL>{
        -[CRE+SMP]/
        -[SMP+SIP+SLP]}}
```

LHa1

```
rlLH-|iSLPF|-o[SLP+LH]
```

LHa2

```
rlSLP-|iSLPF|-o[LH+SLP]
```

LHa3

```
rlAVLP-|pLHF|-o[LH+SLP]
```

LHa4

```
rlAVLP-|lVLPF|-o[LH+SLP]
```

LHd1

```
raSIP-<raSIP>{
    -o[AOTU]-|AOTU-SPSF|-[SPS+PLP]/
    -o[AOTU+SIP+SMP]-|AOTUC|-o[SMP'+SIP'+AOTU']/
    -o[AOTU]-<SLP>{
        -|PYF|-o[LH]/
        -o[SLP]-|ADC|-o[SLP']}}
```

LHl1

```
rlLH-<rlLH>{
    -o[LH+SLP+AVLP]/
    -|PYF|-o[SLP+SIP+LH]/
    -o[SCL+SLP+SIP]}
```

LHl2

```
rlSLP-<rlSLP>{
    -|aSLPF|-|aAOTUF|-o[SMP+SLP+LH]/
    -[AVLP+PVLP+SLP+SCL+ICL+GOR]-|SAC|-
     [ICL'+GOR'+SCL'+SLP'+AVLP']}
```

LHl3

```
rlSLP-<rlSLP>{
    -[LH+SLP]-o[AVLP]/
    -|PLP-LO|-<PLP>{
        -o[PLP]/
        -[LO]}}
```

LHl4

```
rlLH-<rlLH>{
    -o[LH+SLP]/
    -<PLP>{
        -o[PLP+SPS+SCL+ICL+SLP]/
        -|PLP-LOF|-[LO]}}
```

LHp1

```
rpLH-[LH+SLP]
```

LHp2

```
rpSLP-<rpSLP>{
    -o[LH+SLP+SMP]/
    -<PLP>{
        -|PLF|-o[PLP+WED+AVLP]/
        -|PLF|-o[WED+SAD+LAL]/
        -|sPLPC|-<ATL>{
            -o[ATL+SMP]/
            -<ATL'>{
                -o[ATL'+SMP']/
                -|sPLPC|-<PLP'>{
                    -|PLF'|-o[PLP'+WED'+AVLP']/
                    -|PLF'|-o[WED'+SAD'+LAL']}}}}}
```

MBp1

```
rpCA-<rpCA>{
    -o[CA]-|CA-PEDF|-o[PED+SPU+ML(γ)]/
    -o[CA]-|CA-PEDF|-o[PED+VL(α')+ML(β')]/
    -o[CA+ACA]-|CA-PEDF|-o[PED+VL(α)+ML(β)]}
```

MBp2

```
rpCA-<rpCA>{
    -o[CA]-|CA-PEDF|-o[PED+SPU+ML(γ)]/
    -o[CA]-|CA-PEDF|-o[PED+VL(α')+ML(β')]/
    -o[CA+ACA]-|CA-PEDF|-o[PED+VL(α)+ML(β)]}
```

MBp3

```
rpCA-<rpCA>{
    -o[CA]-|CA-PEDF|-o[PED+SPU+ML(γ)]/
    -o[CA]-|CA-PEDF|-o[PED+VL(α')+ML(β')]/
    -o[CA+ACA]-|CA-PEDF|-o[PED+VL(α)+ML(β)]}
```

MBp4

```
rpCA-<rpCA>{
    -o[CA]-|CA-PEDF|-o[PED+SPU+ML(γ)]/
    -o[CA]-|CA-PEDF|-o[PED+VL(α')+ML(β')]/
    -o[CA+ACA]-|CA-PEDF|-o[PED+VL(α)+ML(β)]}
```

PSa1

```
riAL-<riAL>{
    -|FLA-IFSF|-|IFS-VESF|-<VES>{
        -[SPS+VES+FLA+SAD+SEG]/
        -<SPS>{
            -o[ICL+SCL]/
            -o[ICL'+SCL']/
        -|VES-GORF|-<GOR>{
            -o[GOR+ICL+PVLP+AVLP]/
            -|GORC|-o[GOR'+ICL'+PVLP'+AVLP']}}/
    -|FLA-IPSF|-<IPS>{
        -[IPS]/
        -o[ICL+SCL+GOR+PVLP+AVLP]/
        -|POC|-o[ME]-o[LOP]}}
```

Table S3 (part 3) Arborization patterns of clonal units.

PSp1

```
rpSPS-<SPS>{
    -[SPS+ICL+SCL+GOR+SLP]/
    -[SPS+IPS+PLP]/
    -[SPS+IB+SPS']/
    -|SPS-IB|-[IB+ATL]/
    -|SPS-LALF|-[LAL+CRE]}
```

PSp2

```
rpSPS-<SPS>{
    -[SPS+IPS]/
    -|SPS-GCF|-|GC-CVF|-|CV|-}
```

PSp3

```
rpICL-<rpICL>{
    -<PLP>{
        -o[PLP+ICL+SCL]/
        -|PLP-LOF|-[LO]}/
    -<PLP>{
        -o[PLP+SPS+ATL+IB+ATL'+SPS']/
        -|PLP-LOF|-[LO]}/
    -|SPS-GCF|-<GC>{
         -|GC-VESF|-o[VES+FLA+LAL]/
         -|GC-AVLPF|-<AVLP>{
              -[AVLP+PVLP+AMMC]/
              -|ICCF|-|CV|-}}}
```

SlPa1

```
rlSLP-<rlSLP>{
    -|pLHF|-o[SLP+PLP+SCL+ATL]/
    -|PYF|-o[SLP+SIP+SMP]}
```

SLPa&l1

```
riAOTU-<riAOTU>{
    -o[SLP+PLP+SCL+ICL]/
    -|VLP-SCLF|-o[SLP+SCL+ICL]}

rlSLP-<PLP>{
    -[PLP+IPS]/
    -|PLP-LO|-[LO]/
    -|AOT|-o[LAL+VES]}
```

SLPad1

```
rpSLP-<rpSLP>{
    -|pSLPF|-<SLP>{
        -[LH]/
        -|PYF|-o[SLP+SIP+SMP]/
    -|pSLPF|-o[SLP+SCL+ICL+PVLP]}/
    -<PLP>{
        -|SLP-PLPF|-[PLP+SPS]/
        -|PLF|-o[SLP+PVLP+AVLP]}/
    -|SLP-PLPF|-<PLP>{
        -|PLF|-[PLP]/
        -|sPLPC|-[ATL]-|ATLC|-[ATL']}}
```

SLPal1

```
rlSLP-|aSLPF|-o[SLP+LH+SIP]
```

SLPal2

```
rlSLP-|aSLPF|-o[SLP+SCL+LH]
```

SLPal3

```
rlAOTU-<rlAOTU>{
    -[AOTU+SIP+SMP+ATL]/
    -|PYF|-o[SLP+SCL]/
    -|PLF|-[SLP+PLP+SIP]-|MDC|-o[SIP'+SMP'+CRE'+LAL']}
```

SLPav1

```
rlSLP-<rlSLP>{
    -|lSLPF|-o[SLP+SMP+SMP']/
    -<PLP>{
        -o[PLP+SPS+ICL+SCL+SLP]/
        -|PLP-LOF|-[LO]}/
    -<PLP>{
        -o[PLP+SLP]/
        -|PLP-AMEF|-[AME]}/
    -<PLP>{
        -o[PLP+SLP]/
        -|AOT|-o[ICL+SPS]}}
```

SLPav2

```
rlSLP-|lSLPF|-<SMP>{
    -o[SMP+SLP+SCL+AOTU]/
    -<SMP>{
        -o[SMP+CRE+LAL]/
        -|aSEC|-o[SMP'+CRE'+LAL']}/
    -o[SMP+ATL]-|ATLC|-o[ATL'+SMP']-o[SMP'+SLP'+SCL'+PLP']}
```

SLPav3

```
rlSLP-|lSLPF|-o[SLP+SMP+SCL+ICL]
```

SLPp&v1

```
rlLH-<rlLH>{
    -o[SLP+LH+PLP+SCL+ICL]/
    -<SLP>{
        -|PLF|-[IPS+SPS+IB+ATL]/
        -|sPLPC|-|PLF'|-o[IPS'+SPS'+IB+ATL']}

rpPLP-|PLP-EPAF|-<EPA>{
    -o[EPA+PVLP+ICL]/
    -|EPA-PVLPF|-o[PVLP+AVLP]/
    -|EPA-SIPF|-[SIP+AOTU]/
    -|EPA-SCLF|-[SIP+AOTU]/
    -|EPA-SADF|-<SAD>{
        -o[SAD+SEG]/
        -|ICCF|-o[SAD+SEG]}}}
```

SLPpl1

```
rpLH-<rpLH>{
    -<PLP>{
        -[PLP+SLP+SMP]/
        -|PLF|-|PLP-AMEF|-o[AME+ME]}/
    -<SLP>{
        -o[SLP+SCL+ICL+SMP]/
        -|PLF|-|PLP-LOF|-[LO]}}
```

SLPpl4

```
rsLH-|aSLPF|-|aAOTUF|-o[SLP+SMP]
```

SLPpm1

```
rpSLP-o[SLP+SCL+ICL+PLP]
```

Table S3 (part 4) Arborization patterns of clonal units.

SMPad1

```
rmaSMP-<rmaSMP>{
    -o[SMP+SIP+SMP']/
    -<SMP>{
        -o[SMP]-|MBDL|-o[FLA]/
        -|SMPC|-o[SMP']-|MBDL'|-o[FAL']}}
```

SMPad2

```
raSMP-<raSMP>{
   -|vSMPF|-[SMP+SIP+AOTU]/
   -|vSMPF|-[SMP+CRE]-<CRE>{
       -|MBDL|-[VES]/
       -|MBDL'|-[VES']}/
   -|vSMPF|-[SMP+SLP+SCL+ICL]-<ICL>{
       -[PLP]/
       -[IB+SPS+SPS']}}
```

SMPp&v1

```
rpSMP-<rpSMP>{
   -|SMP-SFSF|-<SFS>{
       -o[SMP+SCL+ICL]/
       -o[SMP+SIP+CRE]}/
   -|SMP-SFSF|-o[SMP+ATL]-|ATLC|-o[ATL'+SMP']-<SMP'>{
       -o[SMP'+SCL'+ICL']/
       -o[SMP'+SIP'+CRE']}}

rpSPS-<rpSPS>{
  -|IB-SMPF|-<SMP>{
       -|AOTUC|-o[SMP+SIP+AOTU]/
       -|AOTUC|-o[SMP'+SIP'+AOTU']}/
   -<IB>{
       -o[IB+SPS+ATL+SMP+SIP+AOTU]/
       -o[IB+SPS'+ATL'+SMP'+SIP'+AOTU']}/
   -<IB>{
       -|IBC|-[ICL+SCL+SLP+PLP]/
       -|IBC|-o[ICL'+SCL'+SLP'+PLP']-<PLP>{
           -|POC|-o[LOP']/
           -|POC|-o[ME']}}}
```

SMPp&v2

```
rpSMP-<rpSMP>{
   -|SMP-SFSF|-<SFS>{
       -o[SMP+SCL+ICL]/
       -|SFS-SPSF|-[SPS+IB]}/
   -|SMP-SFSF|-<SFS>{
       -o[SMP+SCL+ICL]/
       -|MDBL'|-o[FLA'+VES']}/
   -|SMP-SFSF|-o[SMP+SIP+AOTU]-|ADC|-o[SMP'+SIP'+AOTU']}

rpPB-<rpPB>{
   -<IB>{
       -o[IB+ATL+SMP]/
       -o[IB+ATL'+SMP']}/
   -<IB>{
       -|IB-SCLF|-<SCL>{
           -[SCl+ICL+SLP+PLP]/
           -|SCL-PVLPF|-[PVLP+AVLP]}/
       -|IB-PLPF'|-<PLP'>{
           -o[PLP'+SCL'+ICL'+SLP']/
           -|POC|-o[ME']}}}
```

SMPpd1

```
rpSMP-<rpSMP>{
   -|SMP-SFSF|-<SFS>{
       -o[SLP+SCL+PLP]/
       -o[SMP+SIP]-|SMPC|-o[SMP']}/
   -|SMP-SFSF|-<SFS>{
       -|SFS-SLPF|-[SMP+SIP+AOTU]/
       -|SFS-PVLPF|-[PVLP+AVLP]}}
```

SMPpd2

```
rpSMP-o[SLP+SCL+SMP]-o[SMP']
```

VESa1

```
rimAMMC-<rimAMMC>{
   -o[VES+FLA+GOR+ICL+SPS]/
   -|AL-FLAF|-<FLA>{
       -o[SAD+CAN]/
       -|FLA-AVLPF|-o[AVLP+WED+EPA]}/
   -o[VES+FLA]-|VES-GORF|-<GOR>{
       -o[GOR+ICL]/
       -|GORC|-<GOR'>{
           -o[VES']/
           -o[GOR'+ICL']}}}
```

VLPa1

```
raAVLP-o[AVLP+PVLP]
```

VLPa2

```
rlAL-<rlAL>{
   -|AL-GCF|-<GC>{
       -o[PVLP+AVLP]-|PVLP-MEF|-o[ME]/
       -|GC-IPSF|-[IPS+SEG]/
       -|GC|-o[PVLP'+AVLP']-|PVLP-MEF'|-o[ME']}/
   -|AL-GCF|-<GC>{
       -o[PVLP+AVLP]/
       -|GC-WEDF|-[WED+SAD+AMMC]/
       -|GC|-o[PVLP'+AVLP']}}
```

VLPd&p1

```
raSLP-<SLP>{
   -|LVF|-o[PVLP(VGa)]/
   -|MDC|-|LVF'|-o[PVLP'(VGa)]}

rpSLP-<rpSLP>{
   -|pSLPF|-<SLP>{
       -o[LH+SLP+SCL+SMP]/
       -o[SLP+SCL+SIP+SMP+AOTU]/
   -|SLP-PLPF|-<PLP>{
           -[PLP]/
           -[LO]}}
```

VLPd1

```
raSLP-<raSLP>{
   -|LVF|-o[PVLP+SCL+ICL+SLP]-|mlALT|-o[FLA+SAD+SEG]/
   -|LVF|-[PVLP+AVLP+SLP]-|AVLP-FLAF|-o[FLA+SAD+SEG]/
   -|LVF|-<PVLP>{
       -o[PVLP+SCL+ICL+SLP]/
       -|PVLP-LOF|-[LO]}}
```

VLPd2

```
raAOTU-|LVF|-<PVLP>{
    -[PLVP+AVLP+SLP]/
    -o[ICL+SCL+GOR]}
```

Table S3 (part 5) Arborization patterns of clonal units.

VLPl&d1

```
rlAVLP-<rlAVLP>{
    -o[AVLP+PVLP+WED+AMMC]/
    -|GC|-o[AVLP'+PVLP']}

raAVLP-<raAVLP>{
    -<AVLP>{
        -o[AVLP+PVLP]/
        -|VLP-SCLF|-o[SCL+ICL+SLP]}/
    -<AVLP>{
        -o[AVLP+PVLP]/
        -|vVLPF|-|pSEC|-o[SCL'+ICL'+SLP']}/
    -<AVLP>{
        -o[AVLP+PVLP]/
        -|vVLPF|-|pSEC|-|vVLPF'|-o[AVLP']}}
```

VLPl&p1

```
raAVLP-<raAVLP>{
    -<AVLP>{
        -o[AVLP+PVLP]/
        -|vVLPF|-o[SCL+ICL+SLP]}/
    -<AVLP>{
        -o[AVLP+PVLP]/
        -|vVLPF|-|pSEC|-o[SCL'+ICL'+SLP']}/
    -<AVLP>{
        -o[AVLP+PVLP]/
        -|vVLPF|-|pSEC|-|vVLPF'|-o[AVLP']}}

rpPLP-<rpPLP>{
    -<PLP>{
        -|PLP-PVLPF|-o[PVLP+SCL+ICL+GOR]/
        -|PLF|-o[SIP+SMP+CRE+LAL]}/
    -|PLP-CRE|-<CRE>{
        -o[LAL+CRE+SMP+SIP]/
        -|aSEC|-o[SMP'+SIP'+CRE']}}
```

VLPl&p2

```
raAVLP-<raAVLP>{
    -o[AVLP]-|lALT|-o[LH]/
    -<AVLP>{
        -o[AVLP+PVLP]/
        -|vVLPF|-o[SCL+ICL+SLP]}/
    -<AVLP>{
        -o[AVLP+PVLP]/
        -|vVLPF|-|pSEC|-o[SCL'+ICL'+SLP']}/
    -<AVLP>{
        -o[AVLP+PVLP]/
        -|vVLPF|-|pSEC|-|vVLPF'|-o[AVLP']}}

rpPLP-<rpPLP>{
    -|LEF|-<PVLP>{
        -o[PVLP+AVLP]/
        -|PVLP-AMMCF|-[AMMC]/
        -|GC|-o[EPA'+PVLP'+AVLP']}/
    -|LEF|-<PVLP>{
        -o[PVLP+AVLP]/
        -|PVLP-WEDF|-[WED+AMMC+SAD]/
        -|GC|-o[EPA'+PVLP'+AVLP']}}
```

VLPl1

```
rlWED-<rlWED>{
    -o[AVLP+PLVP+WED]/
    -o[WED+SAD+AMMC]}
```

VLPl2

```
raAVLP-<raAVLP>{
    -o[AVLP]-|lALT|-o[LH]}/
    -|hVLPF|-o[AVLP+SLP+PVLP+EPA]/
    -<AVLP>{
        -o[AVLP+PVLP]/
        -|PVLP-LOF|-[LO]}/
    -<AVLP>{
        -o[AVLP+SLP+PVLP+EPA]/
        -|GC|-o[PVLP'+AVLP']}/
    -|VLP-ICLF|-<ICL>{
        -o[ICL+GOR+SCL+SLP]/
        -|SAC|-o[ICL'+GOR'+SCL'+SLP']}}
```

VLPl3

```
rlAVLP-<rlAVLP>{
    -|hVLPF|-o[AVLP+PVLP+ICL+SCL]/
    -|hVLPF|-o[AVLP+SLP+SCL+ICL]}
```

VLPp&l1

```
rpPLP-|PLP-PVLPF|-o[PVLP+AVLP+SLP]

rpPLP-<PLP>{
    -[LO]/
    -|LO-PLPF|-o[PLP+SCL+ICL+SLP]}

rpLOP-<LOP>{
    -[LOP]/
    -|LOP-IPSF|-o[IPS]}
```

VLPp1

```
rlPLP-|iVLPF|-o[AVLP+PVLP]
```

VLPp2

```
rpSPS-<rpSPS>{
    -|SPS-GCF|-<VES>{
        -[VES+PVLP+ICL]/
        -[VES+CAN+SPS+IPS]}/
    -|SPS-GCF|-<VES>{
        -[VES+PVLP+ICL]/
        -|VESC|-o[VES'+CAN'+SPS'+IPS']}}
```

Table S3 (part 6) Arborization patterns of clonal units.

VPNd1

```
rlPLP-<rlPLP>{
    -<LO>{
        -o[LO]-o[LOP]/
        -|LO-PLPF|-o[PLP(PGe+PGg)+PVLP(VGi)]}/
    -o[PLP+SPS+ICL+SCL+SLP]-|SAC|-
    o[ICL'+SCL'+ICL'+SPS'+PLP']-|PLP-LOF'|-o[LO']}
```

VPNd2

```
rlLH-<LO>{
    -[LO]/
    -|AOT|-o[AOTU]}
```

VPNd3

```
rlLH-<rlLH>{
    -<LO>{
        -o[LO]/
        -|AOT|-o[PVLP(VGb)]}/
    -<LO>{
        -o[LO]/
        -|AOT|-o[PVLP(VGk)]}}
```

VPNd4

```
rlPLP-<LO>{
    -[LO]/
    -|LO-PVLPF|-|LVF|-<SLP>{
        -o[SLP]/
        -|SLP-ICL'C|-<ICL'>{
            -|ICL-SLPF'|-o[SLP']/
            -o[PVLP'+AVLP']}}}
```

VPNl&d1

```
rlAVLP-<ME>{
    -o[ME]/
    -[IPS+SPS]-|POC|-[IPS'+SPS']-o[ME']}

rlSLP-|lSLPF|-o[LH+SLP]
```

VPNp&v1

```
rlPLP-<rlPLP>{
    -o[PLP+PVLP+AVLP]/
    -o[PLP+WED+AVLP]/
    -<PLP>{
        -o[PLP+SCL+ICL+SLP]/
        -|PLP-LOF|-[LO]}/
    -<PLP>{
        -o[PLP+SCL+ICL+SLP]/
        -|sPLPC|-o[SCL'+ICL'+SLP'+PLP']}}

rpPLP-<rpPLP>{
    -<PLP>{
        -o[PLP+SLP]/
        -|PLP-CAF|-o[CA]}/
    -|PLP-SPSF|-[SPS+IB+SPS']/
    -<PLP>{
        -o[PLP+PVLP]/
        -|sPLPC|-<ATL>{
            -[ATL+IB]/
            -|ATLC|-<ATL'>{
                -[ATL'+IB]/
                -|sPLPC|-o[PVLP'+PLP']}}}}
```

VPNp1

```
rlPLP-<rlPLP>{
    -<LO>{
        -[LO]/
        -|LO-PVLPF|-o[PVLP+AVLP]}/
    -<LO>{
        -[LO]/
        -|GC|-o[VES+LAL+CRE]}/
    -<LO>{
        -[LO]/
        -|GC|-o[VES'+LAL'+CRE']}/
    -<LO>{
        -[LO]/
        -|GC|-o[PVLP'+PLP']}/
    -<LO>{
        -[LO]/
        -|GC|-|PVLP-LOF'|-o[LO']-o[ME']}}
```

VPNp2

```
rlPLP-<LO>{
    -[LO]/
    -|LO-PVLPF|-o[PVLP(VGh)]}
```

VPNp3

```
rlPLP-<rlPLP>{
    -<LO>{
        -[LO]/
        -|LO-PVLPF|-o[PVLP(VGd)]}/
    -<LO>{
        -[LO]/
        -|LO-PVLPF|-o[PVLP(VGe)]}}
```

VPNp4

```
rlPLP-<LO>{
    -[LO]/
    -|LO-PLPF|-o[PLP+ICL+SCL+SLP]}
```

VPNv1

```
rlWED-<LO>{
    -[LO]/
    -|LO-PVLPF|-[PVLP(VGf)]}
```

VPNv2

```
rlWED-<LO>{
    -[LO]/
    -|LO-PVLPF|-o[PVLP(VGa)]}
```

VPNv3

```
rlWED-<rlWED>{
    -o[LO]/
    -|LO-PVLPF|-o[PVLP(VGj)+EPA+AVLP]}
```

Table S3 (part 7) Arborization patterns of clonal units.

WEDa1

rlAMMC-o[AMMC+SAD+WED+SEG+IPS]

WEDa2

```
rlAMMC-<rlAMMC>{
    -|AMMC-IFSF|-o[WED+PLP+SLP+SIP+SMP]/
    -|AMMC-IFSF|-|IFS-LALF|-o[LAL+CRE+SIP+SMP]}
```

WEDd1

```
raAOTU-|AOTU-IFSF|-[VES]-<IFS>{
    -[WED]/
    -|CV|-}
```

WEDd2

```
rsAL-|AL-VESF|-<VES>{
    -|VES-WEDF|-o[WED+PLP]/
    -|VESC|-<VES'>{
        -|VES-WEDF'|-o[WED'+PLP']/
        -o[VES'+CAN'+SAD']}
```

SLPpm4*

```
rmpSMP-<ATL>{
    -|ATL-SLPF|-o[SLP+SCL+PLP]/
    -|ATL-PLPF|-o[PLP+SCL+SLP]}
```

SMPad4*

```
raSMP-<CRE>{
    -o[CRE+SMP+SIP+SLP]/
    -|CRE-FBF|-o[FB+NO+NO']}
```

Table S3 (part 8) Arborization patterns of clonal units.

Table S3 (part1-8) Arborization patterns of clonal units.

The projection and arborization patterns of the clonal units, documented using newly developed formulae. The rule of the formulae is as follows:

- First letters of the formula (starting with “r”) indicates the position of cell bodies in the cell body rind.
- <A> indicates a branching point of neural fibers. (A is a cell body position, neuropil, or fiber bundle).
- If <A> is a cell body position, {-formula 1/ -formula 2/ -formula 3…} that follow <A> indicate the projection patterns of the subgroups of neurons in the clonal cell body cluster (i.e. projection subgroups), each of which shares similar neural pathways and innervation sites that are distinct from those of other subgroups.
- If <A> is a neuropil or fiber bundle, {-formula 1/ -formula 2/ -formula 3…} that follow <A> indicate the set of branches arising from the branch point. Each formula may contain further projections, branches, and arborizations.
- -|A|- indicates fiber bundles (fascicles or commissures) that the fibers pass through without forming arborizations.
- -[A] indicates the neuropils of arborizations. If the presence of presynaptic or postsynaptic sites is known, a small letter “o” (for output) or “i” (for input), respectively, is added in front of [A]. In this study we use only “o” because we did not examine postsynaptic sites.
- -[A+B+…] indicates a contiguous arborization that spans neuropils A, B, etc.
- A’ is a contralateral neuropil of A (in the other brain side).
- A(B) means subregion B of the neuropil A.
- Elements in the formulae are joined with hyphens.

	Neuropil	k	k_{in}	k_{ex}	k_{ex}/k_{in}	s	s_{in}	s_{ex}	s_{ex}/s_{in}	s/k	s_{in}/k_{in}	s_{ex}/k_{ex}	BC
Community 1	AVLP	43	17	26	1.529	204	109	95	0.872	4.744	6.412	3.654	24.672
	AVLP'	43	17	26	1.529	204	109	95	0.872	4.744	6.412	3.654	24.672
	PVLP	44	18	26	1.444	175	80	95	1.188	3.977	4.444	3.654	25.589
	PVLP'	44	18	26	1.444	175	80	95	1.188	3.977	4.444	3.654	25.589
	WED	37	16	21	1.313	125	65	60	0.923	3.378	4.063	2.857	27.381
	WED'	37	16	21	1.313	125	65	60	0.923	3.378	4.063	2.857	27.381
	VES	37	14	23	1.643	116	48	68	1.417	3.135	3.429	2.957	8.741
	VES'	37	14	23	1.643	116	48	68	1.417	3.135	3.429	2.957	8.741
	SAD	41	18	23	1.278	111	70	41	0.586	2.707	3.889	1.783	32.450
	SAD'	41	18	23	1.278	111	70	41	0.586	2.707	3.889	1.783	32.450
	SEG	38	12	26	2.167	82	32	50	1.563	2.158	2.667	1.923	71.160
	FLA	31	13	18	1.385	72	30	42	1.400	2.323	2.308	2.333	26.282
	FLA'	31	13	18	1.385	72	30	42	1.400	2.323	2.308	2.333	26.282
	AMMC	23	13	10	0.769	51	38	13	0.342	2.217	2.923	1.300	7.033
	AMMC'	23	13	10	0.769	51	38	13	0.342	2.217	2.923	1.300	7.033
	CAN	23	14	9	0.643	44	30	14	0.467	1.913	2.143	1.556	3.504
	CAN'	23	14	9	0.643	44	30	14	0.467	1.913	2.143	1.556	3.504
	EPA	14	10	4	0.400	21	16	5	0.313	1.500	1.600	1.250	1.106
	EPA'	14	10	4	0.400	21	16	5	0.313	1.500	1.600	1.250	1.106
Community 2	SLP	55	21	34	1.619	369	213	156	0.732	6.709	10.143	4.588	191.221
	SLP'	55	21	34	1.619	369	213	156	0.732	6.709	10.143	4.588	191.221
	SCL	43	18	25	1.389	316	197	119	0.604	7.349	10.944	4.760	24.619
	SCL'	43	18	25	1.389	316	197	119	0.604	7.349	10.944	4.760	24.619
	ICL	40	18	22	1.222	281	185	96	0.519	7.025	10.278	4.364	18.002
	ICL'	40	18	22	1.222	281	185	96	0.519	7.025	10.278	4.364	18.002
	PLP	49	21	28	1.333	218	119	99	0.832	4.449	5.667	3.536	90.966
	PLP'	49	21	28	1.333	218	119	99	0.832	4.449	5.667	3.536	90.966
	SPS	44	17	27	1.588	182	106	76	0.717	4.136	6.235	2.815	16.633
	SPS'	44	17	27	1.588	182	106	76	0.717	4.136	6.235	2.815	16.633
	IPS	34	16	18	1.125	80	49	31	0.633	2.353	3.063	1.722	25.334
	IPS'	34	16	18	1.125	80	49	31	0.633	2.353	3.063	1.722	25.334
	GOR	30	11	19	1.727	112	69	43	0.623	3.733	6.273	2.263	3.918
	GOR'	30	11	19	1.727	112	69	43	0.623	3.733	6.273	2.263	3.918
	LH	11	6	5	0.833	46	29	17	0.586	4.182	4.833	3.400	3.415
	LH'	11	6	5	0.833	46	29	17	0.586	4.182	4.833	3.400	3.415
	AL	11	5	6	1.200	25	12	13	1.083	2.273	2.400	2.167	5.584
	AL'	11	5	6	1.200	25	12	13	1.083	2.273	2.400	2.167	5.584
	LO	31	13	18	1.385	99	59	40	0.678	3.194	4.538	2.222	8.718
	LO'	31	13	18	1.385	99	59	40	0.678	3.194	4.538	2.222	8.718
	LOP	11	8	3	0.375	13	10	3	0.300	1.182	1.250	1.000	0.337
	LOP'	11	8	3	0.375	13	10	3	0.300	1.182	1.250	1.000	0.337
	ME	17	12	5	0.417	32	26	6	0.231	1.882	2.167	1.200	1.004
	ME'	17	12	5	0.417	32	26	6	0.231	1.882	2.167	1.200	1.004
	AME	6	4	2	0.500	9	6	3	0.500	1.500	1.500	1.500	0.215
	AME'	6	4	2	0.500	9	6	3	0.500	1.500	1.500	1.500	0.215
Community 3 non-CX	SMP	50	19	31	1.632	364	234	130	0.556	7.280	12.316	4.194	117.564
	SMP'	50	19	31	1.632	364	234	130	0.556	7.280	12.316	4.194	117.564
	SIP	44	19	25	1.316	249	181	68	0.376	5.659	9.526	2.720	86.742
	SIP'	44	19	25	1.316	249	181	68	0.376	5.659	9.526	2.720	86.742
	LAL	45	19	26	1.368	171	107	64	0.598	3.800	5.632	2.462	71.934
	LAL'	45	19	26	1.368	171	107	64	0.598	3.800	5.632	2.462	71.934
	ATL	35	12	23	1.917	169	93	76	0.817	4.829	7.750	3.304	4.665
	ATL'	35	12	23	1.917	169	93	76	0.817	4.829	7.750	3.304	4.665
	IB	38	12	26	2.167	164	62	102	1.645	4.316	5.167	3.923	18.054
	CRE	42	18	24	1.333	163	110	53	0.482	3.881	6.111	2.208	84.903
	CRE'	42	18	24	1.333	163	110	53	0.482	3.881	6.111	2.208	84.903
	AOTU	34	14	20	1.429	147	104	43	0.413	4.324	7.429	2.150	15.794
	AOTU'	34	14	20	1.429	147	104	43	0.413	4.324	7.429	2.150	15.794
	PRW	8	4	4	1.000	15	8	7	0.875	1.875	2.000	1.750	0.155
	PRW'	8	4	4	1.000	15	8	7	0.875	1.875	2.000	1.750	0.155
Community 3 CX	FB	21	15	6	0.400	142	132	10	0.076	6.762	8.800	1.667	25.569
	EB	19	15	4	0.267	54	50	4	0.080	2.842	3.333	1.000	14.622
	NO	16	12	4	0.333	46	40	6	0.150	2.875	3.333	1.500	5.046
	NO'	16	12	4	0.333	46	40	6	0.150	2.875	3.333	1.500	5.046
	PB	5	5	0	0.000	32	32	0	0.000	6.400	6.400	0.000	0.000
	PB'	5	5	0	0.000	32	32	0	0.000	6.400	6.400	0.000	0.000
	BU	11	8	3	0.375	20	17	3	0.176	1.818	2.125	1.000	2.164
	BU'	11	8	3	0.375	20	17	3	0.176	1.818	2.125	1.000	2.164
Community 4	ML	14	5	9	1.800	56	42	14	0.333	4.000	8.400	1.556	106.730
	VL	19	4	15	3.750	56	30	26	0.867	2.947	7.500	1.733	94.181
	CA	9	5	4	0.800	46	40	6	0.150	5.111	8.000	1.500	42.025
	PED	5	5	0	0.000	42	42	0	0.000	8.400	8.400	0.000	1.670
	ACA	4	4	0	0.000	16	16	0	0.000	4.000	4.000	0.000	0.000
	SPU	3	3	0	0.000	12	12	0	0.000	4.000	4.000	0.000	0.000
Community 5	ML'	14	5	9	1.800	56	42	14	0.333	4.000	8.400	1.556	106.730
	VL'	19	4	15	3.750	56	30	26	0.867	2.947	7.500	1.733	94.181
	CA'	9	5	4	0.800	46	40	6	0.150	5.111	8.000	1.500	42.025
	PED'	5	5	0	0.000	42	42	0	0.000	8.400	8.400	0.000	1.670
	ACA'	4	4	0	0.000	16	16	0	0.000	4.000	4.000	0.000	0.000
	SPU'	3	3	0	0.000	12	12	0	0.000	4.000	4.000	0.000	0.000

Table S4 Node properties for different neuropils.

Table S4 Node properties for different neuropils.

Node degree (k), extrinsic node degree (k_{ex}), intrinsic node degree (k_{in}), node strength (s), extrinsic node strength (s_{ex}), intrinsic node strength (s_{in}), their ratios, and betweenness centrality (BC) are indicated.